AD-A108 716 ARMY ENGINEER WATERWAYS EXPERIMENT STATION VICKSBURG--ETC F/G 13/2
BOMB CRATER REPAIR TECHNIQUES FOR PERMANENT AIRFIELDS. REPORT I--ETC(U)
OCT 81 D L COOKSEY
UNCLASSIFIED WES/MP/GL-81-12 NL

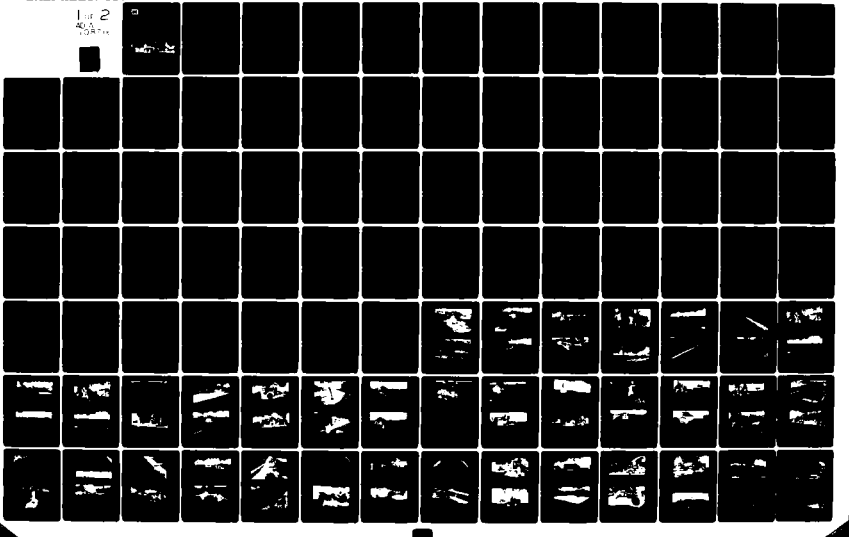

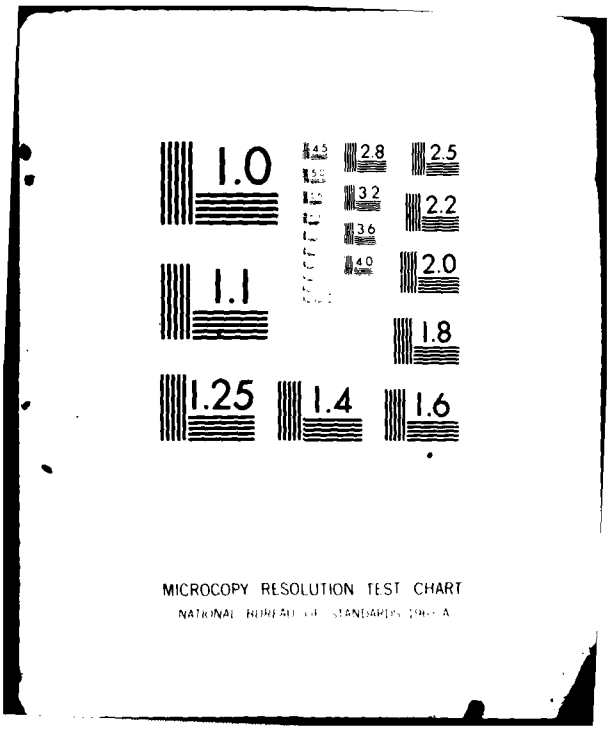
1.0
1.1
1.25
1.4
1.6
1.8
2.0
2.2
2.5
2.8
3.2
3.6
4.0
MICROCOPY RESOLUTION TEST CHART
NATIONAL BUREAU OF STANDARDS 1963-A

TECHNICAL REPORT GL-81-12

BOMB CRATER REPAIR TECHNIQUES FOR PERMANENT AIRFIELDS

Report 1

SERIES 1 TESTS

by

David L. Cooksey

Geotechnical Laboratory
U. S. Army Engineer Waterways Experiment Station
P. O. Box 631, Vicksburg, Miss. 39180

October 1981

Report 1 of a Series

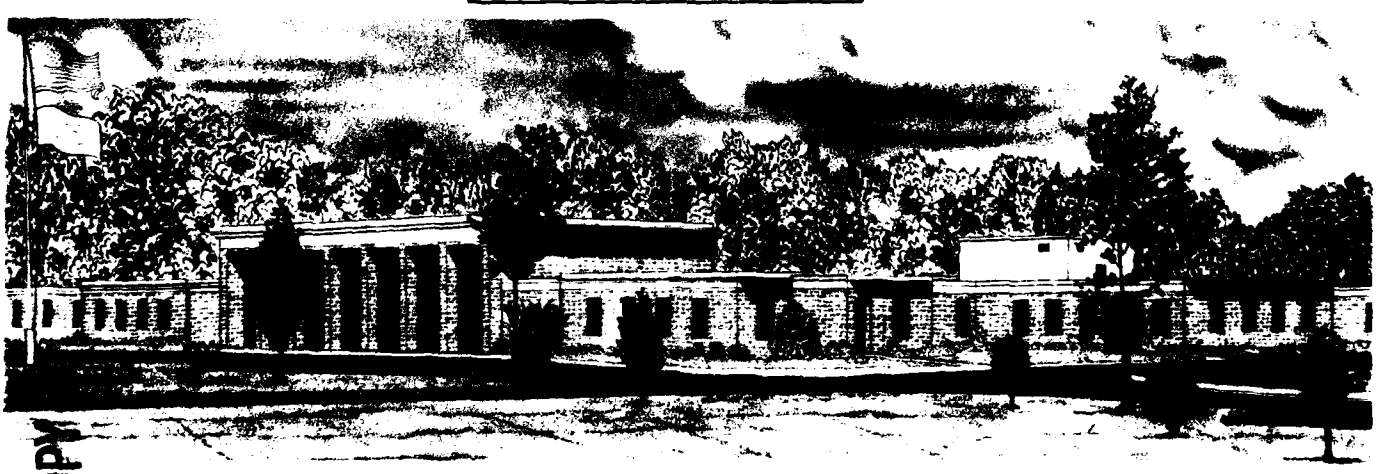

Prepared for Office, Chief of Engineers, U. S. Army
Washington, D. C. 20314

Under Project AT40, Task CO, Work Unit 002

Destroy this report when no longer needed. Do not return it to the originator.

The findings in this report are not to be construed as an official Department of the Army position unless so designated by other authorized documents.

The contents of this report are not to be used for advertising, publication, or promotional purposes. Citation of trade names does not constitute an official endorsement or approval of the use of such commercial products.

DISCLAIMER NOTICE

THIS DOCUMENT IS BEST QUALITY PRACTICABLE. THE COPY FURNISHED TO DTIC CONTAINED A SIGNIFICANT NUMBER OF PAGES WHICH DO NOT REPRODUCE LEGIBLY.

Unclassified
SECURITY CLASSIFICATION OF THIS PAGE (When Data Entered)

VVL-S-Lib

REPORT DOCUMENTATION PAGE

READ INSTRUCTIONS BEFORE COMPLETING FORM

1. REPORT NUMBER: Technical Report GL-81-12	2. GOVT ACCESSION NO.: AD-A108 716
3. RECIPIENT'S CATALOG NUMBER	
4. TITLE (and Subtitle): BOMB CRATER REPAIR TECHNIQUES FOR PERMANENT AIRFIELDS; Report 1, SERIES 1 TESTS	5. TYPE OF REPORT & PERIOD COVERED: Report 1 of a series
	6. PERFORMING ORG. REPORT NUMBER
7. AUTHOR(s): David L. Cooksey	8. CONTRACT OR GRANT NUMBER(s)
9. PERFORMING ORGANIZATION NAME AND ADDRESS: U. S. Army Engineer Waterways Experiment Station, Geotechnical Laboratory, P. O. Box 631, Vicksburg, Miss. 39180	10. PROGRAM ELEMENT, PROJECT, TASK AREA & WORK UNIT NUMBERS: Project AT40, Task CO, Work Unit 002
11. CONTROLLING OFFICE NAME AND ADDRESS: Office, Chief of Engineers, U. S. Army, Washington, D. C. 20314	12. REPORT DATE: October 1981
	13. NUMBER OF PAGES: 123
14. MONITORING AGENCY NAME & ADDRESS (if different from Controlling Office)	15. SECURITY CLASS. (of this report): Unclassified
	15a. DECLASSIFICATION/DOWNGRADING SCHEDULE

16. DISTRIBUTION STATEMENT (of this Report)

Approved for public release; distribution unlimited.

17. DISTRIBUTION STATEMENT (of the abstract entered in Block 20, if different from Report)

18. SUPPLEMENTARY NOTES

Available from National Technical Information Service, 5285 Port Royal Road, Springfield, Va. 22151.

19. KEY WORDS (Continue on reverse side if necessary and identify by block number)

Blast effects	Runway damage
Bomb crater repair	Runway repair
Craters	

20. ABSTRACT (Continue on reverse side if necessary and identify by block number)

A test section with six simulated bomb craters was constructed at the U. S. Army Engineer Waterways Experiment Station for the purpose of developing an improved field method of repair and restoration of air base runways damaged by enemy attack. The crater repair materials tested in the reconstruction were a high-quality crushed stone, grouted concrete, portland cement concrete (PCC), and asphaltic concrete (AC). The performances of the different materials were evaluated under full-scale load testings with the F-4 and C-141 aircraft loadings.

(Continued)

DD FORM 1 JAN 73 1473 EDITION OF 1 NOV 65 IS OBSOLETE

Unclassified
SECURITY CLASSIFICATION OF THIS PAGE (When Data Entered)

20. ABSTRACT (Continued).

The gravity grout solution and the high-quality crushed stone method performed beyond required coverage levels and seem to be the two high candidate material systems for further research. The solutions were accomplished with the time, manpower, equipment, and performance constraints of operational requirements.

PREFACE

The investigation reported herein was sponsored by the Office, Chief of Engineers, U. S. Army, and was conducted under Project AT40, Task CO, Work Unit 002, "Repair and Restoration of Paved Surfaces (REREPS)" during the period July to November 1978. The responsibility for conducting the study was assigned to the Geotechnical Laboratory (GL) of the U. S. Army Engineer Waterways Experiment Station (WES), Vicksburg, Miss.

The investigation was conducted under the general direction of Dr. W. F. Marcuson III and Mr. J. P. Sale, Chief and former Chief, GL, and under the direct supervision of Messrs. A. H. Joseph and R. L. Hutchinson, Chief and former Chief, Pavement Systems Division (PSD), GL. Engineers and technicians of the PSD actively engaged in the planning, testing, analyzing, and reporting phases of this study were Dr. G. M. Hammitt and Messrs. H. L. Green, C. L. Rone, R. W. Grau, S. J. Alford, and D. L. Cooksey. This report was prepared by Mr. D. L. Cooksey.

Commanders and Directors of the WES during the course of this study and the preparation and publication of this report were COL Nelson P. Conover, CE, and COL Tilford C. Creel, CE. The Technical Director was Mr. Fred R. Brown.

CONTENTS

CONVERSION FACTORS, U. S. CUSTOMARY TO METRIC (SI) UNITS OF MEASUREMENT

U. S. customary units of measurement used in this report can be converted to metric (SI) units as follows:

Multiply	By	To Obtain
cubic feet	0.2831685	cubic metres
Fahrenheit degrees	5/9	Celsius degrees or Kelvins*
feet	0.3048	metres
gallons per minute	3.785412	cubic decimetres per minute
gallons per square yard	4.5273	cubic decimetres per square metre
inches	2.54	centimetres
mils	0.0254	millimetres
ounces	28.34952	grams
pounds (force)	4.44822	newtons
pounds (force) per square inch	6894.757	pascals
pounds (mass)	0.4535924	kilograms
pounds (mass) per cubic foot	16.0185	kilograms per cubic metre
square inches	6.4516	square centimetres

* To obtain Celsius (C) temperature readings from Fahrenheit (F) readings, use the following formula: $C = (5/9)(F - 32)$. To obtain Kelvin (K) readings, use: $K = (5/9)(F - 32) + 273.15$.

BOMB CRATER REPAIR TECHNIQUES FOR PERMANENT AIRFIELDS

SERIES 1 TESTS

PART I: INTRODUCTION

Background

1. The responsibility for emergency war damage repair of U. S. Air Force air base facilities, including pavement and structures, is assigned to the U. S. Air Force for accomplishment within their organic service capabilities. The U. S. Air Force normally uses specially designed landing mat crater repair kits for emergency repair of pavements. All war damage repairs which exceed the organic capabilities of the U. S. Air Force are the responsibility of the U. S. Army. The Army is further assigned the responsibility of developing improved repair and restoration systems for paved surfaces (REREPS) that would consider variations in both damage levels from aggressor attacks and in U. S. forces operational requirements. The systems to be evaluated were to include materials, equipment, and procedures that are designed to reduce the personnel requirements, repair time, and cost, as well as to improve the permanency of the repair. During early stages of hostilities, REREPS are among the most vital engineer support missions. Experience in recent conflicts has vividly illustrated the criticality of rapid repair of specific airbase facilities.

2. This report addresses the repair and restoration of war damaged runways after emergency repairs have been made to permit utilization by logistic aircraft as well as the tactical aircraft.

3. The 18th Engineer Brigade in Germany and the U. S. Army Engineer Waterways Experiment Station (WES) have been collaborating to develop a solution to the REREPS problem. In April 1977, WES and the 18th Engineer Brigade demonstrated an Army capability for REREPS using

regulated-set concrete.* Subsequently, full-scale loading studies were conducted at WES and as a construction material the regulated-set concrete was adequate; however, it has many disadvantages, such as limited shelf-life, all weather constraints, very large number of ready-mix trucks required, etc. Regulated-set concrete is not considered an optimum solution but will be kept in inventory while other methods are researched to determine the best one for European airfields.

Purpose

4. This investigation was conducted to evaluate several field methods of repair and restoration of bomb craters in airfields. To accomplish this, a test runway was constructed with simulated crater repairs made and subjected to aircraft loading of F-4C and C-141. The object was to determine which methods would be the most reliable and feasible during and after an enemy attack in which availability of materials and equipment would be of prime concern. Repair concepts were discussed with military field personnel to eliminate those not practical for engineer troop use.

Scope

5. In this study, six simulated craters were repaired with the following materials: (a) a well-graded crushed limestone, (b) an open-graded crushed limestone and grout, (c) portland cement concrete (PCC), and asphaltic concrete (AC). Each method of repair was subjected to F-4C and C-141 loadings at a specified number of passes to examine performance.

---

* R. L. Hutchinson, C. L. Rone, and R. H. Denson. In publication. "Repair and Restoration of Paved Surfaces; Evaluation of Regulated-Set Cement Concrete Repair Procedure," Technical Report C-78-2, Report 2, U. S. Army Engineer Waterways Experiment Station, CE, Vicksburg, Miss.

PART II: LAYOUT OF TEST SITE, SECTION CONSTRUCTION, AND TEST EQUIPMENT USED

Test Site

6. A test site was selected at WES on a well-drained ridge that consisted of a natural lean clay soil deposit. A general view of the site prior to grading is shown on Photo 1. The initial rough grading and compaction of the site was accomplished with D-4, D-6, and D-7 bulldozers (Photo 2), with the D-4 towing a single-drum sheepsfoot roller for compaction of the fills. This rough grading covered an area 400 ft* long by 65 ft wide. The top 6 to 10 in. of the subgrade was processed with a pulvimixer (Photo 3) to break down the soil and reduce the water content. A four-wheel pneumatic-tired roller (Photo 4), loaded to 50,000 lb, with tires inflated to 90 psi, was used for compaction. Final grading of the site was accomplished with a motor grader (Photo 5). The section was graded to both a longitudinal slope and a crown of 1.5 percent. Plate bearing and CBR tests were run and soil samples were taken on the lean clay subgrade prior to setting the wooden forms for the test lanes to be paved with concrete (Photos 6-8).

Section Construction

7. The forms for the 11-in.-thick concrete sections of the north and south lanes (each 20 by 275 ft) were set first (Photo 9). The north lane contained forms that produced a longitudinal keyway (Photo 10) and the south lane had both forms and No. 5 tie bars, 30 in. long, placed at 30-in. intervals in the center of the keyway (Photo 11). Concrete was placed in the south lane first, directly from ready-mix trucks. The concrete was vibrated using hand vibrators and then screeded with a wooden straightedge on which two small gasoline-powered vibrators were

---

* A table of factors for converting U. S. customary units of measurement to metric (SI) units is presented on page 3.

mounted (Photos 12 and 13). Fiberboard, 1/4 in. thick, was placed in the wet concrete to a depth of 4 in. to form a weakened plane for creating transverse joints. A rough finish was accomplished by hand using bullfloats, trowels, and burlap cloth drags. The same procedure was used the next day to pour concrete in the north lane. In preparation for pouring the center lane, forms were set and cross forms were placed at 25-ft intervals to make 25- by 25-ft sections (Photo 14). Eleven days after the south lane was completed, concrete, 11 in. thick, was placed in alternate 25- by 25-ft sections in the center lane, following the same placing and finishing procedures as those used in the south and north lanes (Photo 15). Forms from all lanes were removed as soon as possible after placing the concrete. This method of construction resulted in a total of 28 slabs in the test section and 6 simulated 25-ft square craters. The north and south lanes each contained 11 slabs and the center lane contained 6 slabs.

8. As soon as the water sheen began to disappear, the south lane was sprayed with a curing compound meeting the requirements of test method CRD-C 300* (Photo 16). The north lane and center slabs were sprayed with the curing compound and also covered with burlap and wet cured for approximately 7 days. All exposed edges were sprayed after the forms were removed from the concrete.

9. A 65- by 65-ft flexible pavement test section was placed on the east end of the rigid pavement test section. This section consisted of 3 in. of AC placed over 6 in. of crushed stone and 17 in. of sandy gravel.

10. Maneuver areas were constructed on each end of the test sections to provide the load carts with an area in which to shift wheel paths and traffic lanes. The west maneuver area, which consisted of 15 in. of lime-stabilized clayey gravel, was 65 ft wide and 30 ft long. The east maneuver area, which consisted of 3 in. of AC over 16 in. of lime-stabilized clayey gravel, was 65 ft wide and 30 ft long.

---

* U. S. Army Engineer Waterways Experiment Station, CE. 1977. "Specifications for Membrane-Forming Compounds for Curing Concrete," Handbook for Concrete and Cement, CRD-C 300-77, Vicksburg, Miss.

11. Since the rigid pavement portion of the test section was to be overlain with 4 in. of AC, a tack coat of SS-1 asphalt emulsion was applied to the surface of the PCC at the rate of approximately 0.05 gal/sq yd (Photo 17). The AC, at a temperature of 300°F, was placed on the test area after the concrete cured for 40 days. Using an asphalt spreader, 11-ft-wide lanes were paved on each pass (Photo 18). Breakdown compaction of the asphalt was accomplished with a vibratory self-propelled roller (Photo 19). A pneumatic self-propelled roller, with 90-psi tire pressure and weighing 50,000 lb, made 12 passes (Photo 20), and for final compaction, one pass was applied with the steel-wheel vibratory roller. The density of the AC averaged 136.8 pcf and the average asphalt content was 4.4 percent.

12. The test section, as shown in Figure 1, was constructed to simulate existing European airfield pavements containing bomb craters requiring repair/restoration.

13. The pavements around craters 1-6 were designed as medium-load pavements capable of withstanding 5,000 coverages of the C-141 aircraft with a gross weight of 320,000 lb.

Test Equipment

14. Two specially designed load carts which simulated aircraft wheel loading were used in these tests. To simulate the single-wheel loadings of the F-4C fighter aircraft, a load cart with a single-wheel load of 25,000 lb was used as one of the test carts (Photo 21). As shown, the load cart was fitted with an outrigger wheel to prevent overturning and was powered by the front wheels. The test wheel had a 30.0×11.5, 24-ply tire inflated to 250 psi to produce a contact area of 111 sq in. and an average contact pressure of 225 psi.

15. In order to simulate the heavier loads of the C-141, a larger load cart was used (Photo 22). The load box, supported by four tires in a twin-tandem gear arrangement, was used to traffic the pavement. The independent action of the outrigger and the load box provided a condition where the load on the outrigger wheels had no influence on the test

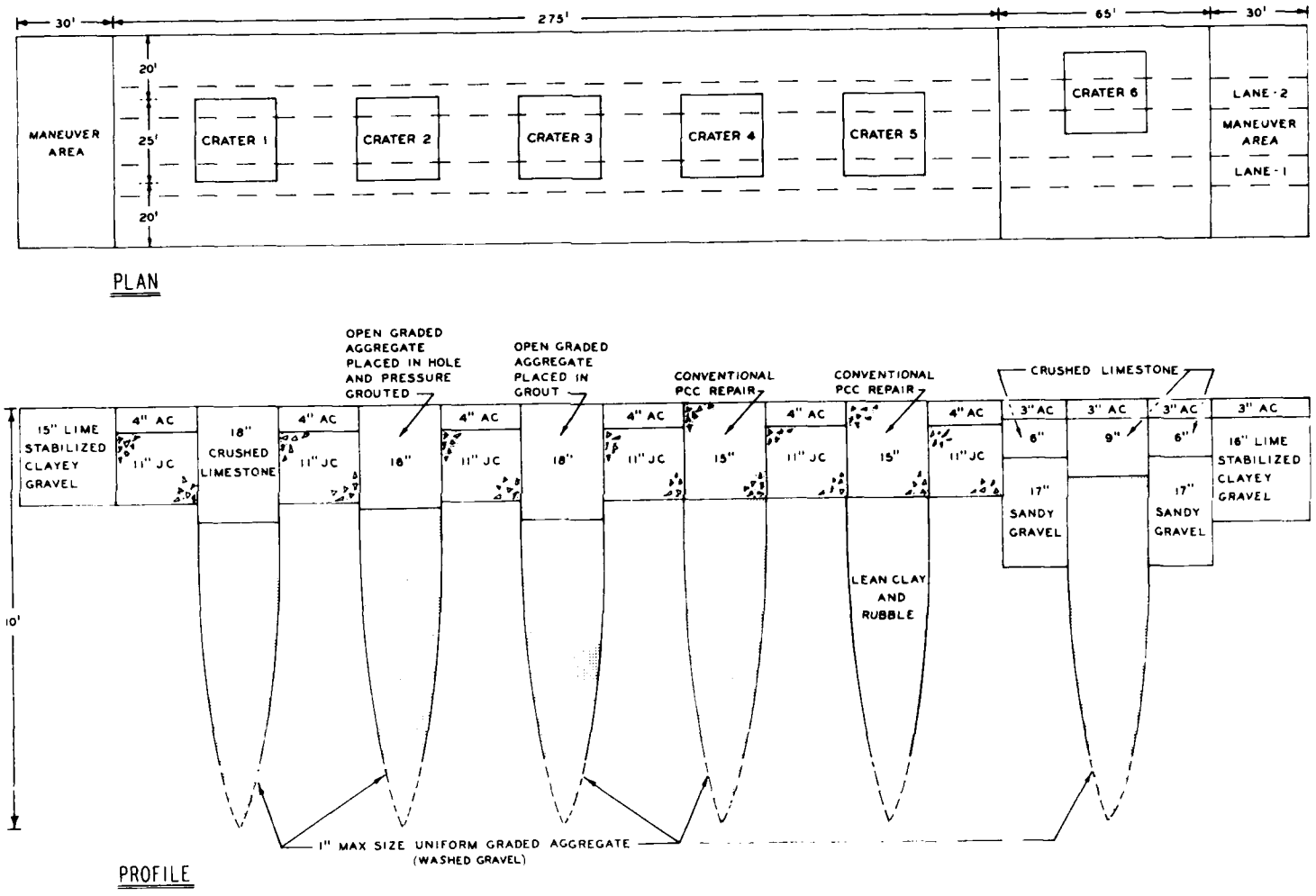

Figure 1. Test site for the REREPS

wheels. In simulating conditions of the C-141 aircraft, the test tires were inflated to 185 psi and the cart was loaded to a total gross weight of 144,000 lb, resulting in a 208-sq-in. contact area per tire. To simulate as nearly as possible the effects of the aircraft, the respective aircraft tires and wheel spacings were used.

PART III: CONSTRUCTION OF TEST CRATERS

Crater Excavation and Backfill

16. The test section for the REREPS is shown in Figure 1. Six simulated craters, each 25 by 25 ft, were constructed (Photo 23) in the test section. Each crater was excavated to an approximate center depth of 10 ft (Photo 24). Craters 1, 2, 3, 4, and 6 were backfilled with washed Vicksburg, Mississippi River gravel up to within 9 to 18 in. of the top surface depending on the test material to be placed in the craters. The washed gravel was smooth and had a maximum size of 1 in. and was uniformly graded. The washed gravel was dumped into the craters from dump trucks and spread with a backhoe (Photo 25). A vibrator foot attached to the backhoe was used to compact the washed gravel as it was being spread (Photo 26). To simulate a more hasty repair that might be expected in a hostile environment, crater 5 was backfilled with a lean clay and broken concrete. The rubble material was placed in lifts approximately 1 ft thick and spread with the backhoe. It was compacted with the vibrator foot and a gasoline-powered tamper (Photo 27). The final lift of backfill material was rolled with the vibratory steel-wheel roller. Gradation curves for the clayey gravel, crushed limestone, and washed gravel used in the maneuver areas and the lower portion of craters 1, 2, 3, 4, and 6 are shown in Figure 2. Gradation curves for materials used in the upper portion of craters 2 and 3 and the subbase of crater 6 are shown in Figure 3.

Crater Surfacing and Joining Devices

17. The surfacing of each crater varied in type of material, thickness of material, method of placement, and/or types of devices used in tying in the crater material to the adjoining concrete. Detailed descriptions of each crater surfacing material and the types of joining devices used are given below. Sketches of the various types of joining devices are depicted in Figure 4. The results of both the density and

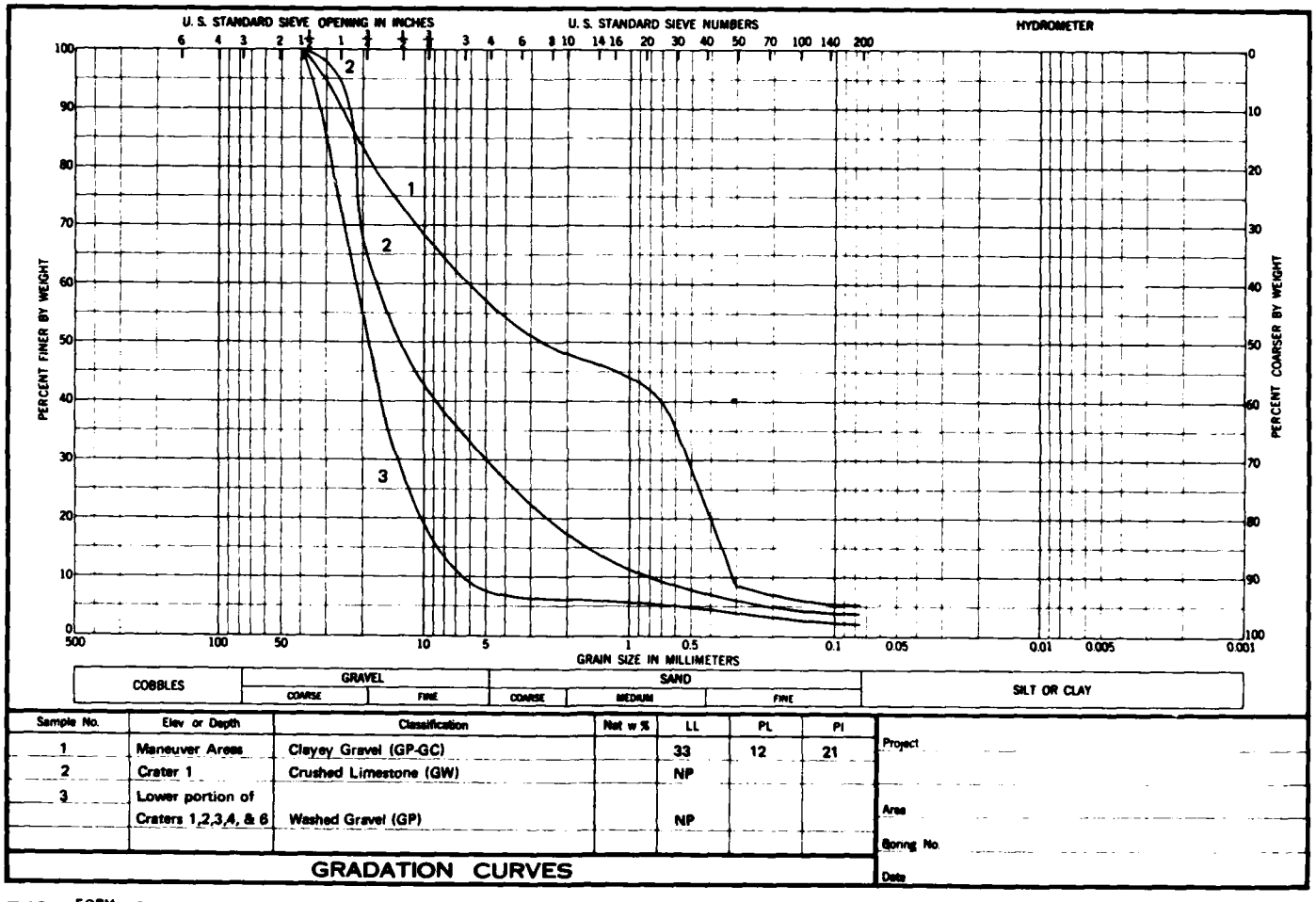

ENG FORM 1 MAY 63 2087

Figure 2. Gradation curves for clayey gravel, crushed limestone, and washed gravel

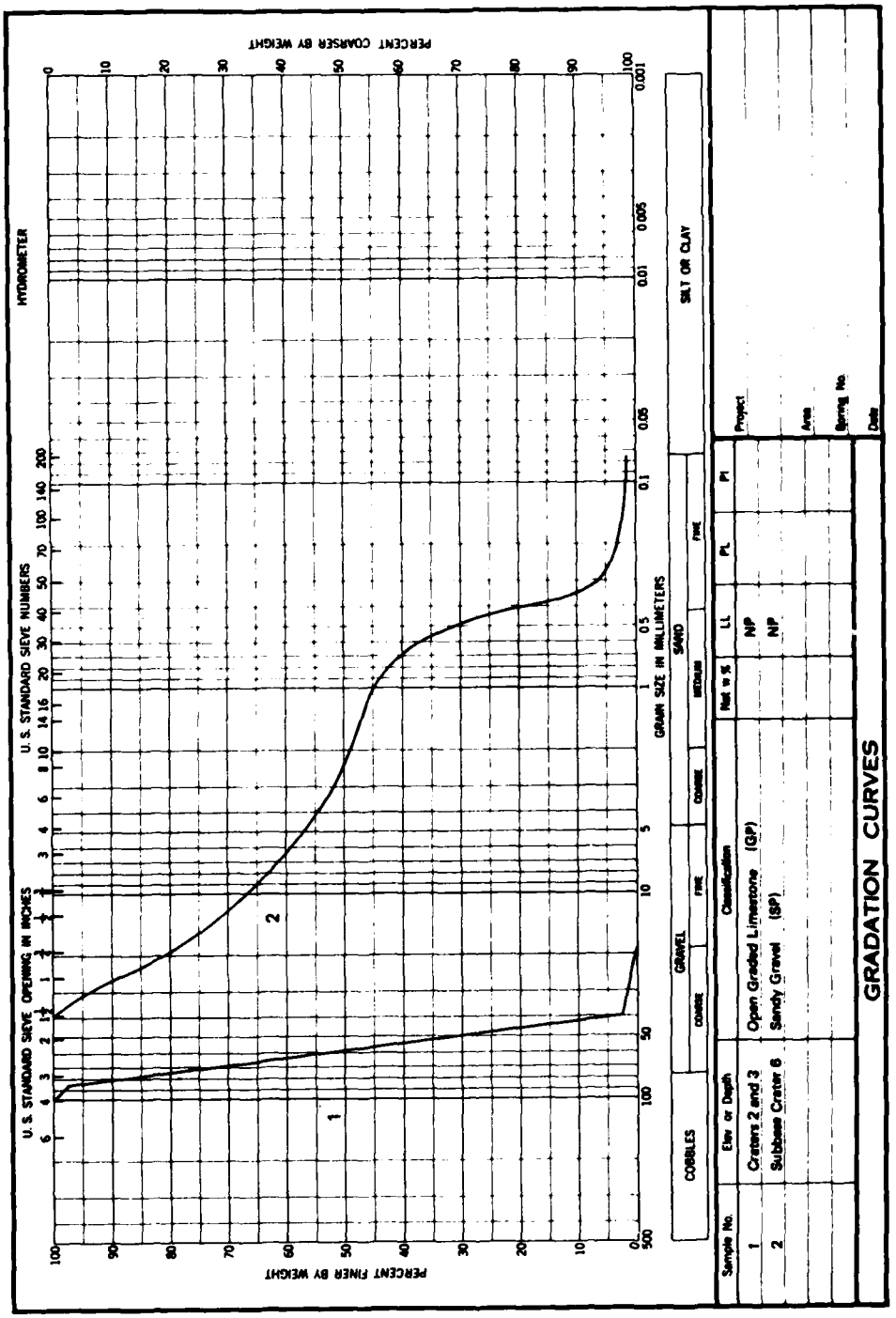

Figure 3. Gradation curves for open-graded limestone and sandy gravel

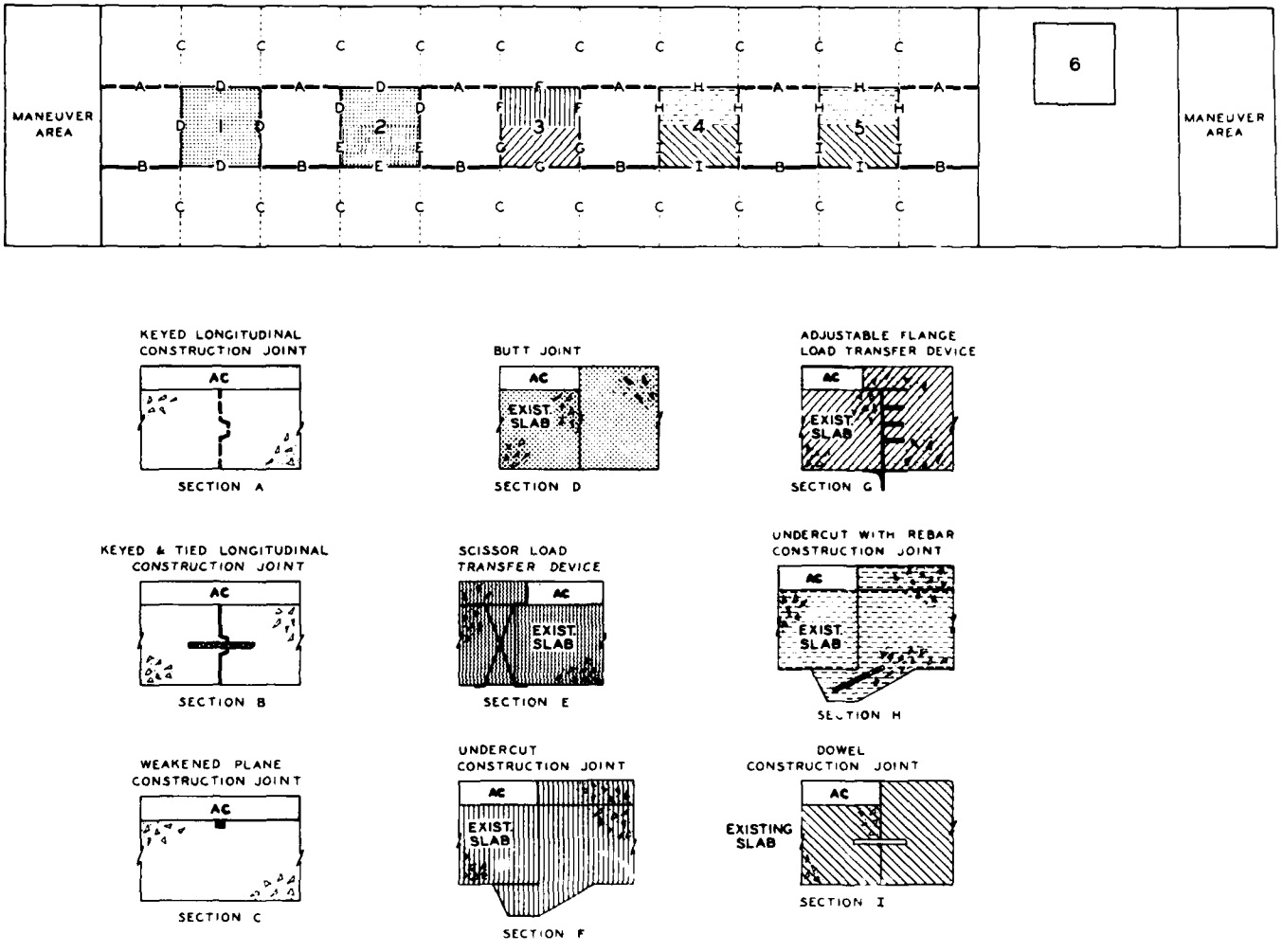

Figure 4. Moment transfer devices

water content measurements taken in craters 1-4 during excavations are shown on Table 1. These measurements were not taken at craters 5 and 6. Soil data taken at various locations during the testing are shown in Table 2.

Crater 1

18. After backfilling the bottom portion of the crater with washed gravel, approximately 18 in. of crushed limestone was used to finish filling the crater (Photos 28 and 29). The limestone was placed in three lifts. Each lift was rolled with eight coverages of the vibratory steel-wheel roller (Photo 30). The fill around the edges of the crater was compacted using the vibrator foot (Photo 31). The final lift was rolled an additional 8 coverages with the vibratory steel-wheel roller and 48 coverages with the pneumatic roller weighing 110,000 lb with tire pressure of 90 psi (Photo 32). This was considered to be the simplest repair method for filling the crater since no special equipment or materials were required. There were no specially prepared joining devices required to tie the crushed limestone to the surrounding concrete and asphalt. The limestone was also to be used as the final surfacing on which the load cart would travel.

Crater 2

19. Prior to the filling of the top 16 in. of crater 2, a scissor-type moment transfer device was placed in the perimeter of the crater along the south side of the center line. That portion of the crater north of the center line had no special joining devices. The scissor-type devices were fabricated from 1/2-in. steel plate and were placed on 4-ft centers with just enough of the asphalt overlay cut out to allow the devices to be clamped onto the existing PCC slab (Photo 33). A sketch of the device is shown in Figure 5. Since this crater was to be grouted, a layer of sand and dry bentonite approximately 1 ft wide and 1 to 2 in. deep was placed on the washed gravel around the entire edge of the crater in order to prevent the grout from flowing into the gravel under the existing slab. The gravel in the open crater was also covered with two sheets of 6-mil polyethylene film to keep the grout from penetrating into it. A total of seven 4-in.-diam grout pipes made

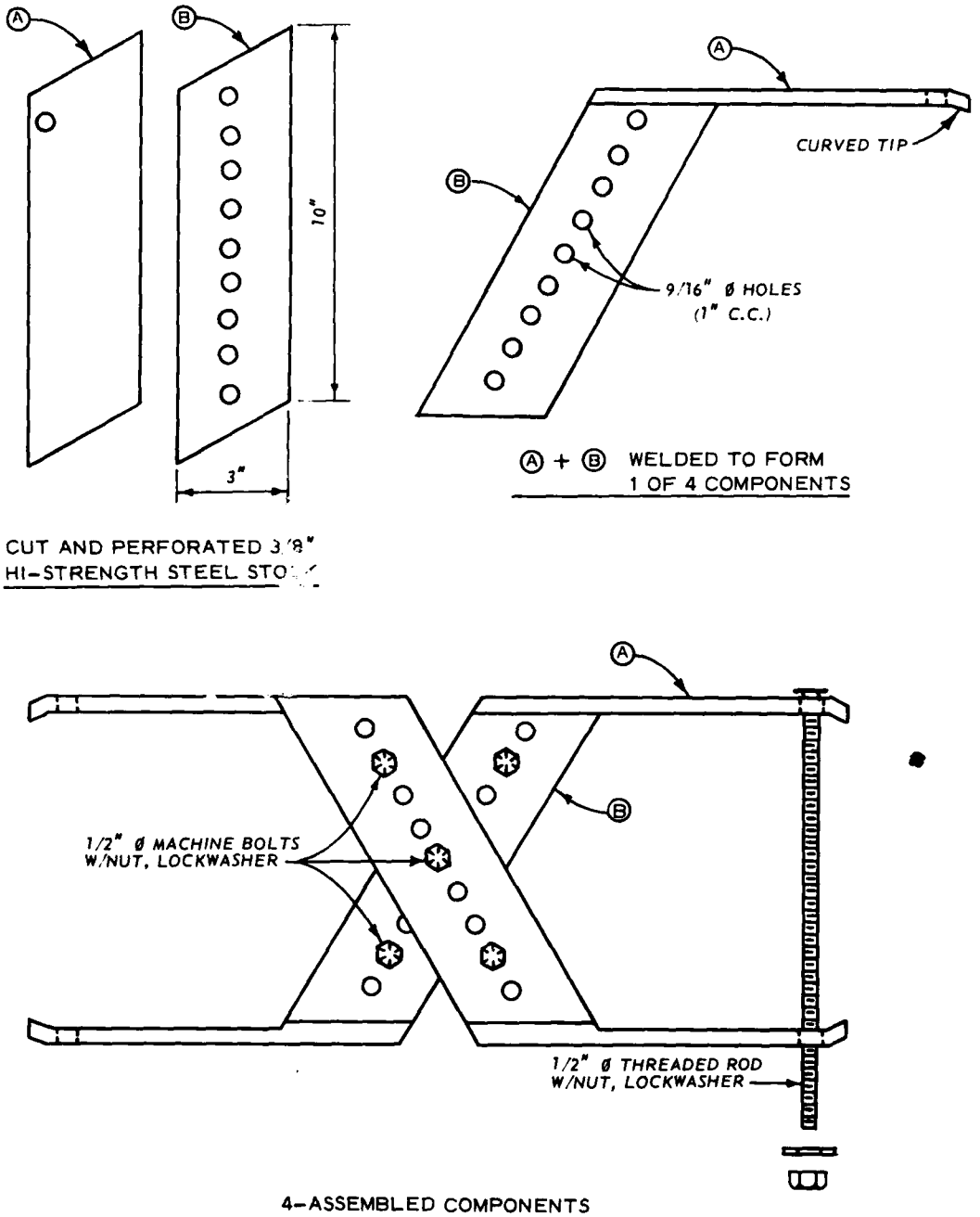

Figure 5. Scissor-type moment transfer device

of polyvinyl chloride (PVC), 20 ft long, were installed in the crater on top of the plastic film (Photo 34). One end of the pipes was capped and the opposite end contained a 45-deg connector and a 4-ft extension added to reach out of the crater and above the limestone. The pipes contained 1/2-in.-wide longitudinal slots spaced throughout the entire 20-ft pipe length. The pipes were placed on 4-ft centers approximately 2.5 ft from the crater edges. One pipe was placed perpendicular to the others beneath the extensions coming out of the crater. For pumping the grout, 27-ft-long flexible rubber hoses with inside diameters of 3 in. were inserted inside the seven PVC pipes until they were 1 ft from the capped end. Approximately 15 in. of open-graded limestone was placed into the crater over the pipes using a front-end loader and a dump truck (Photos 35 and 36). The limestone was spread by a backhoe and by dragging the bucket of a front-end loader (Photos 37 and 38). The limestone was sprayed lightly with water to prevent the grout mixture water from being absorbed by the dry limestone and to facilitate the passage of the fluid grout around the individual particles of limestone (Photo 39). The grout was prepared and pumped under a contract using commercial equipment (Photo 40). The large commercial equipment was used to facilitate construction and would not be available under combat conditions. Ready-mix transit trucks or other means of delivery could be used. The grout that was used in craters 2 and 3 consisted of PCC (Class A), flake calcium chloride, friction reducer, and water. The grout had a density of 117 pcf and contained the following percentages by weight: cement--68 percent, water--31 percent, calcium chloride--1 percent, and a friction reducer--0.2 percent (approximately). The grout was designed to have an unconfined compressive strength of 800 psi minimum after 8 hr of curing time. The grout was very fluid and level seeking and was pumped at the rate of approximately 42-168 gal/min (1-4 barrels/min (one oil field barrel is 42 gal)). The grout flow was 15-20 sec through a flow cone.*

---

* U. S. Army Engineer Waterways Experiment Station, CE. 1980. "Test Method for Flow of Grout Mixtures (Flow-Cone Method)," Handbook for Concrete and Cement, CRD-C 611-80, Vicksburg, Miss.

20. The grout pump was connected to two of the hoses and grout was pumped until it appeared on the surface of the limestone. As the grout began to appear on the surface, the pumps were switched to two other hoses. As the crater filled with grout (Photo 41), the rubber hoses were progressively drawn out of the PVC pipes until the crater was completely filled with grout. The perpendicular pipe was the last one into which grout was pumped. The PVC pipes were then cut off approximately 6 in. below the surface.

21. The crater was screeded using a 28-ft-long box aluminum beam, and the surface was covered with a sheet of polyethylene during curing. There was approximately a 1-hr time lapse from start of grout pumping until the crater was covered.

22. Specimens for flexure and unconfined compressive strength tests were cast during the grouting operations. Eight steel beam molds, 48 in. long, 9 in. wide, and 9 in. deep, were filled with the same crushed limestone aggregate used to fill field test items, and fluid grout was pumped over the rocks through a rubber hose. Seven 10-in.-diam by 20-in.-long steel cylinders were filled in the same manner. Six 6-in.-diam by 12-in.-long cardboard cylinder molds were filled with grout only. The flexure test was performed according to ASTM C 78-75.* The unconfined compressive strength tests were performed according to ASTM C 39-72.** Data on the results of laboratory tests on these specimens are shown in Tables 3-5. The strength versus time relationships for the grouted aggregate are shown in Figure 6.

Crater 3

23. Crater 3 contained two types of moment transfer devices as shown in Figure 4. The northern half of the crater used an undercut construction joint beneath the existing slab to provide a stronger joint

---

* American Society for Testing and Materials. 1978. "Flexural Strength of Concrete (Using Simple Beam with Third-Point Loading), Designation: C 78-75, 1978 Book of ASTM Standards, Part 14, Philadelphia, Pa.

** American Society for Testing and Materials. 1978. "Compressive Strength of Cylindrical Concrete Specimens," Designation: C 39-72, 1978 Book of ASTM Standards, Part 14, Philadelphia, Pa.

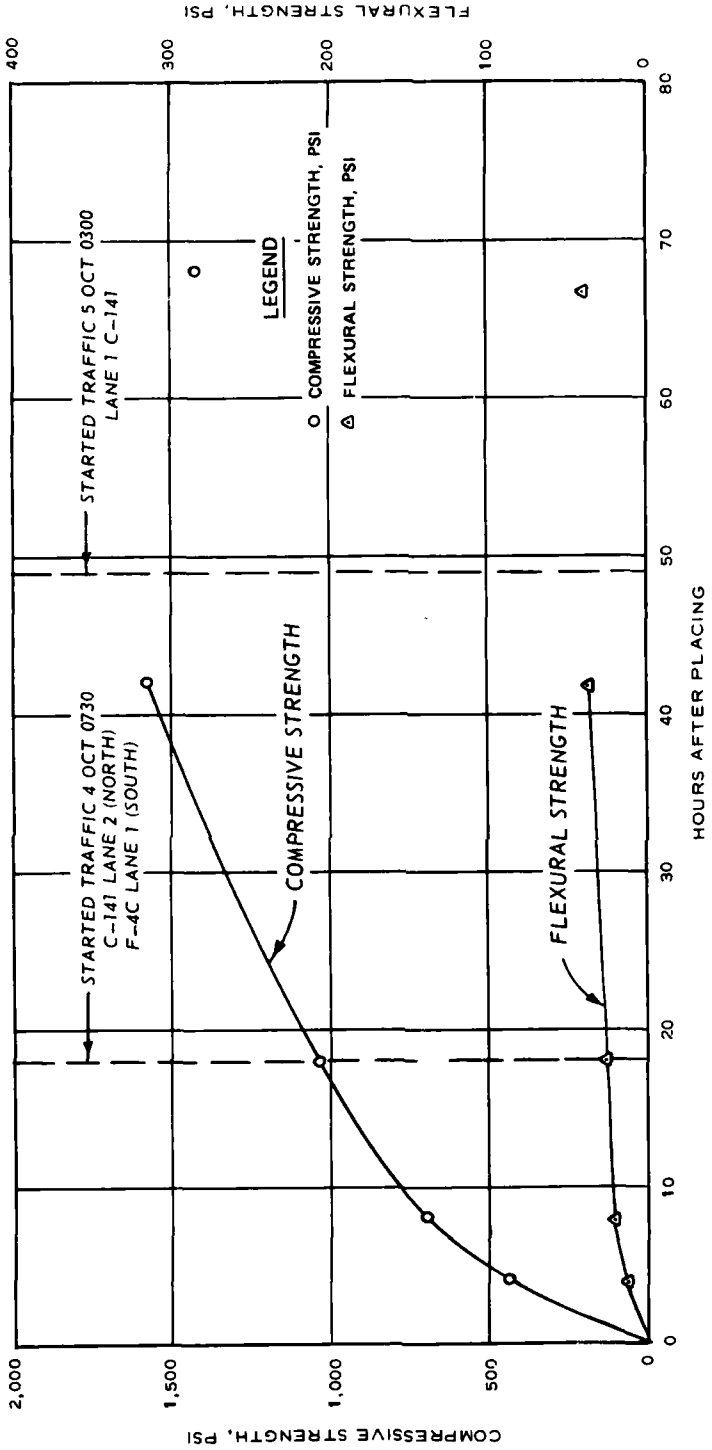

Figure 6. Strength versus time relationship for the grouted craters

directly beneath the intersection of the existing slab and the grout and limestone that was to be placed in the crater. The subgrade under the edge of the existing slab had to be undercut approximately 6 by 6 in. to create a cavity into which the grout could flow. The south half of the crater contained an adjustable flange moment transfer device fabricated from a 1/2-in.-thick steel plate and reinforcement bars welded to the vertical face (Photo 42). A sketch of this device is shown in Figure 7. These devices were placed along the crater edges on 4-ft centers. Again, the purpose of these devices was to allow a continuity between the surrounding concrete slab and the repaired crater. The top 18 in. of crater 3 remained to be filled after placement of the washed gravel in the bottom portion. As in crater 2, sand, dry bentonite, and polyethylene were placed to seal the gravel (Photo 43). Limestone was stockpiled close to the crater and sprayed lightly with water. Next, approximately one-third of the top portion of the crater was filled with grout (Photos 44 and 45). A front-end loader was then used to dump and spread the stockpiled limestone in the crater to within 1 in. of the top surface (Photo 46). The limestone was then compacted with a vibratory steel-wheel roller (Photo 47). Grouting of the crater from the top was then resumed and the grout was hand finished and covered with polyethylene. Total time from start of grouting until covering was approximately 2 hr. The grout mixture in craters 2 and 3 was the same. The flexural and compressive strengths are given in Tables 3-5.

Crater 4

24. After the uniform-graded washed gravel had been placed in the lower portion of the crater, approximately 15 in. remained to be filled. Two types of systems were selected as moment transferring devices. In the north half of the crater, a 6- by 12-in. undercut beneath the existing slab was excavated (Photo 48). For reinforcement, No. 5 steel bars 30 in. long were placed on 18-in. centers. These bars were tied together with 1/2-in. bars. This system was similar to the north half of crater 3 except that steel was added to the undercut in crater 4 for additional strength. The south half of the crater contained 1-in. steel dowels, 16 in. long, placed on 12-in. centers around the vertical face

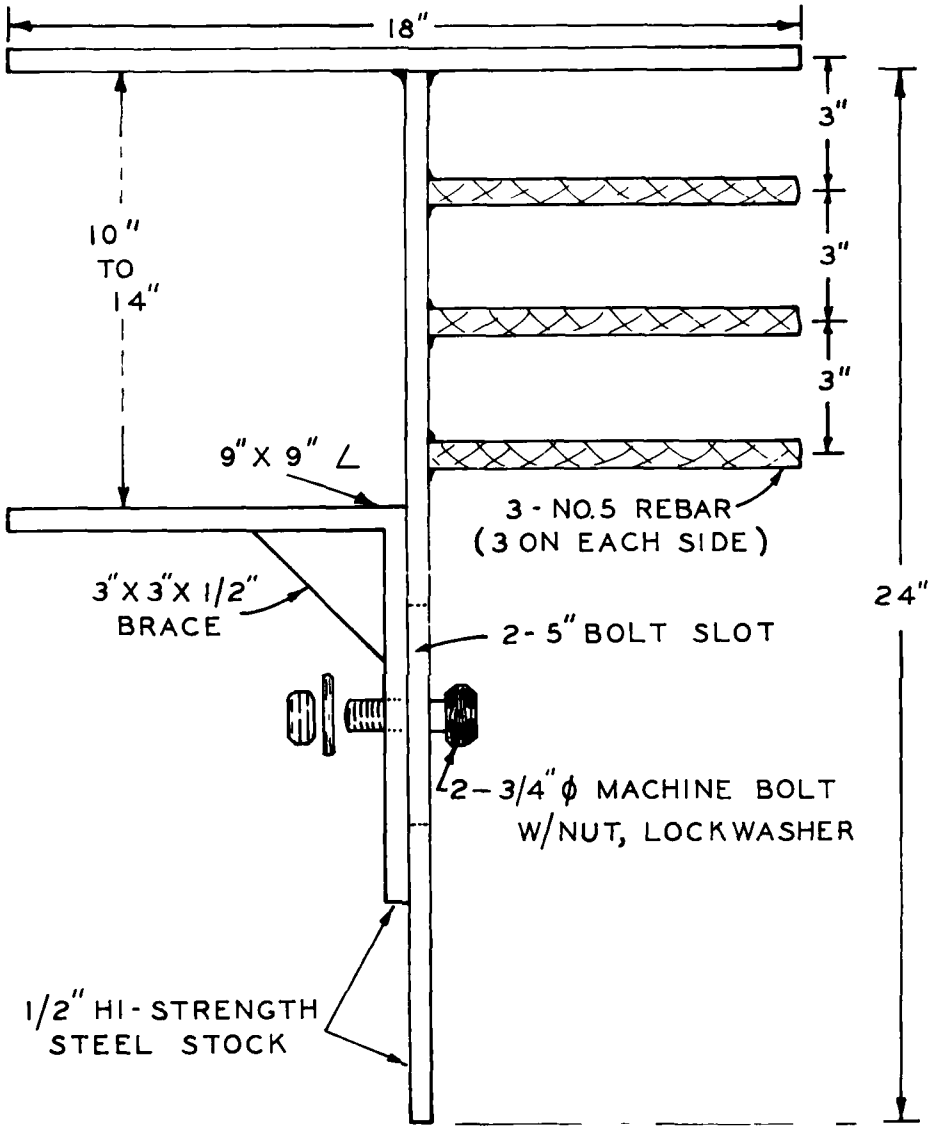

Figure 7. Adjustable flange moment transfer device

of the existing concrete slab at a depth of 6 in. below its top. Holes for the dowels were drilled using an electric roto-core drill mounted on the face of the concrete (Photos 49 and 50). The dowels were inserted 8 in. into the holes and grouted using an epoxy resin mixed with sand. After the grout had set, the exposed 4 in. of the dowels were coated with oil to prevent bonding to the concrete that was to be placed in the crater (Photo 51). The craters were lightly sprayed with water to prevent the gravel from drawing moisture from the concrete. Concrete was placed into the crater directly from the ready-mix trucks (Photo 52). It was spread as necessary by hand and vibrated using internal vibrators. The surface was screeded and finished using a vibrating straightedge, bullfloats, and trowels, followed by a wet burlap drag (Photo 53). The exposed concrete surface was covered with burlap and sprayed with water and then covered with polyethylene to prevent moisture evaporation. The burlap was wet each day as necessary to maintain proper moisture during curing (Photo 54). During the pouring of the concrete, cylinders and beams were made from various batches of concrete for laboratory compressive and flexure tests. The concrete was cured for 24 hr prior to traffic. The results of these tests are presented in Table 6.

Crater 5

25. Crater 5 was very similar to crater 4 in that it was initially backfilled to within 15 in. of the top and was then filled with ready-mix concrete. The moment transfer devices were also the same. The difference in the two craters was that the lower portion of crater 5 was backfilled with a mixture of lean clay and rubble rather than washed gravel (Photo 55) to simulate compaction applied by troops in the field. The material selected was chosen to be more nearly like the concrete rubble that would be available at an actual crater site in the field in the event washed gravel was not available. The top 15 in. was filled with concrete as previously described for crater 4 (Photo 56). Compressive and flexural strengths are shown in Table 6.

Crater 6

26. Crater 6 was a conventional AC repair consisting of 3 in. of AC over 9 in. of dense graded crushed limestone. The limestone was

placed in two lifts over the washed gravel. A front-end loader was used to place and spread the limestone (Photo 57). The first lift was rolled with 8 coverages of a vibratory steel-wheel roller (Photo 58) and 12 coverages of a 110,000-lb pneumatic-tired roller with four tires inflated to 90-psi pressure (Photo 59). The second lift was rolled with 16 coverages of each roller. Dry density, CBR, and water content data are given in Table 2. A prime coat of SS-1 was applied at 0.5 gal/sq yd (Photo 60). The AC was dumped into the crater from dump trucks (Photo 61) and spread with a motor grader (Photo 62). The AC was rolled with a vibratory steel-wheel roller (Photo 63) and a 50,000-lb self-propelled roller with rubber tires inflated to a pressure of 90 psi. There were eight coverages with each roller. The density of the AC was 139.8 pcf.

PART IV: TRAFFICKING ON TEST SITE

Lane Descriptions

27. Two parallel traffic lanes were established on the test section to allow concurrent traffic on both the north and south sides of the craters. Guidelines were painted on the sections to assist the operator in maneuvering the load carts along the test section. These were supplemented by metal poles placed at one end of the section to provide a visual reference guide to the operators while backing the load carts. An aerial view of the test section with the C-141 test cart positioned in lane 1 between craters 3 and 4 is shown in Photo 64. Figure 1 shows the location of traffic lanes with respect to the test craters and the overall test section.

Types of Data Recorded

28. Foundation material densities, water contents, in-place CBR's, and plate bearing measurements were taken before and after traffic at representative locations. Cross sections and profiles of the traffic lanes and craters were taken prior to, during, and after the completion of traffic. Visual observations of the surfaces of the craters, crater behavior, and the surface of the slabs encompassing the craters were made and recorded throughout the periods of traffic and were supplemented by photographs.

Application of Traffic

29. Traffic on the test section was distributed across the width of the traffic lanes in a manner that would represent the actual traffic distribution on a runway. Under normal aircraft operations, traffic on a runway is distributed following a normal distribution curve. This type distribution was simulated for the C-141 and F-4C traffic using the distribution shown in Figure 8. These distributions provide for the

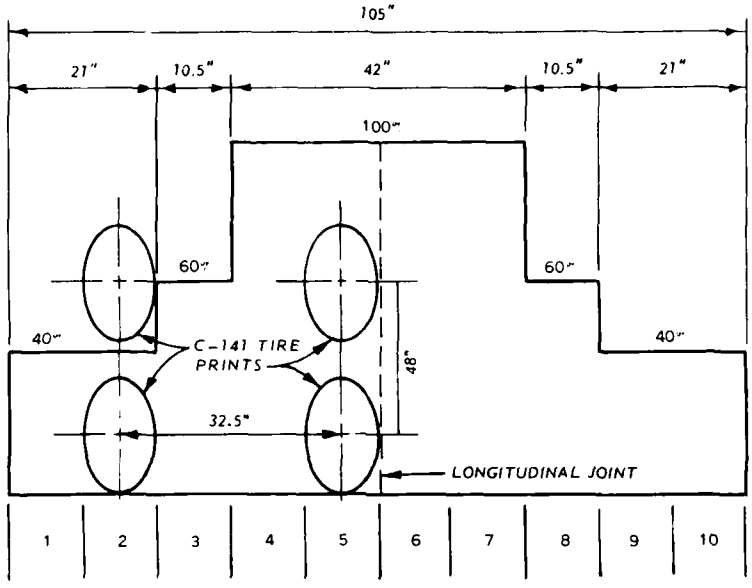

C-141 TRAFFIC PATTERN

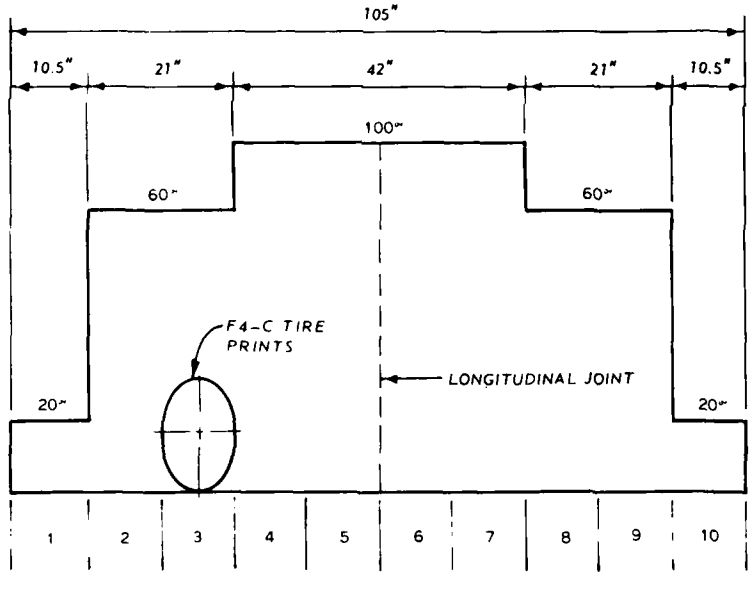

F-4C TRAFFIC PATTERN

Figure 8. Traffic distribution

majority of the traffic to occur in the central portions of the traffic lane with lesser amounts of traffic on the outer edges of the traffic lane. Shown on this plot is the number of passes of the load cart applied to the indicated width of the traffic lane expressed as a percent of the number of passes applied to the center of the traffic lane. The space between traffic lines represents the tire print width and location of individual tire passes. Profiles of the center of traffic lanes 1 and 2 are shown in Figures 9 and 10, respectively.

30. An overall view of the test section showing the F-4C and C-141 load carts operating in lanes 1 and 2, respectively, is shown in Photo 65. To accelerate the traffic testing, the two traffic lanes were laid out on the test section to allow simultaneous testing. The center line of lane 1 was located so as to coincide with the southern edge of the craters, and the center line of lane 2 coincided with the northern edge. This allowed for meandering of the load wheels both along and on either side of the joint as well as allowing the entire gear to be supported by both the repaired crater and the unrepaired pavement. Initially, 760 passes of the F-4C load cart were applied to lane 1 followed by 4692 passes of the C-141 load cart. Traffic was resumed after 4 months with the C-141 loading and an additional 408 passes were applied. This resulted in a total of 760 passes of the F-4C loading and 5100 passes of the C-141 loading on lane 1. Only the C-141 load cart was used to traffic lane 2 with 3400 passes being applied initially, followed by an additional 1700 passes applied after the 4-month weathering period. This resulted in a total of 5100 passes of the C-141 load cart on lane 2. After the F-4C traffic was completed, the C-141 load cart was alternated between lanes 1 and 2 at various pass levels to keep the coverage levels similar with respect to each day's traffic. Behavior of each of the craters during traffic is discussed in the following paragraphs.

Crater 1, lane 1

31. The condition of the portion of crater 1 that was in lane 1 is shown in Photo 66 prior to traffic. As indicated in the photograph, the center line of the 105-in.-wide traffic lane coincides with the

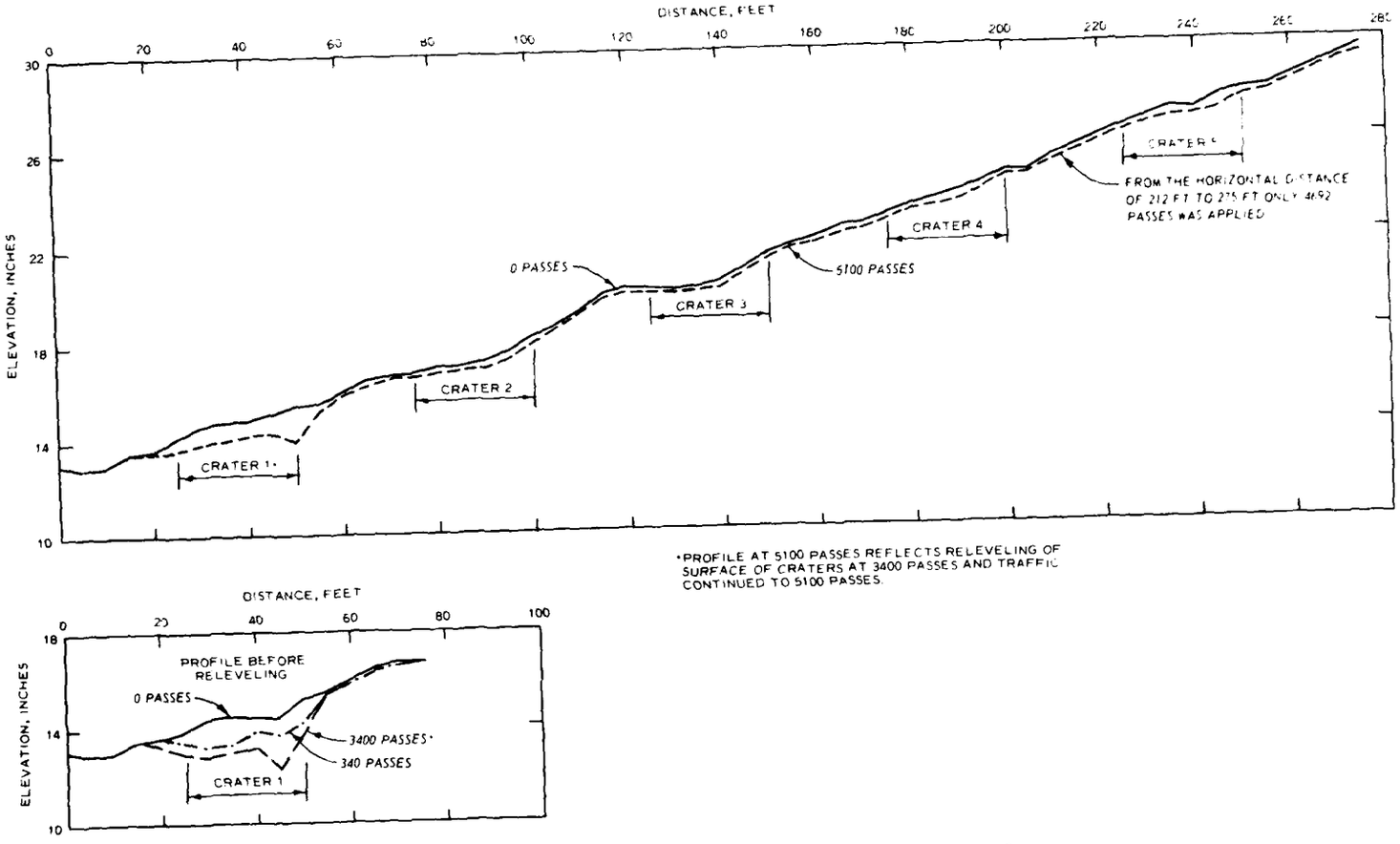

Figure 9. Profile of center of traffic lane 1

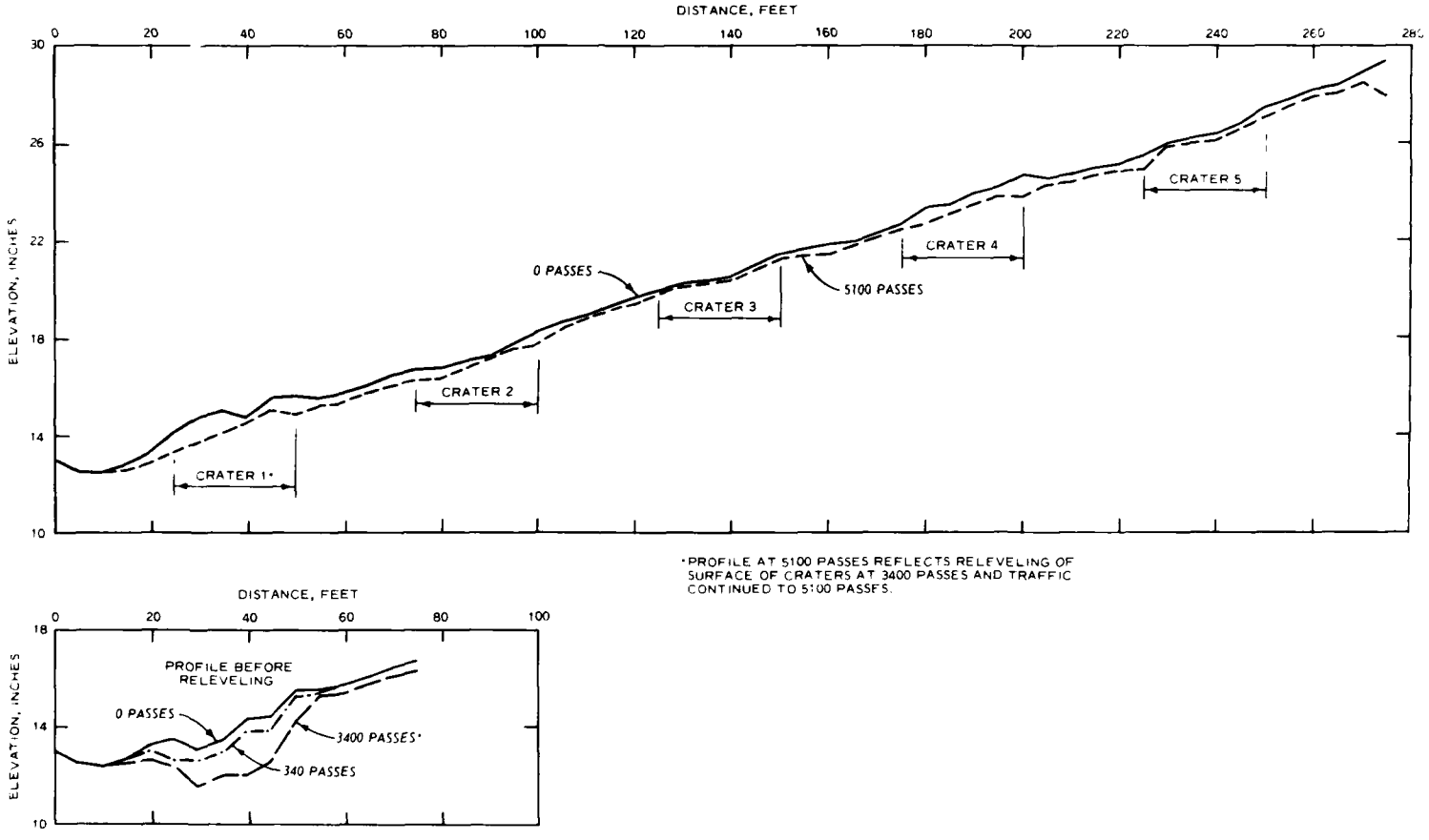

Figure 10. Profile of center of traffic lane 2

joint between the repaired crater and the existing pavement. The initial traffic was applied with the F-4C load cart for the first 760 passes. Of this total, the last 240 passes were applied in the rain. As expected, the F-4C loading caused some densification of the limestone and some limestone was displaced by traffic during the rain. At the completion of 380 passes, the average rut depth was 1.5 in. (Photo 67). After 760 passes of the F-4C load cart, traffic was applied using the C-141 load cart. Only minor densification was noted due to the additional loading imposed by the heavier C-141 loading. After 1020 passes of C-141 traffic, the surface of the limestone appeared to be in good condition (Photo 68). Additional traffic was placed with the C-141 cart under normal weather conditions, including some rainfall, and after 3400 passes, a rut depth of 2.1 in. could be measured in the limestone adjacent to the asphalt pavement (Photo 69).

32. After 3400 C-141 passes of traffic on crater 1, additional limestone was added and the surface releveled. This was considered to be normal maintenance that would occur in the field and would prevent ponding of rainwater and ultimately prevent further breakdown and weakening of the subgrade. The limestone material was transported and spread using a front-end loader (Photo 70). The material was rolled with 24 coverages of the pneumatic-tired roller loaded to 110,000 lb with four tires inflated to 90-psi pressure (Photo 71). After compaction, the surface of the crater was level with the surrounding pavement (Photo 72). Traffic was continued to 4692 passes (plus 760 passes of the F-4C load cart). The average rut depth was approximately 0.6 in. (Photo 73). The crater repair was performing satisfactorily at this time with only the loose limestone aggregate on the surface presenting any problem. Traffic was resumed after 4 months and continued to 5100 passes. The only visible change was a small amount of limestone displaced during traffic. The average rut depth had increased to 0.75 in. when measured from a 10-ft straightedge (Photo 74). This densification would be expected after this amount of traffic indicating some routine maintenance would be required to maintain a smooth surface during operations. The cross sections indicate some subgrade

consolidation as shown on Figure 11. No abnormal ruts were present at the completion of traffic. This is also evident in the profile of lane 1 (Figure 9).

Crater 1, lane 2

33. Simulated C-141 traffic was initiated on the north portion of crater 1 in lane 2 while F-4C traffic was being applied to the south portion of crater 1 in lane 1. The surface of the crater was relatively smooth prior to the start of traffic (Photo 75). Initially, there was some densification of the limestone and some of the limestone fines were displaced due to rainfall which occurred during traffic. The measured rut depth after 510 passes of traffic was 2.2 in. Although the surface was showing the effects of traffic, the problems were not significant (Photo 76). Traffic continued to 1700 passes and the crater gave no indication of stress and continued to perform satisfactorily (Photo 77). Traffic with the C-141 load cart was continued to 3400 passes and, other than the average rut depth increasing to 2.5 in., no other problem areas developed (Photo 78). The cross-section and profile measurements showed some densification of the limestone in the repaired crater, but this was considered minor for the number of passes and gross weight of 144,000 lb on the load cart.

34. One drawback in using this method of repair is the presence of loose limestone aggregate that could be a potential hazard to jet engine ingestion and to metal skins on the aircraft. One possible solution considered in this test was the use of an asphalt-covered fabric which could be placed by hand over the limestone (Photo 79). Some rolling was required to cause the material to adhere to the crater surface (Photo 80). This type material was applied to the portion of crater 1 that included lane 2 (Photo 81). The fabric used in this investigation was a commercially available item and consisted of an 8-oz needle-punched polyester material with each side treated with 0.4 gal of asphalt (AC-10) per sq yd. The material was rolled after placement with a half-ton truck and with the self-propelled rubber-tired roller with a gross weight of 50,000 lb in an attempt to bond the material to the limestone surface. The temperature was cool when the fabric was placed

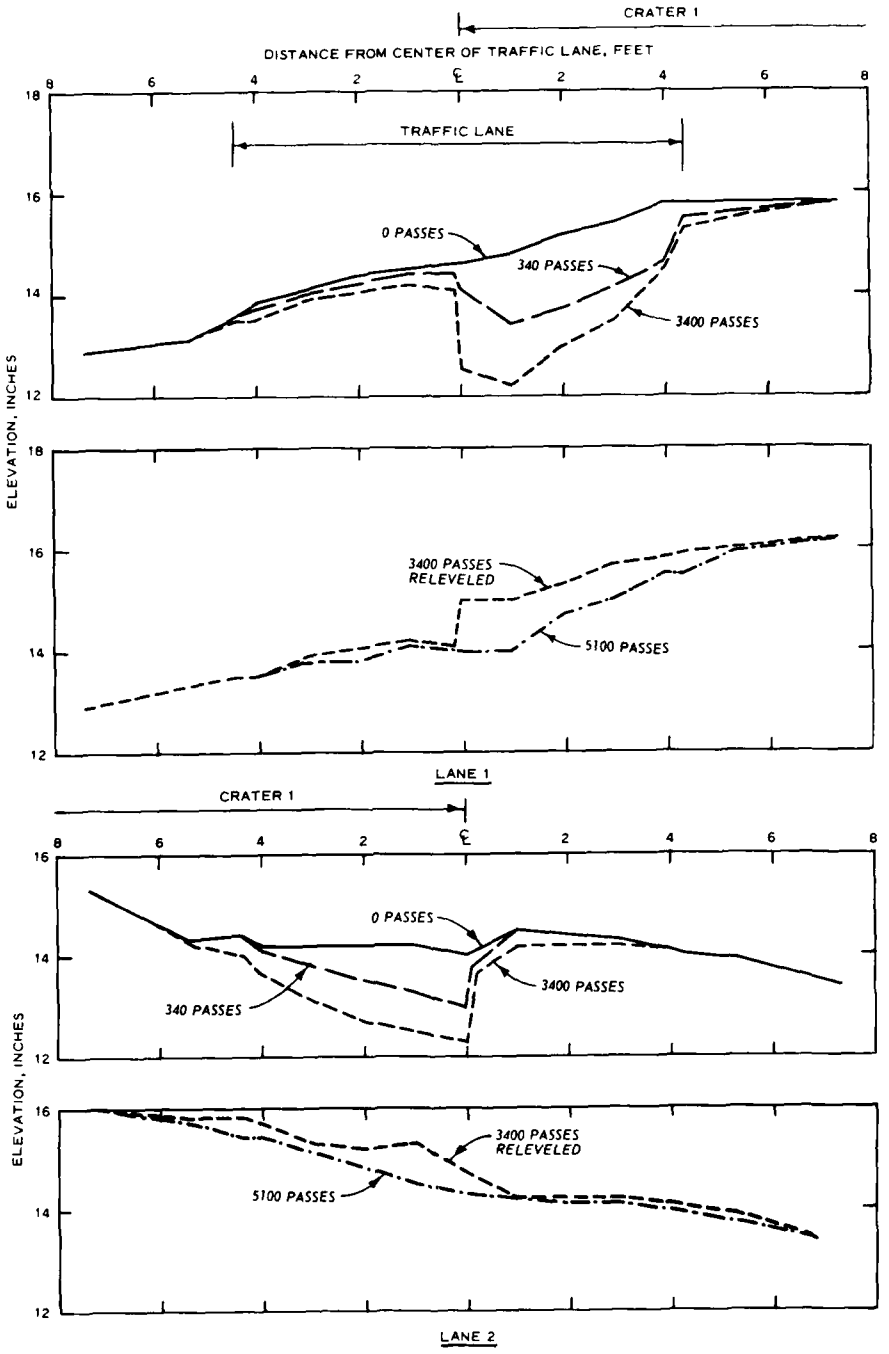

Figure 11. Cross section of crater 1 repair

and it was exposed to the cold and wet climate for 4 months before traffic was resumed. During the initial 10 passes of traffic, the drive wheels of the load cart caused the bond between the fabric and limestone surfaces to fail and wrinkles developed in the fabric (Photo 82). The individual pieces of limestone began to penetrate the film in several places (Photo 83). Moisture was found to be present beneath the fabric and there was little bond to keep the fabric in place. Therefore, the fabric was removed at the completion of 10 passes of traffic. As traffic continued to 5100 total passes with the C-141 load cart, some limestone was displaced due to traffic operations and due to rainfall. The average rut depth had increased to 0.5 in. at the completion of traffic (Photo 84). Figure 11 shows cross sections indicating some densification in the repaired crater. This is also evident in the profile of lane 2 (Figure 10).

Crater 2, lane 1

35. To simulate the actual conditions that would exist in the field in a bomb crater situation, plans were to begin traffic on the crater within 24 hr after repair. The surface condition of repaired crater 2 was relatively smooth immediately after grout placement with some free water standing in low areas (Photo 85). Traffic in lane 1 with the F-4C load cart was begun within 16 hr after the completion of the grouting. The surface of the crater contained numerous shrinkage cracks at this time after the 16-hr curing period. Traffic of the F-4C load cart continued to 760 passes with no apparent damage. After a time lapse of 43 hr following the placement of the grout, the C-141 load cart was used to apply traffic. After 340 passes of the C-141 load cart and 88 hr of curing time, the shrinkage cracks were becoming more pronounced. The larger cracks, which were felt to be load related, were painted white for location purposes and for later comparisons (Photo 86). Both corner breaks and transverse cracks were visible in addition to a slight amount of spalling along the edge of the crater repair. As traffic progressed through 1020 passes, the spalling increased and some of the corner breaks and transverse cracks became more pronounced (Photo 87). However, after 1700 passes there were no additional corner breaks or

cracks, but there was visible spalling over the moment transfer devices (Photo 88). There was some progression of existing corner breaks and spalling in these areas and along the crater joints after 3400 passes of the C-141 load cart (Photo 89). Spalling was the most visible indication of the effect of the prolonged traffic after 4692 passes of C-141 traffic (in addition to 760 passes of the F-4C load cart). A view of the portion of crater 2 located in lane 1 is shown in Photo 90. No structural damage to the repair that would have any effect on traffic was observed at this time. After the 4-month delay, traffic was resumed and an additional 408 passes of C-141 traffic was applied, resulting in a total of 5100 passes of the C-141 load cart. The additional traffic caused no new corner breaks and only a small amount of spalling occurred at the crater edges (Photo 91). The repair method was considered satisfactory from a performance viewpoint. Cross sections of crater 2 are shown in Figure 12. A profile of crater 2, lane 1, is presented in Figure 9.

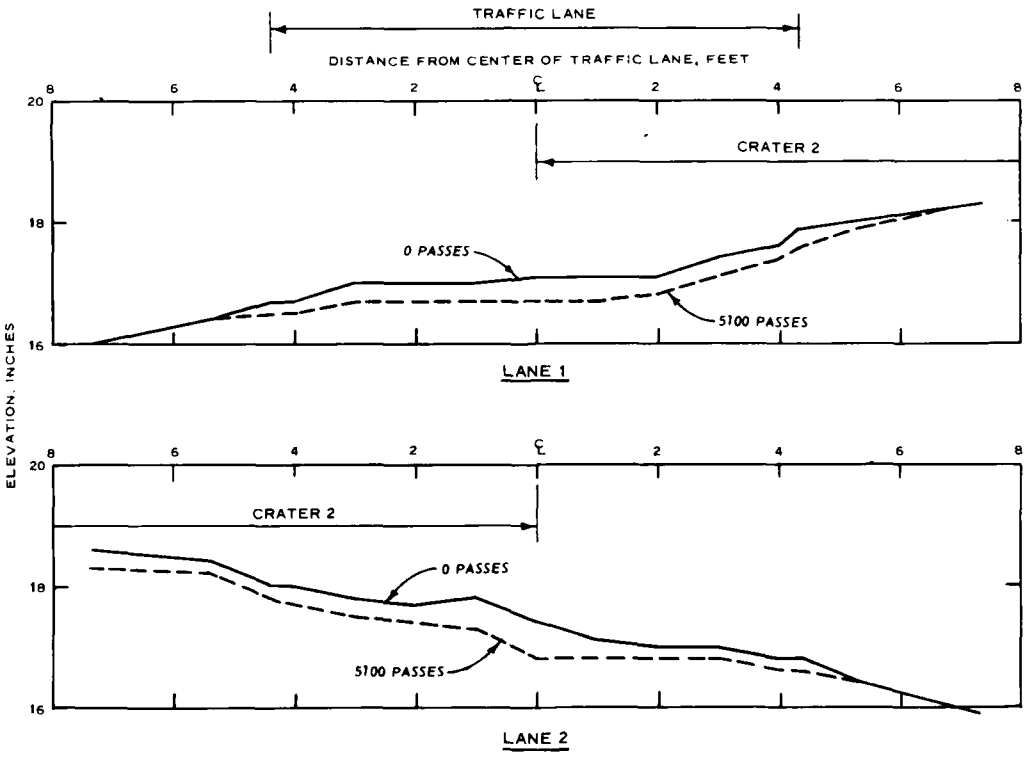

Figure 12. Cross section of crater 2 repair

Crater 2, lane 2

36. After placement of the grout in crater 2, the surface in lane 2 was not completely smooth and small water-filled depressions were visible (Photo 92). The traffic with the C-141 load cart was begun within 16 hr after grout placement. Again, small shrinkage cracks had developed prior to the start of traffic. Corner breaks were observed at both corners of the repair in the traffic lane after 340 passes of the C-141 load cart, and after 510 passes (45-hr curing time) the edges of the crater repair and the hairline curing cracks were starting to spall (Photo 93). With no additional traffic and after 88 total hours curing time, shrinkage caused more corner breaks and transverse cracks to develop. These were painted white for identification and future reference (Photo 94). Due to the shrinkage breaks occurring in this manner, it was difficult to accurately determine which cracks were load related. After 1700 passes of the C-141 loading, spalling at the corners of the repair continued but the breaks did not seem to have increased (Photo 95). As traffic continued up through 3400 passes, the crater repair continued to perform well with no major increases occurring in the breaks. Spalling along the joints and at the corner did not significantly increase with the progression of traffic (Photo 96). As traffic with the C-141 load cart continued to 5100 passes, there was an increase in spalling along the crater edges. This apparently was caused by the method used in filling the crater in which the grout was pumped into the crater in several lifts. This possibly resulted in thin layers of grout as the material began to set rather rapidly during construction. No major breaks developed other than the spalling which was localized near the joints (Photo 97). The profile and cross section of this crater in lane 2 showed only minor changes after traffic (Figures 10 and 12).

Crater 3, lane 1

37. After placement of the grout in crater 3, the hairline shrinkage cracks began to appear. Photo 98 shows a view of lane 1 prior to traffic, approximately 30 min after grout placement. F-4C traffic was begun within 16 hr after grout placement, and 760 passes of the load cart were applied. No apparent damage was caused by this traffic.

Within 48 hr after grout placement and after the F-4C traffic, C-141 traffic was begun. Corner breaks in each corner of the crater repair were first noted after 80 passes of the C-141 load cart. After 1020 passes of traffic, the southwest corner still had one corner break and the southeast corner contained two. As traffic increased to 1700 passes, spalling began to develop and the corner breaks were still quite evident. The main corner breaks were painted for identification (Photo 99). After 3400 passes of traffic, two additional corner breaks were evident and spalling was increased along the crater joints and over the moment transfer devices (Photo 100). Spalling was greatly increased after 4692 passes of C-141 traffic (plus the initial 760 passes of F-4C traffic), but there was no increase in the number or size of the corner breaks (Photo 101). From 4692 passes to 5100 passes only a slight amount of spalling took place, and no new breaks occurred in the crater surface. An overall view of the crater at the completion of traffic showing the repaired test pit is shown in Photo 102. Profiles and cross sections of the portion of crater 3 in lane 1 showed no major changes in the repair other than minor densification of the overall repair (Figures 9 and 13).

Crater 3, lane 2

38. Traffic was started within 16 hr after grout placement using the C-141 load cart (Photo 103). The initial signs of stress in the repair were in the form of spalling and a crack in the northeast section of the repair. A view of this is shown in Photo 104 after 510 passes of traffic. Breaks and spalling at each corner and along the joint were occurring through 1700 passes and the breaks were painted white for identification (Photo 105). After 3400 passes, spalling increased along the edges of the crater repair (Photo 106). However, no major problems had developed. As traffic was continued in lane 2 to a total of 5100 passes, spalling along the crater joint increased and some of the pieces breaking out were up to 1 in. in diameter. This was thought to be caused by the layered method in which the grout cap was placed in the crater. Apparently this caused no major structural problems other than creating an irregular roughened surface along the joints (Photo 107).

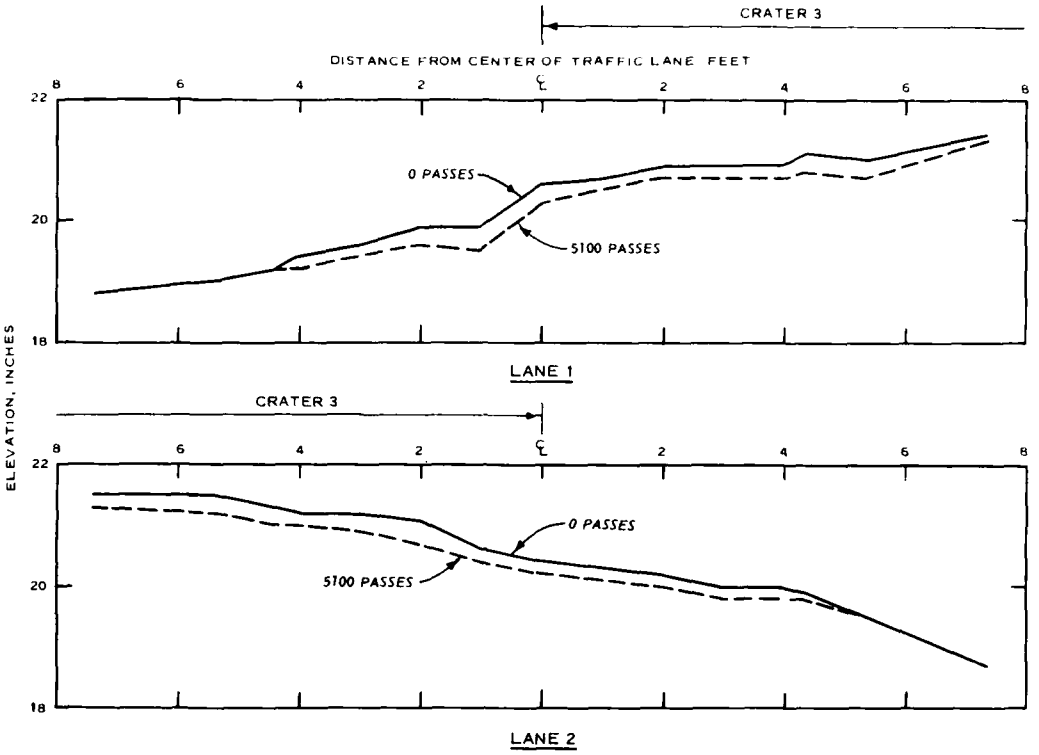

Figure 13. Cross section of crater 3 repair

Profiles and cross sections showed only densifications occurring in the crater repairs (Figures 10 and 13).

Crater 4, lane 1

39. Crater 4 contained conventional PCC in the top portion of the crater. The concrete surface was relatively smooth and had been allowed to cure for 7 days after placement (Photo 108). The initial traffic with the F-4C load cart caused no apparent damage after 760 passes. F-4C traffic was followed on the eighth day after placement by traffic with the C-141 load cart. After 544 passes of the C-141 load cart, one long corner break was observed in the southwest portion of the crater. The break was painted white and is shown after 680 passes of traffic in Photo 109. After 782 passes of C-141 traffic, a crack was observed in the southeast portion of the crater and joined the other cracks and corner break. This condition is shown in Photo 110 after 1020 passes of traffic. Although no new breaks occurred after this time, spalling

began to develop along the edges of the crater and in one of the cracks. An overall view of this condition is shown after 4692 passes (Photo 111). Traffic was continued up to 5100 passes and no additional damage was observed in the crater surface. The surface was relatively smooth and free from any major spalling (Photo 112). Both the profile and cross-section measurements showed only minor consolidation after traffic (Figures 9 and 14).

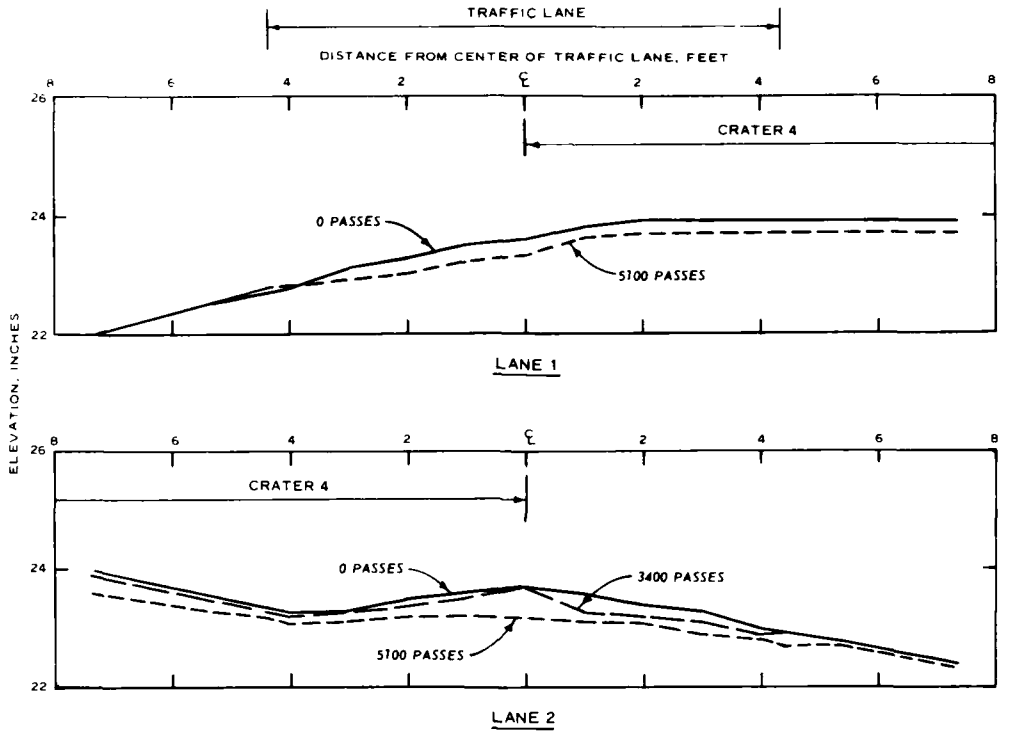

Figure 14. Cross section of crater 4 repair

Crater 4, lane 2

40. As in lane 1 of crater 4, traffic was applied to lane 2 within 7 days after placement of the PCC. The crater was not as level prior to traffic as some of the other repairs, but this was considered to be typical of a field-repaired crater (Photo 113). The C-141 load cart was used for testing. After 1020 passes of traffic, no apparent damage was evident other than some minor spalling (Photo 114). After 3400 passes of the C-141 loading cart, there were no apparent cracks or

corner breaks in the repair and spalling at the crater edges was considered minimal (Photo 115). Traffic was continued with the C-141 load cart to 5100 total passes. At 3842 passes, a transverse crack developed in the concrete surface but caused no problem. A view of the crater at the completion of traffic is shown in Photo 116. Only a small amount of spalling occurred in the crater. Thus, this type repair and the moment transfer device used were considered to be quite successful. The profile and cross-section measurements showed no major changes after 5100 passes of the C-141 load cart (Figures 10 and 14).

Crater 5, lane 1

41. Crater 5 contained a conventional PCC repair at the top surface; however, the bottom portion of the repair contained the lean clay and rubble. The concrete repair patch was slightly irregular and resulted in the top surface being somewhat higher than the adjacent surface (Photo 117). The F-4C traffic was applied within 7 days after concrete placement and 760 passes of traffic caused no visible damage. The C-141 traffic followed and after 544 passes of the C-141 load cart, a corner break was observed in the southeast corner of the repair. After 680 passes, the break had opened slightly and was painted white for identification (Photo 118). Two corner breaks developed after 1428 passes of traffic with one in each corner of the portion of lane 1 in crater 5. As traffic was continued to 3400 passes, some spalling began to occur along the construction joints and one corner and there was a further increase in corner breaks (Photo 119). The profile and cross section showed very little change due to traffic and the repair performed quite well (Figures 9 and 15). After 4692 passes of the C-141 load cart, no further breaks had occurred, although spalling had increased but presented no major problems (Photo 120). At this time a test pit was made, repaired, and the test craters allowed to weather for 4 months. After 4 months, however, traffic could not be resumed due to the weakness of the repair and the wet subgrade beneath the repair. Thus, traffic was not resumed in lane 1 on crater 5.

Crater 5, lane 2

42. After placement of concrete in the top portion of crater 5,

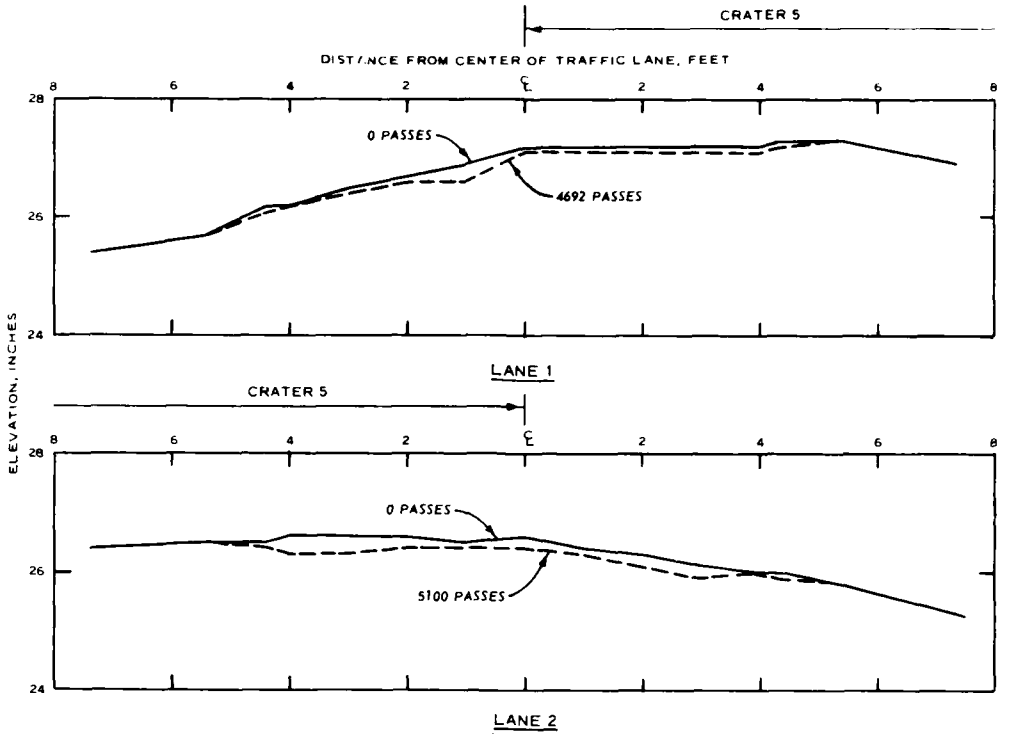

Figure 15. Cross section of crater 5 repairs

the joint between the asphalt and concrete along the center line of the traffic lane was slightly high in elevation (Photo 121). Otherwise, the repair was relatively smooth. The C-141 traffic was initiated on this lane days 7 after concrete placement. Generally, there were no major corner breaks in this crater along lane 2 and only a minor amount of spalling occurred along the joint after 1020 passes (Photo 122). Traffic was continued with the C-141 load cart through 3400 passes, including periods of rainfall, and no major corner breaks or cracks were observed (Photo 123). Spalling continued to occur along the repair joints, but presented no problems. After 4 months, traffic was resumed. While trafficking with the C-141 load cart during a period of rainfall, a small amount of subgrade material was pumped up from the northwestern corner of the crater after 3876 passes (Photo 124). The pumping was continued for approximately 24 hr after the rainfall had stopped, which was after 4928 passes of the load cart. Only one transverse crack had

occurred after 5100 passes of traffic and only minor spalling was evident (Photo 125). A test pit in this area revealed a hairline crack in a concrete moment transfer device near the crater face which allowed the pumping of subgrade material. Otherwise, the moment transfer appeared to have no other structural damage. Profile and cross-section data indicated very little change in elevation (Figures 10 and 15).

Crater 6, lane 2

43. Crater 6 was a conventional AC repair located only in lane 2. Photo 126 shows crater 6 immediately prior to traffic. A total of 5100 passes of the C-141 load cart was applied to this repair. Densification occurred in the crater under traffic. A 10-ft straightedge was used to measure an average deformation of 0.5 in. after 1020 passes (Photo 127). As traffic continued, this deformation increased to 1.2 in. after 3400 passes. At this pass level longitudinal fatigue cracks had developed in the AC pavement section (the entire length of the section) in which the crater had been placed; however, they were just starting to develop in the AC crater repair (Photo 128). A test pit was run at this pass level. CBR and density data obtained in crater 6 are listed in Table 2.

44. After a 4-month delay traffic was continued. The longitudinal cracks did not increase in length. After 5100 passes the average deformation was 1.25 in. The condition of the crater after 5100 passes and also the repair made at 3400 passes is shown in Photo 129. A cross section of crater 6 repair is presented in Figure 16.

Performance of Slabs Encompassing Craters

45. The concrete, upon curing, developed some minor cracks. The south lane contained transverse cracks with one slab, No. 28, containing a corner crack (Figure 17). All slabs in the center section contained transverse cracks, and three contained longitudinal cracks. Seven of the slabs in the north lane contained transverse cracks and two of these also contained longitudinal cracks. In some instances, the transverse cracks continued across two or even three slabs in a seemingly continuous line. All cracks were considered to be shrinkage cracks.

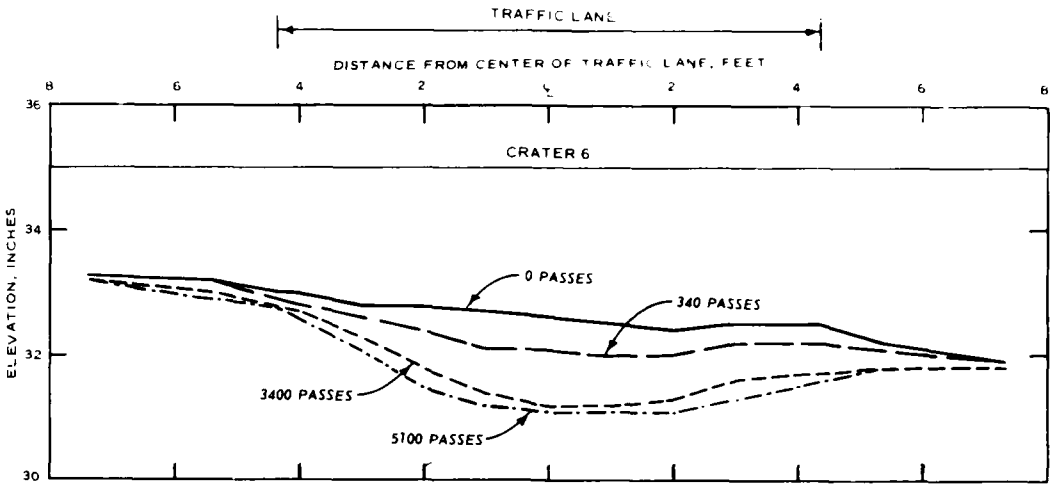

Figure 16. Cross section of crater 6 repair

46. Although all three of the main concrete slabs, which include the 28 individual slabs, received heavy traffic, no reflective cracking was evident in lane 1. Traffic lane 1 received 760 passes of the F-4C loading and 5100 additional passes of the C-141 loading. The tie bars were very effective along the construction joint as a moment transfer device in holding the two main slabs together. The main breaks that had occurred during the progression of traffic are shown in Figure 18. Cracking in lane 1 occurred primarily around crater 1 (Photo 130). None of the structural cracks in lane 2 were considered major.

47. Lane 2 received a total of 5100 passes of C-141 traffic. Reflective cracking was evident in the asphalt overlay above the longitudinal-keyed construction joint in the concrete (Photo 131). After 2856 passes of traffic, reflective cracking indicated that both corner breaks and a keyed joint failure had occurred in slabs 26 and 27 (Photo 132). A cored sample removed from the key joint area shows the failed key joint (Photo 133). Slabs 26 and 27 were located near the end of the test section adjacent to the flexible pavement section and it is believed this contributed to the failures in the concrete since there was densification of the flexible pavement during traffic. Due to this densification the flexible pavement section had a difference in surface

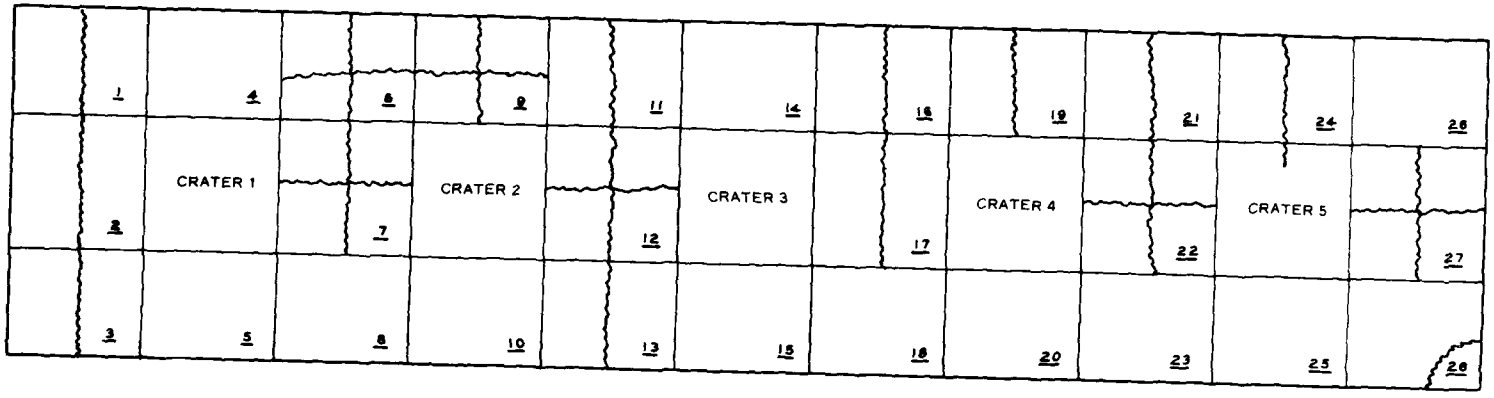

Figure 17. Cracks in concrete prior to asphalt overlay

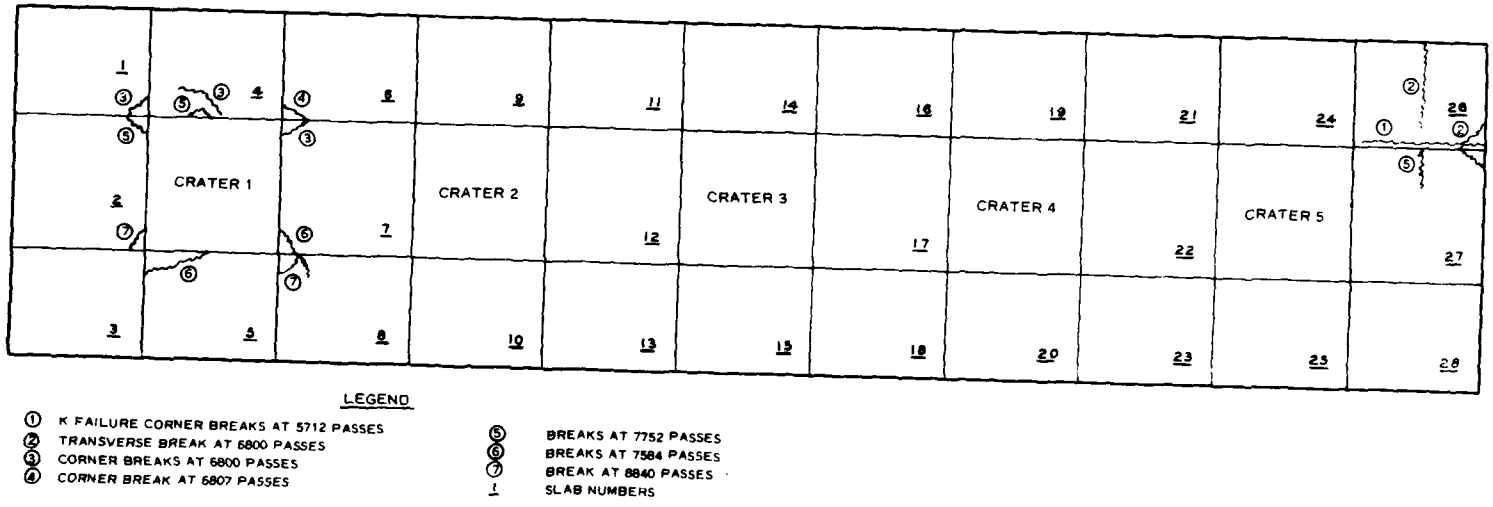

Figure 18. Breaks in asphalt-overlay pavement

elevation and thus problems arose as the load wheels tended to "ramp-up" onto the concrete slabs in the vicinity of crater 1 after 3400 passes of traffic. Also, transverse cracks developed in slabs 26 and 27. Probably the unevenness of the loose limestone in crater 1 contributed to the corner breaks and cracks around this crater by causing load shifting as the load wheels passed over the crater surface. However, after 5100 passes of traffic, there were no major cracks in the surface pavement due to traffic.

PART V: SUMMARY AND CONCLUSIONS

48. A summary of performance is shown in Table 7. All items tested performed satisfactorily, although the crushed stone items would require some maintenance and the AC section did experience densification. The crushed stone should have only accepted 1800 passes but in actuality 5100 passes were placed. The gravity grout and crushed stone method performed beyond required coverage levels and seem to be high candidate material systems for further research.

BIBLIOGRAPHY

Anderson, R., and Ames, T. S. 1968 (May). "Utilization of Fast-Fix Concrete for Rapid Repair of Mortar and Rocket Damaged Runways," AFAPL-TR-68-55, Western Co., Richardson, Tex.

Baird, G. T. 1976 (Mar). "Evaluation of Substitute Input for NCEL Bomb Damage Repair Code," AFCEC-TR-76-4, Civil Engineering Research Center, University of New Mexico, Kirtland AFB, N. Mex.

Baker, W. E., and Westine, P. S. 1973. Similarity Methods in Engineering Dynamics, Hayden Book Co., Rochelle Park, N. J.

Barber, V., Green, H., and Hammitt, G. M. 1979 (May). Airfield Damage Repair, Field Reference Doc, U. S. Army Engineer Waterways Experiment Station, CE, Vicksburg, Miss.

Beal, G. D., and Chandler, R. W. 1971 (Oct). "Rapid Repair and Construction with Fast-Fix Cements," AFWL-TR-71-42, Western Co., Richardson, Tex.

Bell, R. L. 1975 (Feb). "Rapid Runway Repair...A Civil Engineering Mission," Air Force Civil Engineer, Air Force Institute of Technology.

Brooks, G. W., and Davis, H. L. 1974 (Sep). "Development of a Concrete Runway Penetrator Munition - Simulated Runway Static Tests," AMD-ANA10408011-006, Martin Marietta Corp., Orlando, Fla.

Brooks, G. W., et al. 1975 (Oct). "Bomb-Damage Repair Damage Prediction," AFCEC-TR-75-24, Martin Marietta Corp., Orlando, Fla.

Buckingham, E. 1914 (Oct). "On Physically Similar Systems; Illustrations of the Use of Dimensional Equations," Physical Review, Series II-4.

Bussone, P. S., Bottomely, B. J., and Hoff, G. C. 1972 (Jun). "Rapid Repair of Bomb-Damaged Runways; Phase I: Preliminary Laboratory Investigations," Miscellaneous Paper C-72-15, U. S. Army Engineer Waterways Experiment Station, CE, Vicksburg, Miss.

Carr, G. L. 1971 (Feb). "History of Kaiser-Medium Duty Aluminum Sandwich Mat," Miscellaneous Paper S-71-4, U. S. Army Engineer Waterways Experiment Station, CE, Vicksburg, Miss.

Carroll, G. E., and Sutton, P. T. 1965 (Feb). "Developmpnt Test of Rapid Repair Technique for Bomb-Damaged Runways," APGC-TR-65-16, Air Proving Ground Center, Eglin AFB, Fla.

Cassino, V., and Chavez, D. 1975 (Oct). "Effects of Pavement Design on Cratering Damage from Penetrating Weapons," AFWL-TR-74-197, Civil Engineering Research Facility, University of New Mexico, Kirtland AFB, N. Mex.

Daniel, C., and Wood, F. S. 1971. "Fitting Equations to Data," Wiley-Interscience, New York, N. Y.

Department of the Air Force. 1967 (Dec). "Maintenance and Repair of Expeditionary and Theater of Operation Airfield Facilities," AFM 85-33, Washington, D. C.

Department of the Air Force. 1974 (Jul). "Disaster Preparedness and Base Recovery Planning," AFR-93-2, Washington, D. C.

Eash, R., and Hart, G. 1971 (May). "Latex Modification of Fast-Fix C-1 Cement for the Rapid Repair of Bomb-Damaged Runways," WES-CR-C-71-1, Dow Chemical Co., Midland, Mich.

Forrest, J. B., and Crawford, J. 1975 (Aug). "A Structural Evaluation of Rapid Methods of Backfilling for Bomb-Damage Repair," AFWL-TR-74-272, Naval Civil Engineering Laboratory, Port Hueneme, Calif.

Forrest, J. B., and Shugar, T. A. 1974 (Mar). "A Structural Evaluation of Rapid Methods of Backfilling for Bomb-Damage Repair," AFWL-TR-73-29, Naval Civil Engineering Laboratory, Port Hueneme, Calif.

Gerard, C. J. 1969 (May). "Evaluation of Equipment Used for Emplacement of Earth Anchors," Miscellaneous Paper S-69-18, U. S. Army Engineer Waterways Experiment Station, CE, Vicksburg, Miss.

Gerardi, A., and Lohwasser, A. K. 1974 (Apr). "Computer Program for the Prediction of Aircraft Response to Runway Roughness, Volume I-Program Development; Volume II-User's Manual," AFWL-TR-73-109, Air Force Weapons Laboratory, Kirtland AFB, N. Mex.

Green, H. L. and Ellison, D. A. 1969 (Jul). "Installation of XM19 Airfield Landing Mat and Ancillary Items," Instruction Report S-69-4, U. S. Army Engineer Waterways Experiment Station, CE, Vicksburg, Miss.

Guest, P. G. 1961. Numerical Methods of Curve Fitting, Cambridge University Press, London, England.

Harris, T. M. 1974 (Feb). "Dynamic Response of an RF-4C Aircraft to a Bomb-Damage Repair Patch," AFFDL-TM-73-22-FYS, Air Force Flight Dynamics Laboratory, Wright-Patterson AFB, Ohio.

Headquarters, Department of the Army. 1965 (Nov). "Planning and Design for Rapid Airfield Construction in the Theater of Operations," Army Technical Manual 5-336, Washington, D. C.

_____. 1966 (Feb). "Paving and Surfacing Operations," Army Technical Manual 5-337, Washington, D. C.

Headquarters, Departments of the Army and Air Force. 1968 (Sep). "Planning and Design of Roads, Airbases, and Heliports in the Theater of Operations," Army Technical Manual 5-330, Air Force 86-3, Vol II, Washington, D. C.

Headquarters, Naval Air Systems Command. 1967 (Jul). "Handbook-Installation, Maintenance, Repackaging, and Illustrated Parts Breakdown-AM2 Airfield Landing Mat and Accessories," NAVAIR 51-60A-1, Washington, D. C.

Hickman, B. R., et al. 1966 (Mar). "Rapid Repair of Bomb-Damage Runways," AFML-TR-66-141, Monsanto Research Corp.

Hoff, G. C. 1975 (Jul). "A Concept for Rapid Repair of Bomb-Damage Runways Using Regulated-Set Cement," Technical Report C-75-2, U. S. Army Engineer Waterways Experiment Station, CE, Vicksburg, Miss.

Hokanson, L. D. 1973 (Feb). "Soil Property Effects on Bomb Cratering in Pavement Systems," AFWL-TR-72-231, New Mexico State University, Las Cruces, N. Mex.

_____. 1975 (Sep-Oct). "Airfield Bomb Damage Repair," The Miltary Engineer, American Society of Military Engineers.

_____. 1975 (Oct). "Tyndall AFB Bomb Damage Repair Field Test, Documentation and Analysis," AFWL-TR-74-226, Air Force Weapons Laboratory, Kirtland AFB, N. Mex.

_____. 1975 (Nov). "Analysis of Dynamic Aircraft Responses to Bomb Damage Repair," AFWL-TR-75-138, Air Force Weapons Laboratory, Kirtland AFB, N Mex.

Hokanson, L. D., and Rollings, R. S. 1975 (Oct). "Field Test of Standard Bomb Damage Repair Techniques for Pavements," AFWL-TR-75-148, Air Force Weapons Laboratory, Kirtland AFB, N. Mex.

_____. 1976 (Mar). "Bomb Damage Repair Analysis of a Scale Runway, Project Essex," AFCEC-TR-75-27, Air Force Weapons Laboratory, Kirtland AFB, N. Mex.

Kvammen, A., Jr., Pichumani, R., and Dick, J. L. 1972 (Dec). "Pavement Cratering Studies," AFWL-TR-72-6, Air Force Weapons Laboratory, Kirtland AFB, N. Mex.

Classified reference.*

Lehamn, C. T., Koch, A. R., and Wenk, R. J. 1970 (Aug). "Super Strength Gypsum Cement for Rapid Runway Repair," CEC-70-003, United States Gypsum, Co., Chicago, Ill.

Leitheiser, R. H., Hellmer, R. J., and Clocker, E. T. 1967 (Dec). "Water Extended Resin Materials and Methods for Rapid Repair and Construction of Pavements," AFAPL-TR-67-146, Ashland Chemical Co., Minneapolis, Minn.

Lindberg, C., and Currin, D. D. 1971 (Jan). "Maintenance and Repair of Expeditionary and Theater of Operation Airfield Landing Mat Facilities Using Explosive Impulse Welding," AFWL-TR-70-160, Air Force Weapons Laboratory, Kirtland AFB, N. Mex.

Martin Marietta Aluminum. 1967 (Jul). "Instructions for Using the Martin Marietta Aluminum Rapid Runway Repair Kit," Torrance, Calif.

Menza, D. F., and Offen, G. R. 1963 (Jul). "Runway Bomb Damage Repair Test," APGC-TR-63-40, Air Proving Ground Center, Eglin AFB, Fla.

Mueller, F. N. 1971 (Apr). "Rapid Backfilling of Runway Craters," PREC-TR-71-1, Western Co., Richardson, Tex.

* Bibliographic materials for the classified reference will be furnished to qualified agencies upon request.

Nielsen, J. P., and Cassino, V. 1975 (Sep). "Evaluation of Liquid Binder for Airfield Bomb Damage Repair," AFCEC-TR-75-25, Civil Engineering Research Facility, University of New Mexico, Kirtland AFB, N. Mex.

O'Sullivan, J. J. 1951 (Nov). "Time, Equipment, and Costs to Repair Cratered Runways," RM-730, Rand Corp., Santa Monica, Calif.

Peasley, J. A. 1965 (Dec). "Rapid Repair of Bomb-Damaged Runways by Unique Chemical Means," AFAPL-TR-65-12, Raven Industries, Inc., Sioux Falls, S. Dak.

Pichumani, R., and Dick, J. L. 1970 (Dec). "Effects of Small Cratering Charges on Airfield Pavements," AFWL-TR-70-66, Air Force Weapons Laboratory, Kirtland AFB, N. Mex.

Pruitt, G. T., et al. 1968 (Apr). "Rapid Repair of Bomb-Damage Runways," AFAPL-TR-67-165, Vol II, Western Co., Richardson, Tex.

Richardson, C. E. 1975 (Nov). "Time Lapse Movie Analysis of Equipment for Rapid Repair of Bomb Damage Runways," AFWL-TR-75-253, University of New Mexico, Albuquerque, N. Mex.

Rollings, R. S. 1975 (Nov). "Comparison of the British Class 60 Trackway and AM-2 Mat for Bomb Damage Repair Applications," Air Force Weapons Laboratory, Kirtland AFB, N. Mex.

Rooke, A. D., Carnes, B. L., and Davis, L. K. 1974 (Jan). "Cratering by Explosions: A Compendium and an Analysis," Technical Report N-74-1, U. S. Army Engineer Waterways Experiment Station, CE, Vicksburg, Miss.

Seats, J. H., et al. 1972 (Mar). "Bomb Damage Repair Proposal," Air Force Institute of Technology, Wright-Patterson AFB, Ohio.

Setser, W. G., et al. 1968 (Mar). "Rapid Repair of Bomb-Damage Runways," Vol I, AFAPL-TR-67-165, Western Co., Richardson, Tex.

Smith, J. L., and Morris, W. W. 1974 (Feb). "Structural Repair of Bomb Damage to Airfield Runways," AFWL-TR-73-214, Texas Tech University, Lubbock, Tex.

Springston, P. S. 1979 (Oct). "Fiberglass-Reinforced Plastic Surfacing for Rapid Runway Repair by Naval Construction Forces," Naval FAC Eng Command Port Hueneme, Calif.

_____. 1980 (Feb). "Traffic Testing of a Fiberglass-Reinforced Polyester Resin Surfacing for Rapid Runway Repair," Naval FAC Eng Command Port Hueneme, Calif.

Stroup, T., Reed, D., and Hammitt, G. M. 1980 (Dec). "Airfield Damage Recovery Techniques of 18th Engineer Brigade in Europe," Field Reference Document, Office, Chief of Engineer, U. S. Army, Washington, D. C.

U. S. Army Engineer Waterways Experiment Station, CE. 1962 (Aug). "Bomb Crater Repair Study, Fort Bragg, North Carolina," Miscellaneous Paper No. 4-526, Vicksburg, Miss.

Vedros, P. J., Jr. 1980 (Dec). "Airfield Bomb Damage Repair Methods," Field Training Document, Office, Chief of Engineers, U. S. Army, Washington, D. C.

Westine, P. S. 1973 (Feb). "Bomb Crater Damage to Runways," AFWL-TR-72-183, Southwest Research Institute, San Antonio, Tex.

White, D. W. 1969 (Jun). "History of Dow Chemical Extruded Medium-Duty Mat," Miscellaneous Paper S-69-22, U. S. Army Engineer Waterways Experiment Station, CE, Vicksburg, Miss.

_____. 1969 (Jul). "Installation of XM18 Extruded Aluminum Airfield Landing Mat," Instruction Report S-69-3, U. S. Army Engineer Waterways Experiment Station, CE, Vicksburg, Miss.

Whitman, R. V. 1970 (May). "The Response of Soils to Dynamic Loadings," Report 26, U. S. Army Engineer Waterways Experiment Station, CE, Vicksburg, Miss.

Yoshihara, T. 1964 (Jun). "Repair of Bomb-Damaged Runway," NCEL-TR-297, Naval Civil Engineering Laboratory, Port Hueneme, Calif.

Young, C. W. 1967 (May). "The Development of Empirical Equations for Predicting Depth of an Earth-Penetrating Projectile," SC-DR-67-60, Sandia Laboratories, Albuquerque, N. Mex.

Table 1

Subgrade Density and Water Content in Area of Craters

Crater	Material	Depth ft	Dry Density pcf	Water Content percent
1	Washed gravel	2	87.9	19.0
		10	87.5	20.7
2	Washed gravel	2	103.0	18.0
		4	91.9	21.0
		6	96.5	22.0
		8	88.7	24.0
		10	87.1	26.0
3	Washed gravel	2	85.8	24.0
		4	90.9	24.0
		6	84.3	23.0
		8	88.0	23.8
		10	87.0	25.0
4	Washed gravel	2	93.2	21.0
		4	91.3	22.0
		6	83.9	21.0
		8	86.1	23.0
		10	86.9	23.0

Table 2

Summary of Soil Data

Location	Material	Depth in.	CBR	Dry Density pcf	Water Content percent	Modulus of Subgrade Reaction, k
Center line test pad Sta 0+65	Lean clay	Surface	26	101.9	15.3	172
		6	11	91.7	23.3	
		10				164
		12	8	97.1	18.7	
		Avg	15	96.9	19.1	168
Center line test pad STA 1+65	Lean clay	Surface	26	103.1	16.3	227
		6	9	103.5	19.9	
		10				217
		12	9	94.2	23.7	
		Avg	15	100.3	20.0	222
Center line AC test pad	Subbase (sandy gravel)	Surface	23	140.9	4.1	
	Base (limestone)	Surface	140	146.1	2.1	
Crater 1	Washed gravel	Surface			3.1	167
Crater 3	Washed gravel			115.8	2.5	150
Crater 4	Washed gravel	Surface			3.5	182
Crater 5	Rubble				18.0	150
Crater 6	Limestone		125	151.2	3.0	

Note: Strength in Crater 2 assumed to be the same as Crater 1.

Table 3

Flexural Strength of Grout-Limestone Mixture (Steel Beam Molds-48 in. Long, 9 in. Wide, and 9 in. Deep)

Spec No.	Age Hours	Total Load lb	Flexural Strength psi	Average Flexural Strength psi
1	4	1940	70	70
2	8	3030	107	
3	8	2930	106	107
4	18	3180	115	
5	18	4320	155	135
6	42	5320	195	
		5540	196	196
7	67	5400	200	200

Note: Rate of load 150 psi per minute. Same crushed limestone aggregate used that was used to fill the actual test items.

Table 4

Compressive Strength of Grout-Limestone Mixture (Steel Cylinder Molds-10 in. Diameter by 20 in. Length)

Spec No.	Age Hours	Total Load lb	Compressive Strength psi	Average Compressive Strength psi
1	4	34,000	432	432
2	8	60,000	763	
3	8	49,500	630	696
4	18	82,250	1050	
5	18	81,000	1050	1040
6	42	122,500	1560	1560
7	68	110,500	1410	1410

Note: Same crushed limestone aggregate used that was used to fill the actual test items.

Table 5

Compressive Strength of Grout (Cardboard Cylinder Molds-6 in. Diameter by 12 in. Length)

Spec No.	Age Hours	Total Load lb	Compressive Strength psi
1	4	24,600	870
2	8	38,000	1340
3	8	37,500	1330
4	18	56,500	2000
5	18	37,900	1340
6	42	60,500	2140

Note: These are cylinders of grout only (rock).

Table 6

Laboratory Compressive and Flexural Strengths on Concrete Slabs

Location	Compressive Strength of Cylinder, psi			Flexural Strength of Beams, psi		
	7 days	28 days	97 days	7 days	28 days	97 days
South lane	3430	4540	4770		740	810
	3430	4290	4820		--	760
	3480	4450	5670		705	865
	3410	4140	4720		--	730
	3460	4360	5410		580	750
	3500	4120	5140		--	685
Avg	3450	4320	5090		675	770
North lane	3790	4890	5440		755	755
	3690	4830	5320		--	770
	3700	4580	4860		635	695
	3550	4540	4640		--	825
	3700	4820	5270		715	725
	3620	4750	5410		--	775
Avg	3660	4730	5160		700	760
Center lane	3730	4960	5480		760	875
	3700	4820	5820		--	725
	3150	4130	4750		655	760

(Continued)

Table 6 (Concluded)

Location	Compressive Strength of Cylinder, psi			Flexural Strength of Beams, psi		
	7 days	28 days	97 days	7 days	28 days	97 days
Center lane (Continued)	3040	4290	4790		--	875
	3790	4980	5540		800	920
	3730	4750	5360		--	810
Avg	3520	4650	5290		740	840
Crater 4 and 5	4290	4620	--	575	670	
	4220	4500	--	560	695	
	4270	4380	--	--	--	
Avg	4280	4500		570	680	

Table 7

Summary of Traffic Data

Crater Number	Material Capping System Identification	Thickness in.	Operational Pass Level Requirements	Aircraft Gear Used to Traffic Pavement	Number of Passes Applied Lane 1	Number of Passes Applied Lane 2	Structural Performance	Hours After Construction Until the Surface Is Usable
1	Compacted well-graded (3/4 in. maximum limestone aggregate)	18	4760	C-141 F-4C	5100 760	5100 0	Satisfactory with some remedial repair	0
2	Pressure grouted uniform 3 in. aggregate	16	4760	C-141 F-4C	5100 760	5100 0	Satisfactory	8
3	Gravity grouted uniform 3 in. aggregate	18	4760	C-141 F-4C	5100 760	5100 0	Satisfactory	8
4	Portland cement concrete	15	4760	C-141 F-4C	5100 760	5100 0	Satisfactory	24
5	Portland cement concrete	15	4760	C-141 F-4C	5100 760	5100 0	Satisfactory	24
6	Asphaltic concrete crushed stone	3 9	4760	C-141 F-4C	5100 760	5100 0	Satisfactory with some densification	24

Photo 1. Overall view of bomb damage repair test site prior to construction

Photo 2. Initial rough grading of test site

Photo 3. Processing the top of subgrade with a pulvimixer

Photo 4. Compaction of subgrade with roller loaded to 50,000 lb and tires inflated to 90 psi

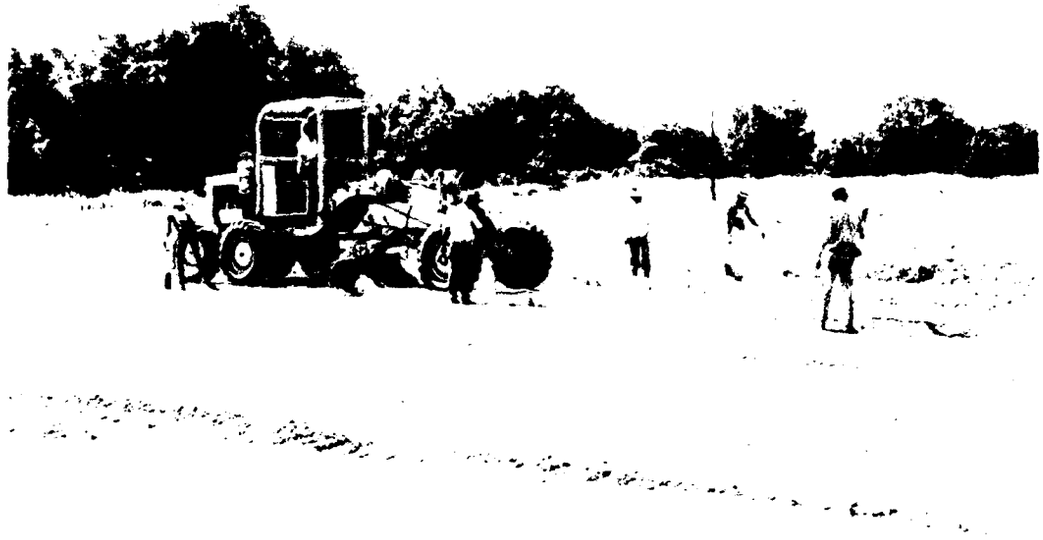

Photo 5. Final grading of the site

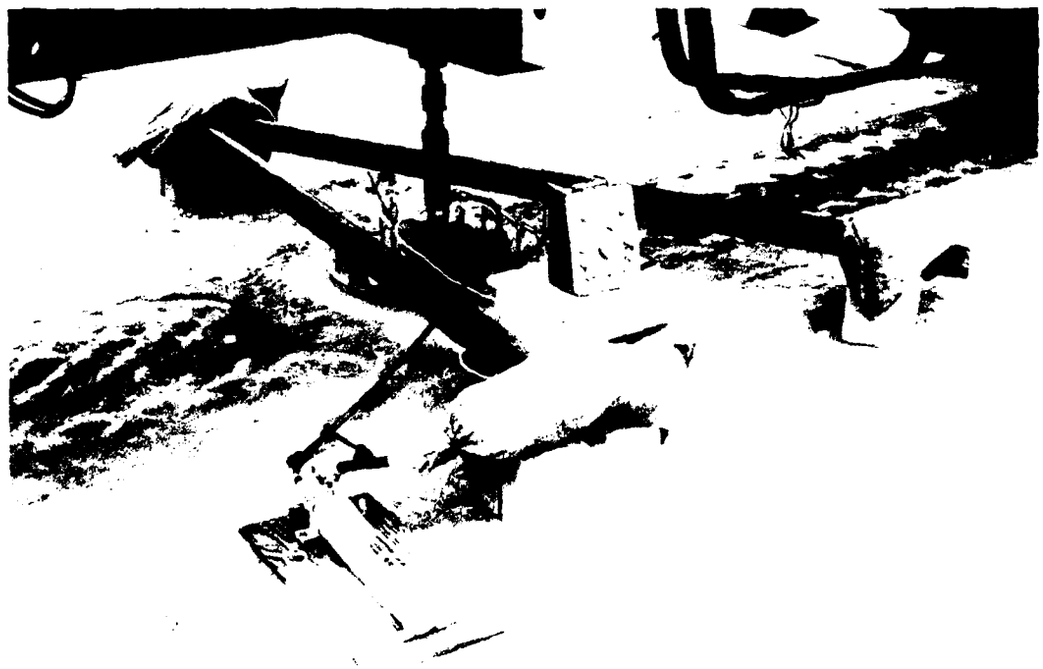

Photo 6. Typical setup of plate bearing test

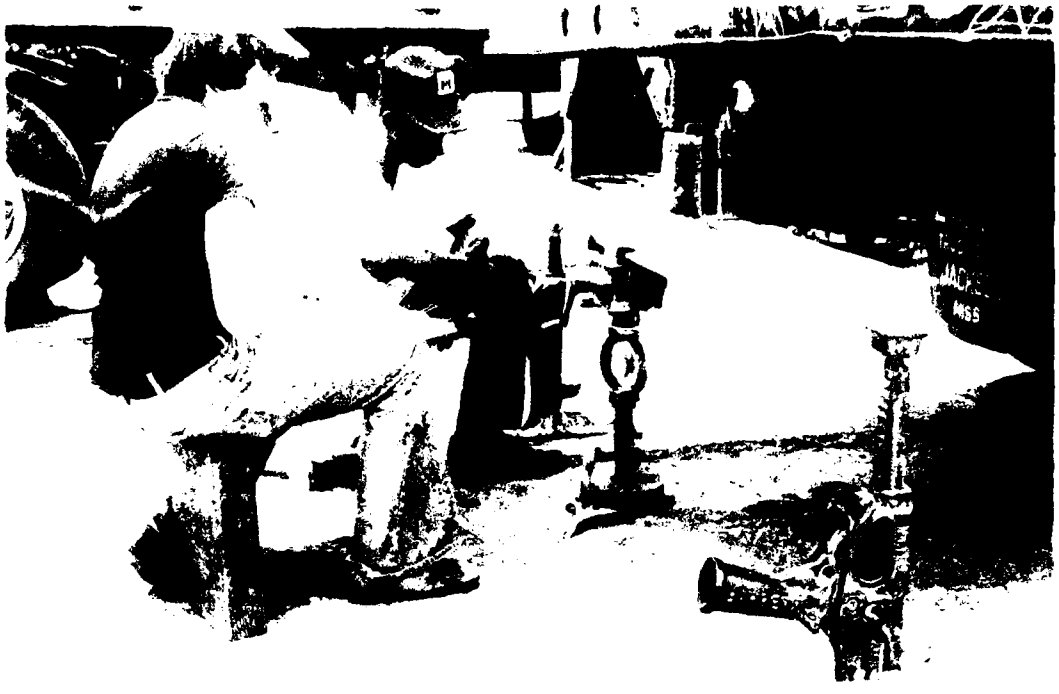

Photo 7. Typical setup for CBR test

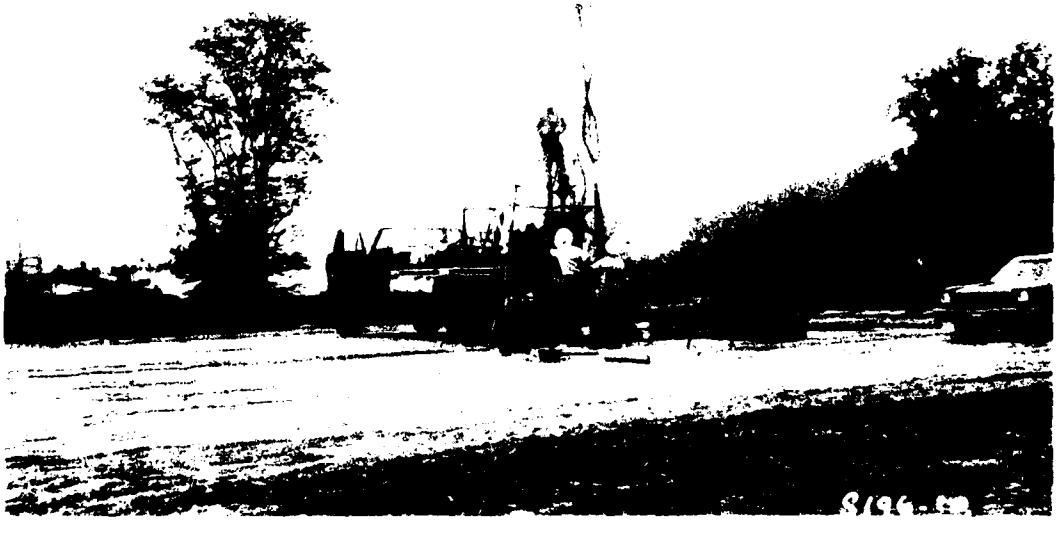

Photo 8. Split spoon soil samples being taken along center line of test section

Photo 9. Test section after setting forms in north and south lanes

Photo 10. Forms in north lane producing a longitudinal keyway

Photo 11. South lane forms and steel tie bars as moment transfer devices

Photo 12. Concrete being placed in south lane from ready-mix truck

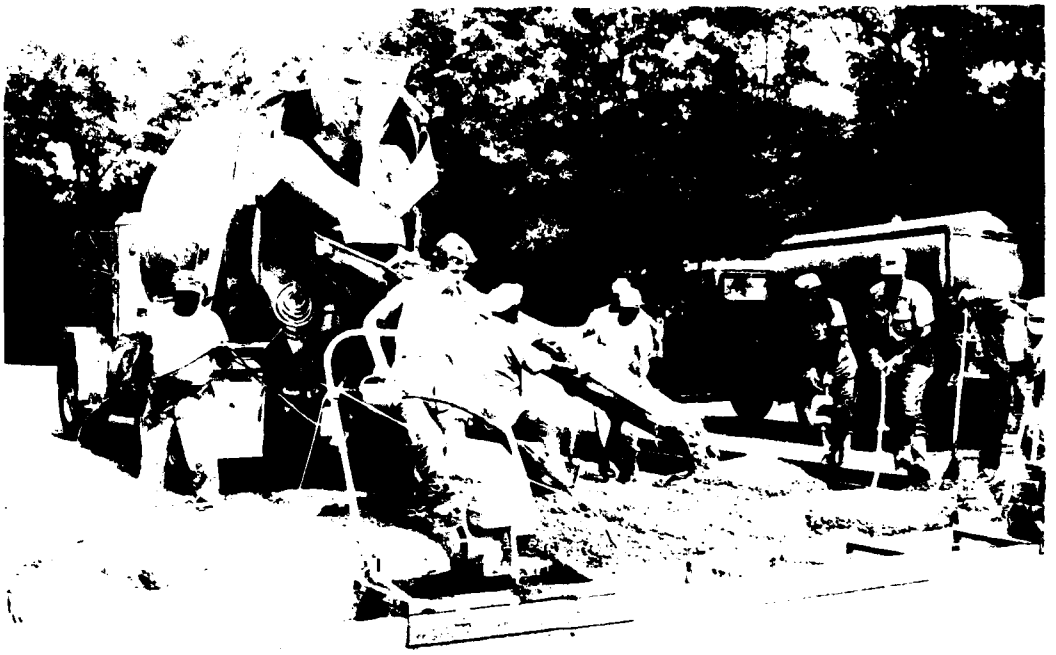

Photo 13. View of concrete placement and use of vibrators

Photo 14. Cross forms used in center lane to form 25- by 25-ft sections. Moment transfers are shown along the sides

Photo 15. Pouring of 25- by 25-ft slabs in center lane between north and south lanes

Photo 16. Spraying of curing compound on south lane

Photo 13. View of concrete placement and use of vibrators

Photo 14. Cross forms used in center lane to form 25- by 25-ft sections. Moment transfers are shown along the sides

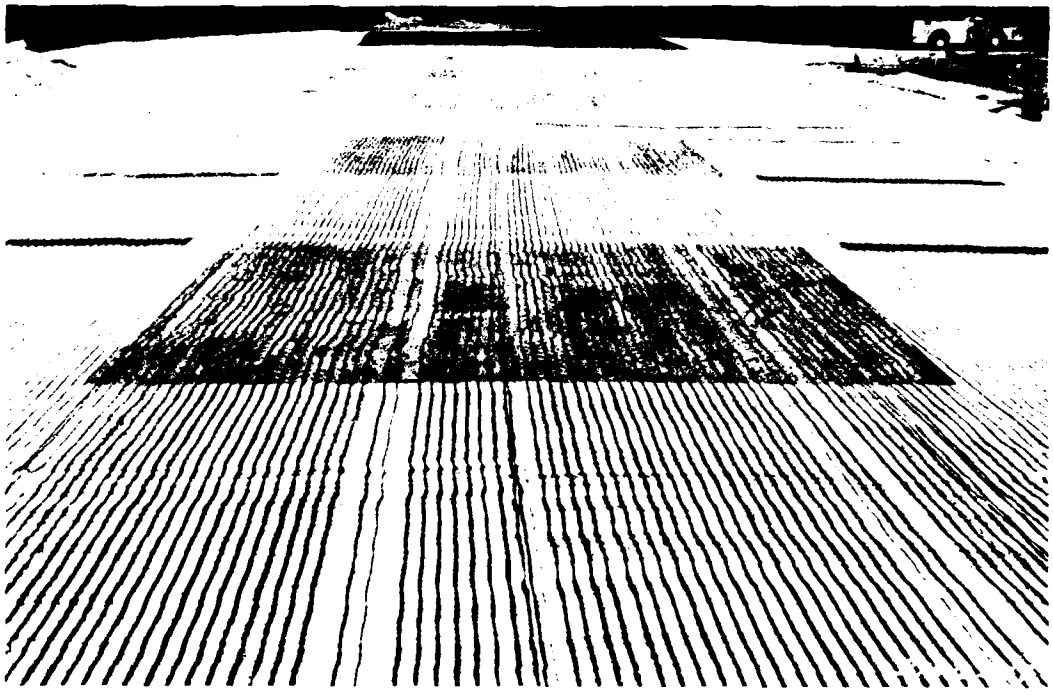

Photo 17. Asphalt emulsion sprayed on portland cement concrete as a tack coat prior to overlaying with asphaltic concrete

Photo 18. Asphaltic concrete overlay being placed on portland cement concrete

Photo 19. Vibratory steel-wheel roller compacting asphaltic concrete

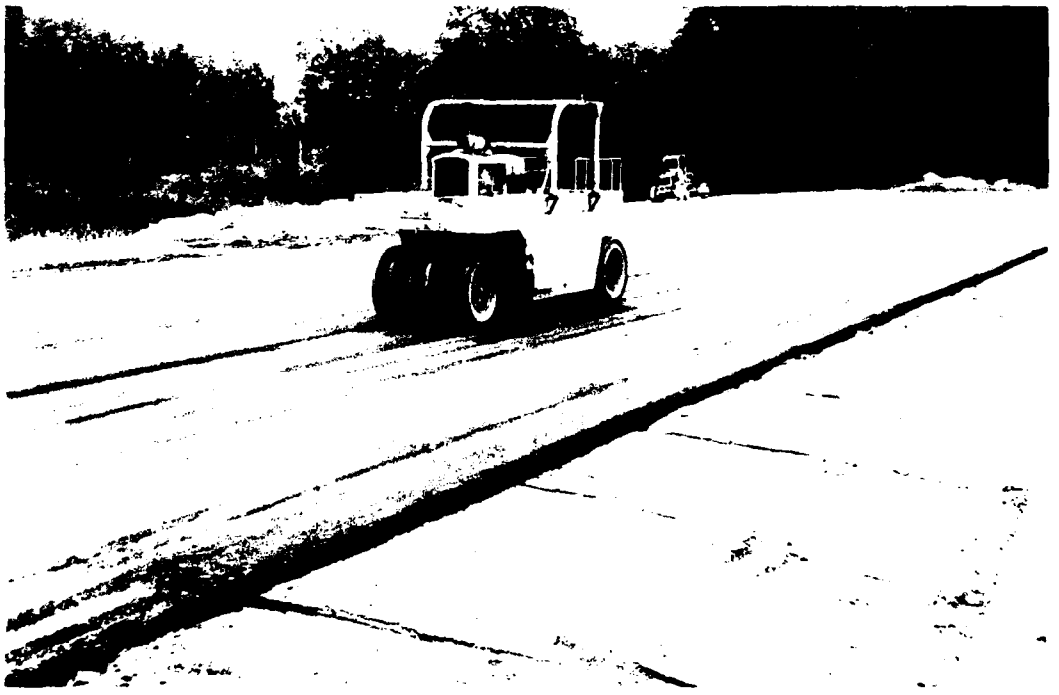

Photo 20. Self-propelled, 50,000-lb pneumatic-tired roller compacting asphaltic concrete

Photo 21. Load cart used in traffic tests to simulate F-4C aircraft loading

Photo 22. Load cart used in traffic test to simulate C-141 aircraft loadings

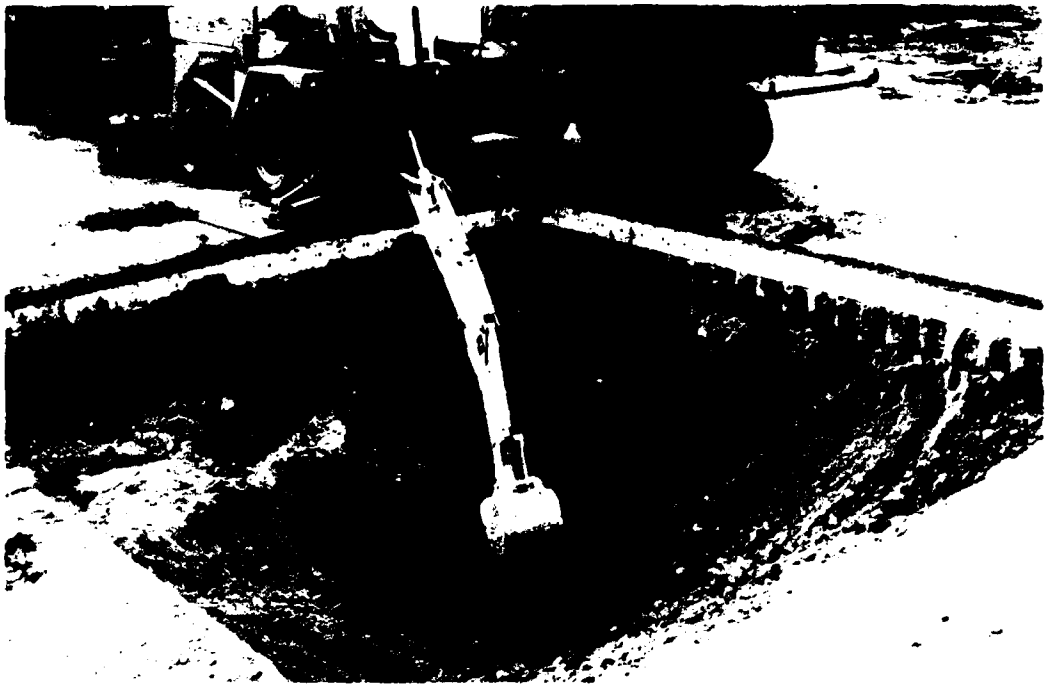

Photo 23. Construction of a simulated crater

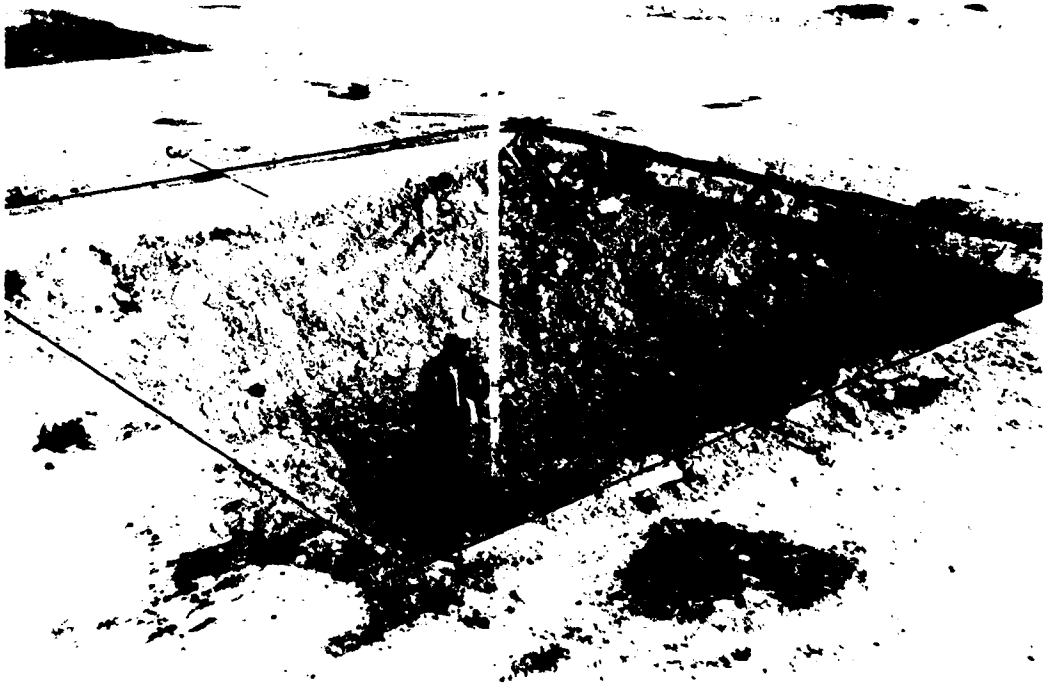

Photo 24. Excavated crater with an approximate center depth of 10 ft

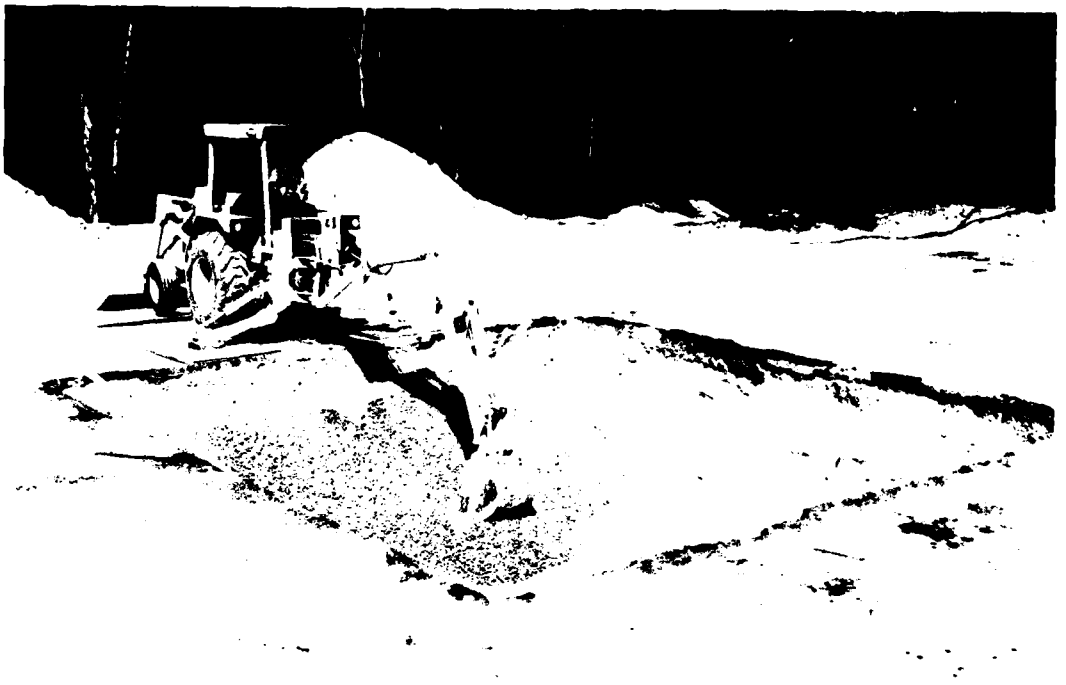

Photo 25. Gravel being spread in bottom of crater with backhoe

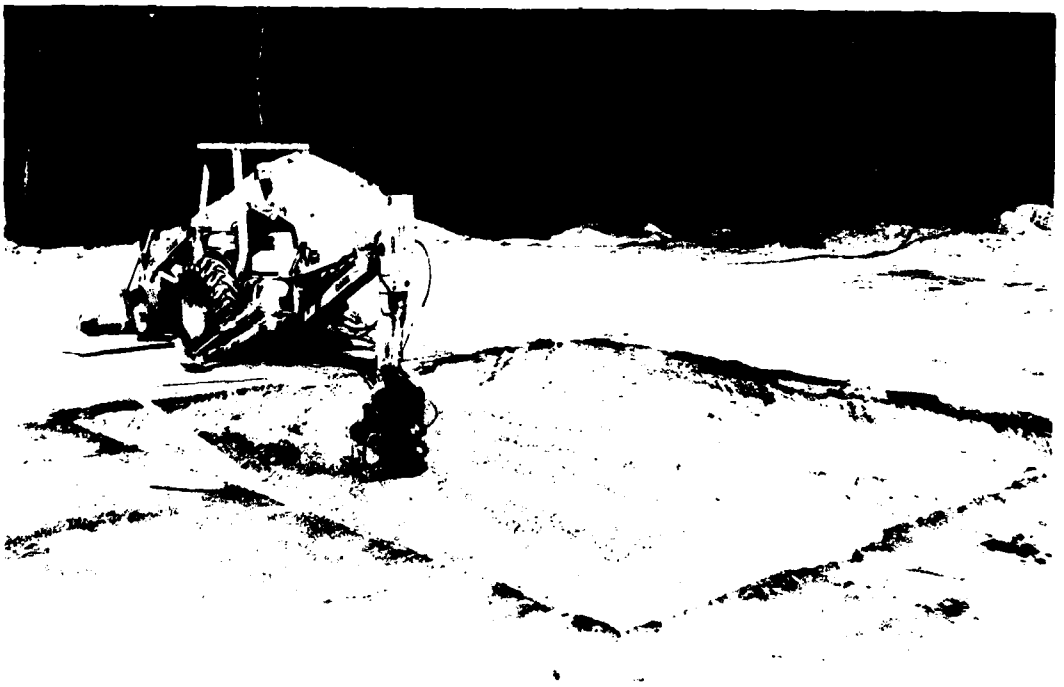

Photo 26. Gravel being compacted with vibrator foot attached to backhoe boom

Photo 27. Rubble being compacted in crater 5

Photo 28. Crater 1 after filling bottom portion with washed gravel and compacting

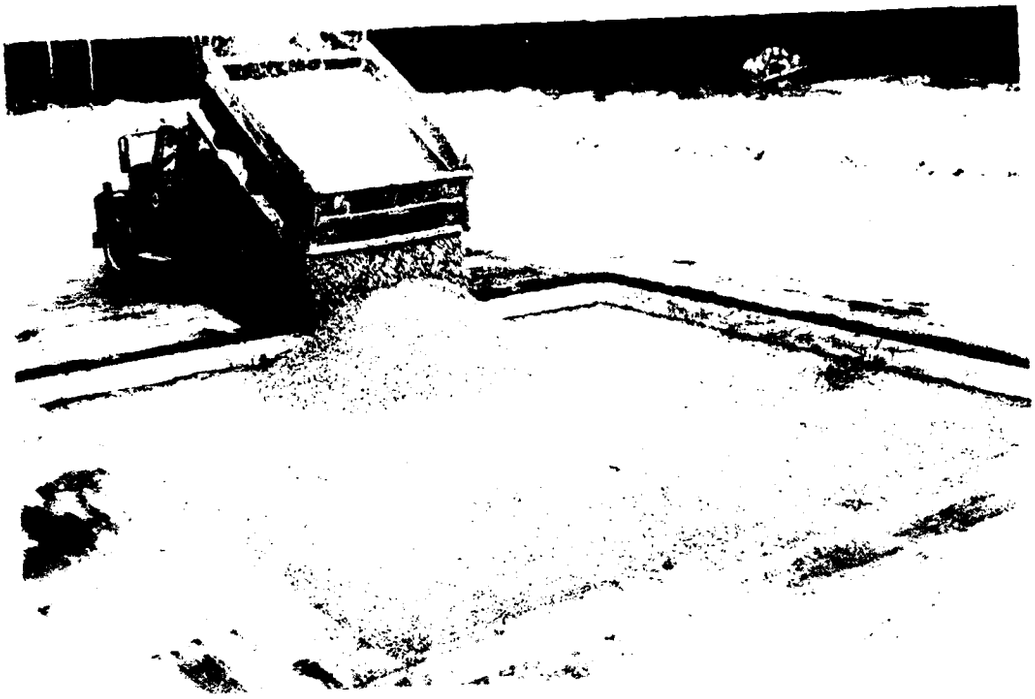

Photo 29. Crushed limestone being placed into upper portion of crater 1

Photo 30. Compaction of crushed limestone with vibratory steel-wheel roller, crater 1

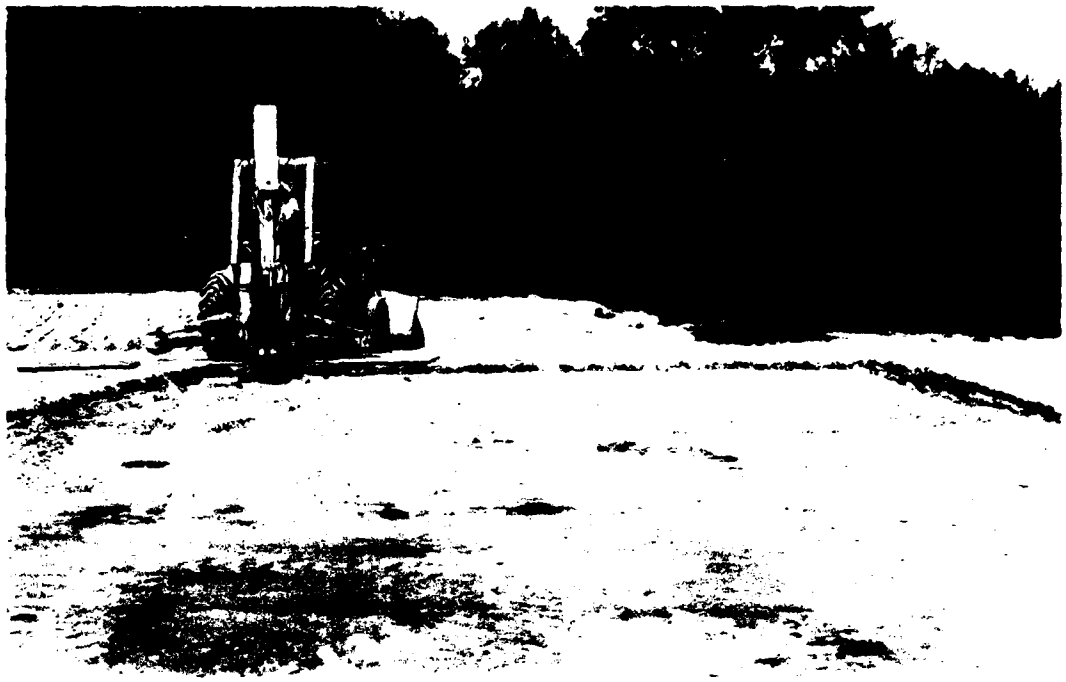

Photo 31. Vibrator foot compacting around edges of crater

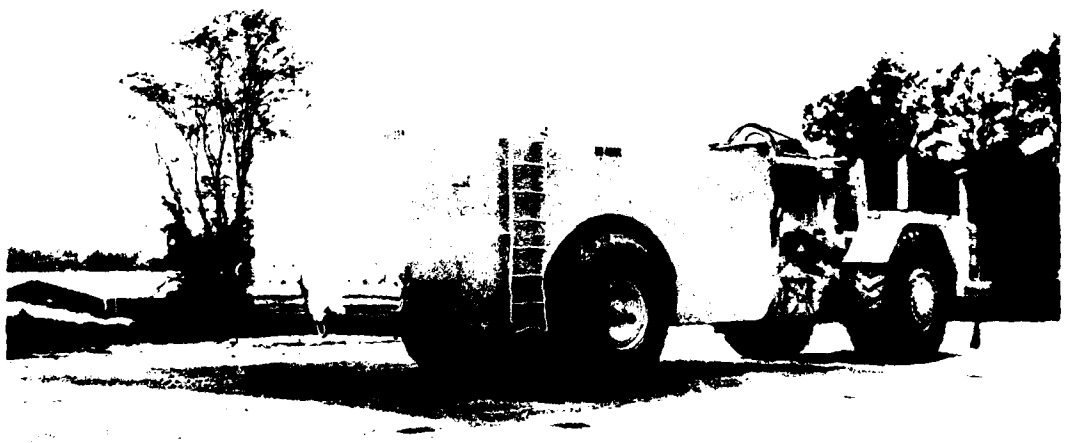

Photo 32. Pneumatic-tired roller compacting final lift in crater 1

Photo 33. Scissor-type moment transfer device installed in crater 2 by clamping to the existing concrete slab

Photo 34. General view of crater 2 showing plastic film and PVC pipes installed prior to grouting. Moment transfer devices are installed along the south half of the crater

Photo 35. Front-end loader placing initial limestone over slotted plastic pipes in crater 2

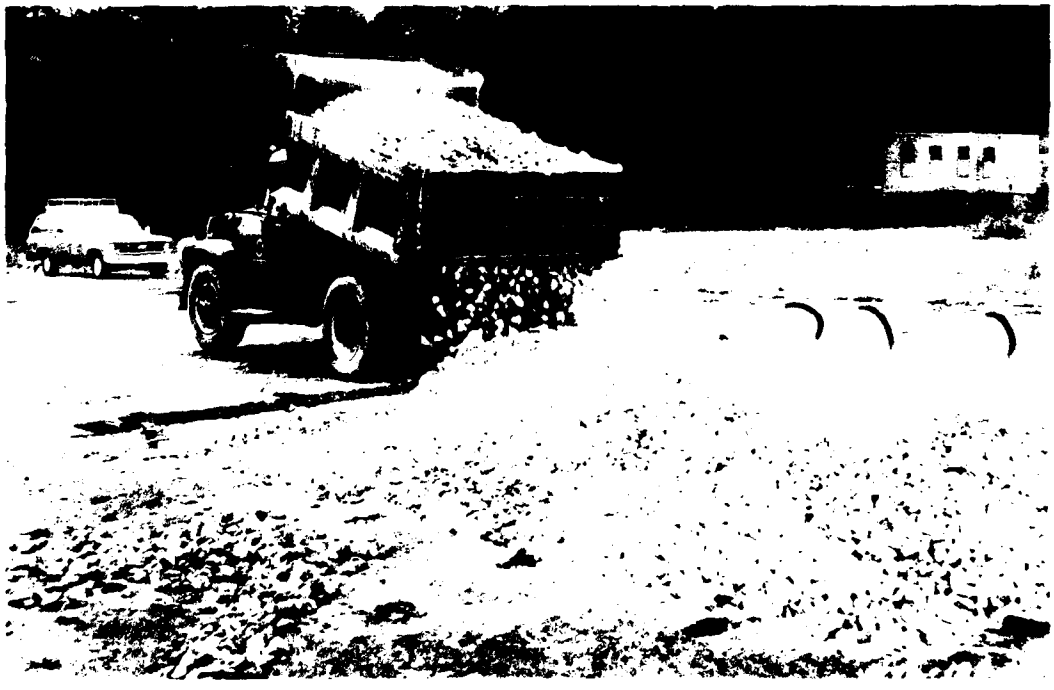

Photo 36. Limestone being dumped into crater 2 directly from truck

Photo 37. Backhoe used to push limestone away from edges of crater

Photo 38. Front-end loader spreading limestone in crater

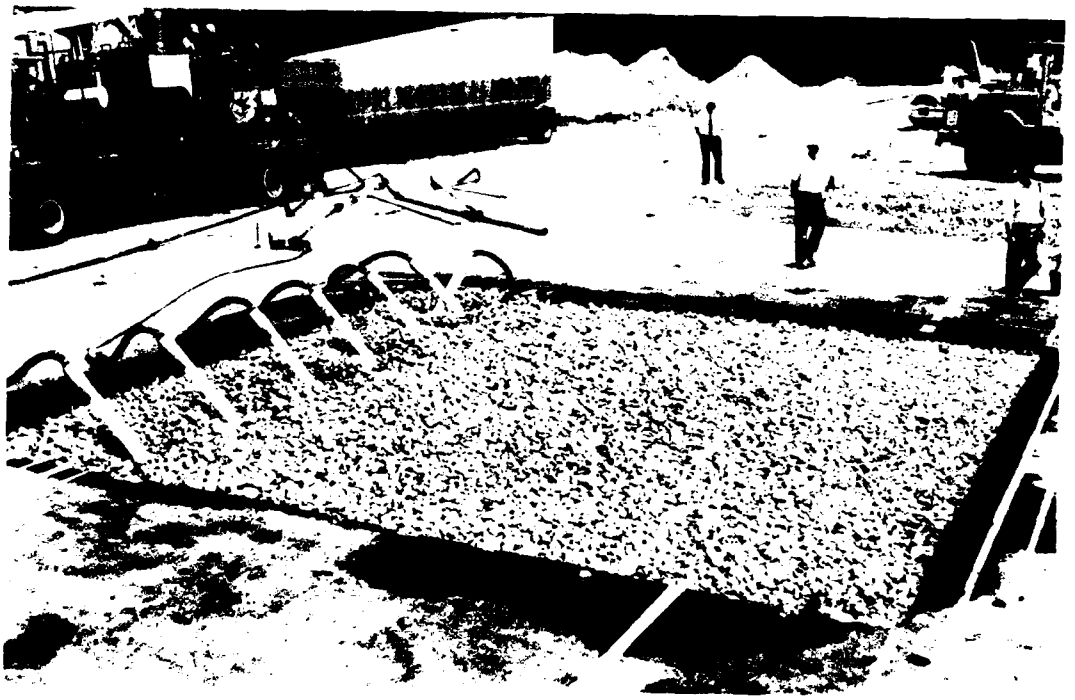

Photo 39. View of crater 2 in foreground after spraying limestone with water and just prior to grouting

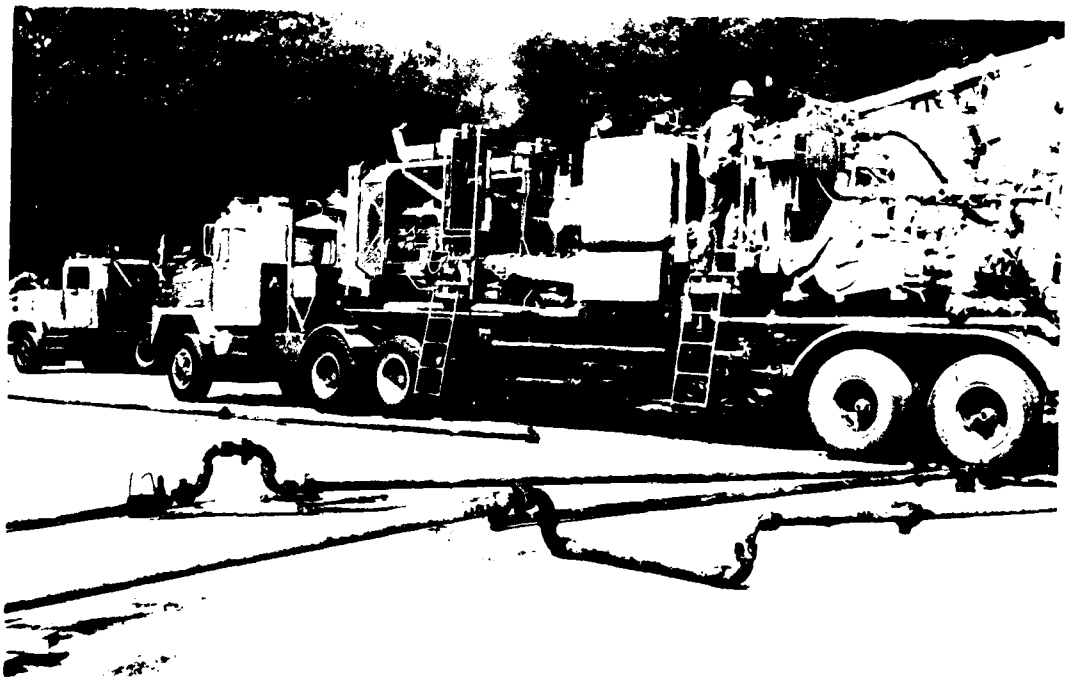

Photo 40. Commercial grout pumping equipment used in grouting of craters 2 and 3

Photo 41. Crater 2 shown almost filled near the end of the grouting operation

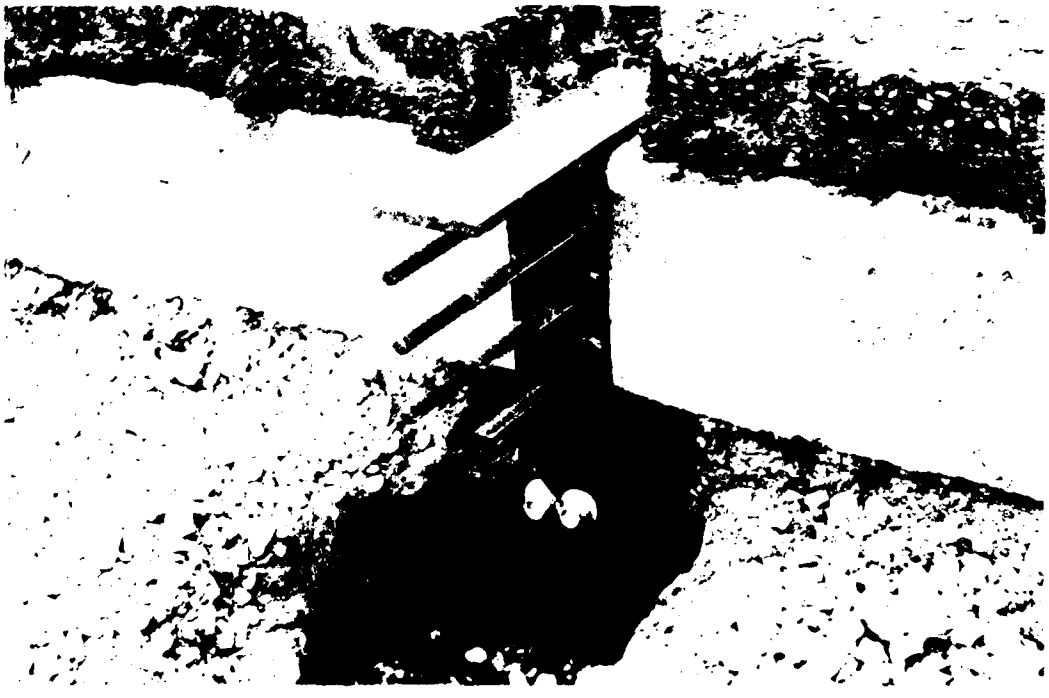

Photo 42. Shop-fabricated moment transfer device used along south half of crater 3. Note cutout in asphalt pavement required to allow device to clamp onto existing concrete slab

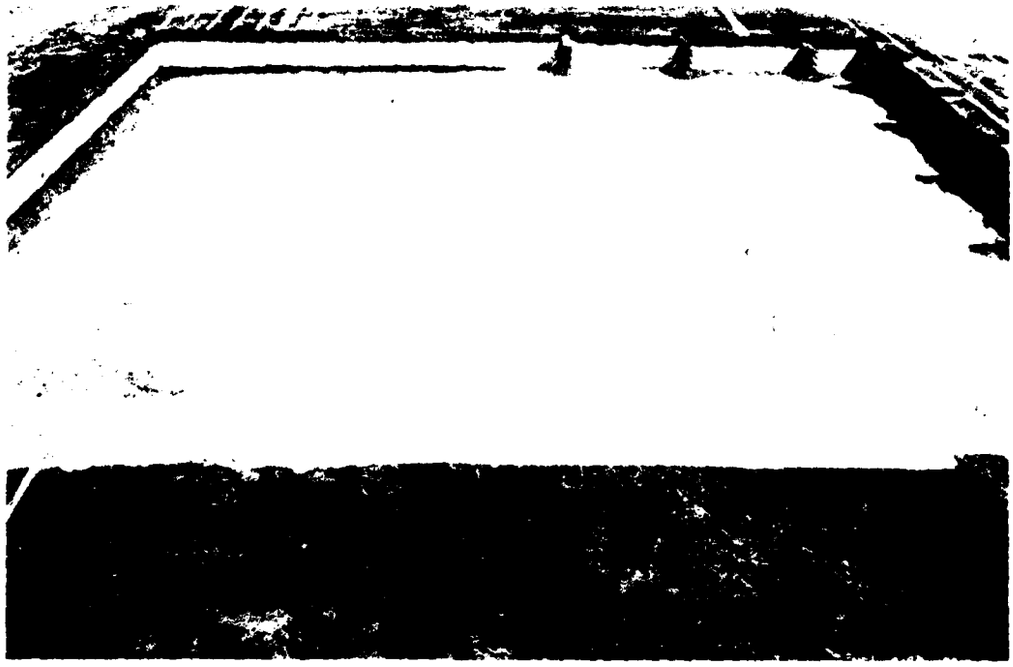

Photo 43. Crater 3 with polyethylene film placed over limestone just prior to grouting. Both the undercut and fabricated moment transfer devices can be observed along the perimeter of the crater

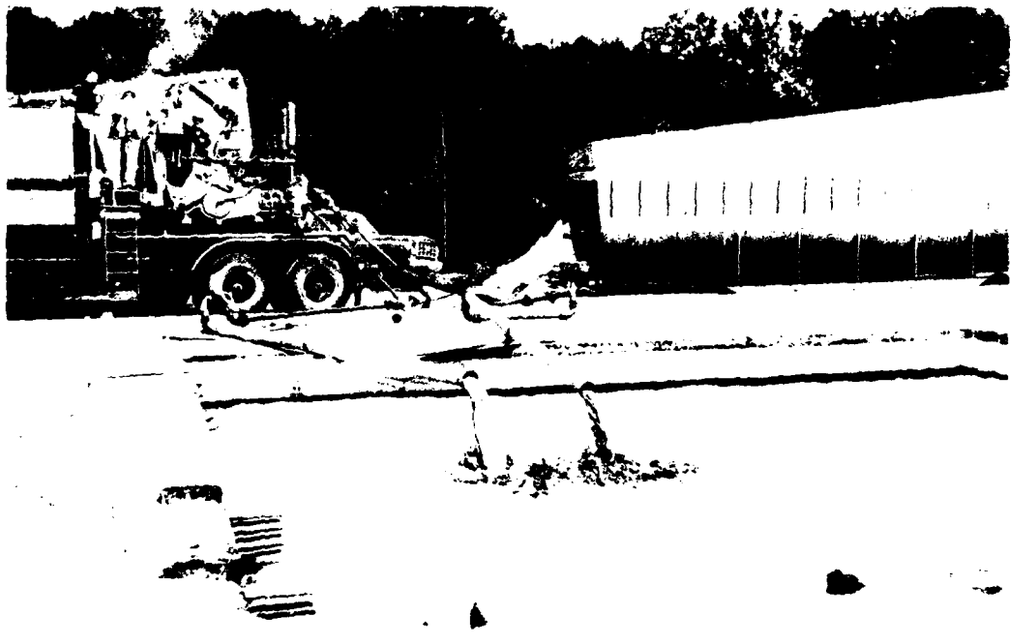

Photo 44. Grout being pumped into top portion of crater 3 prior to placement of limestone

Photo 45. Moment transfer devices located in south half of crater 3 after initial pumping of grout

Photo 46. Front end loader placing limestone in crater 3. Note stockpiled limestone in rear being wetted prior to placement in crater

Photo 47. Vibratory steel-wheel roller compacting limestone in crater 3, while crater 2 (in background) is being filled with grout

Photo 48. Undercut being excavated in north half of crater 4, prior to placement of reinforcement steel

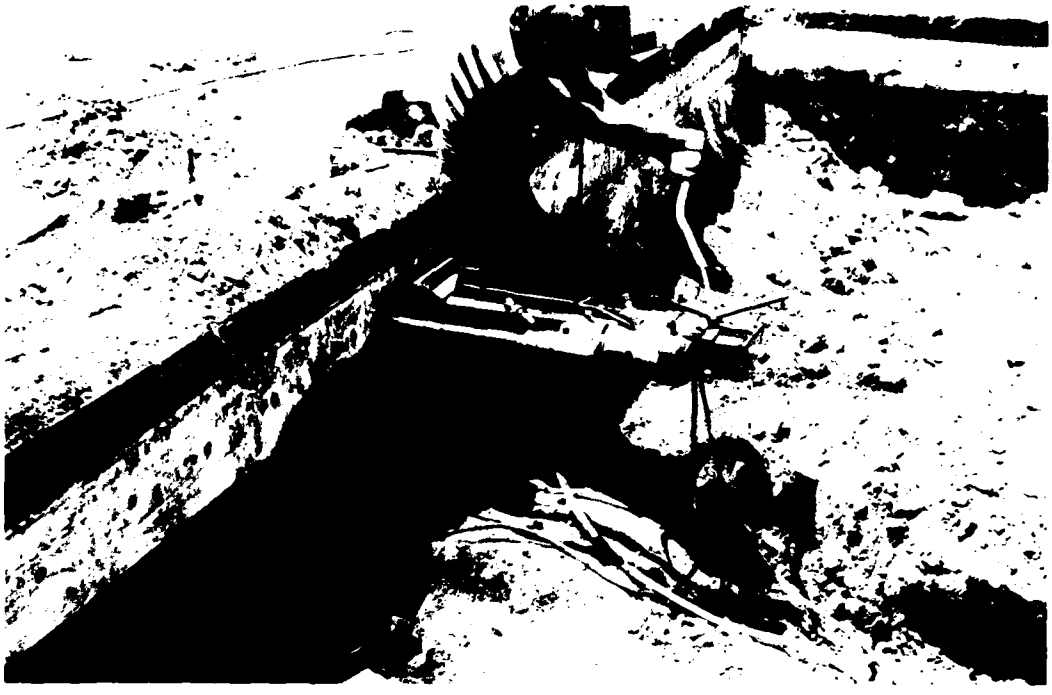

Photo 49. Drilling of 1-1/4-in. holes in existing vertical face of concrete slab for placement of steel dowels in south half of crater 4

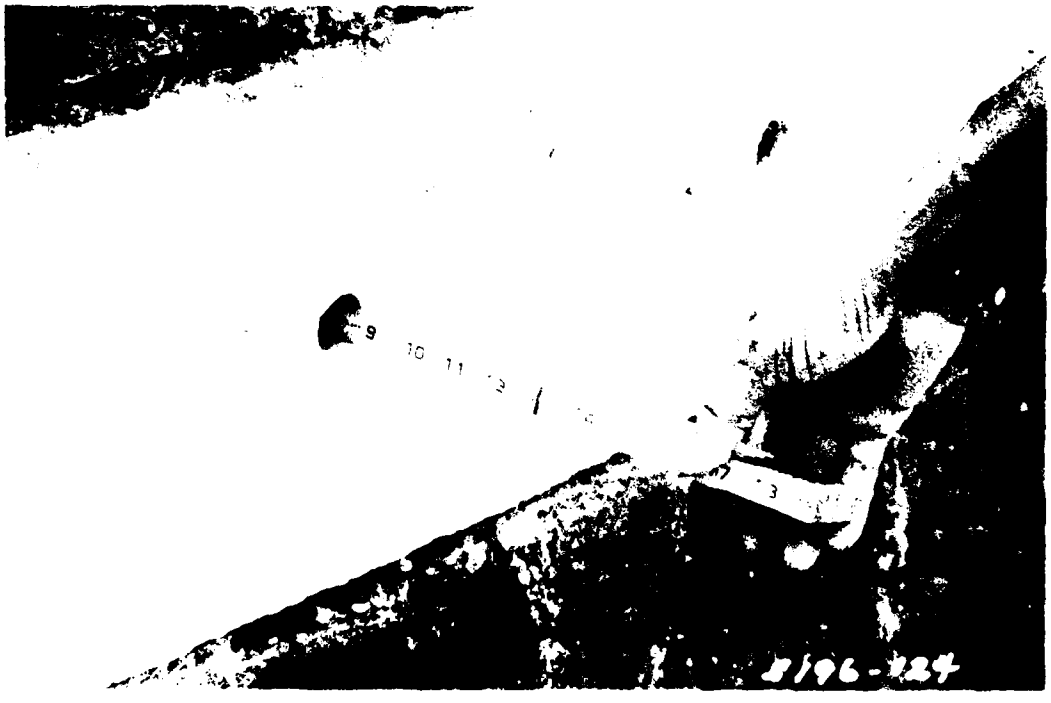

Photo 50. Completed holes in vertical face of concrete slab

Photo 51. View of crater 4 looking west just prior to concrete placement. The undercut section in the north half of the crater has the steel reinforcement in place and the steel dowels are shown protruding from the slab after being grouted in the drilled holes

Photo 52. Concrete being placed in crater directly onto washed gravel in crater 4

Photo 53. Finishing top surface of crater 4 as concrete placement is being completed

Photo 54. Wetting of burlap covering crater 4 to aid in proper curing of the concrete

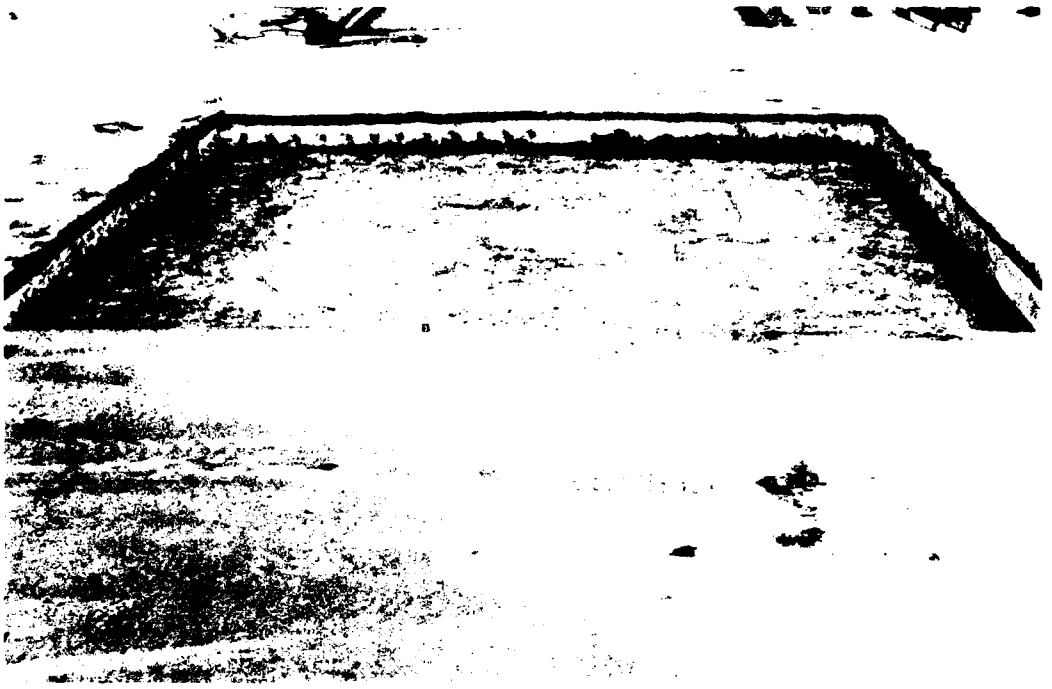

Photo 55. Crater 5 ready for concrete after lower portion was filled with lean clay and rubble

Photo 56. Concrete being placed in the top 15 in. of crater 5

Photo 57. Front-end loader used to place and spread the crushed limestone in two lifts in crater 6

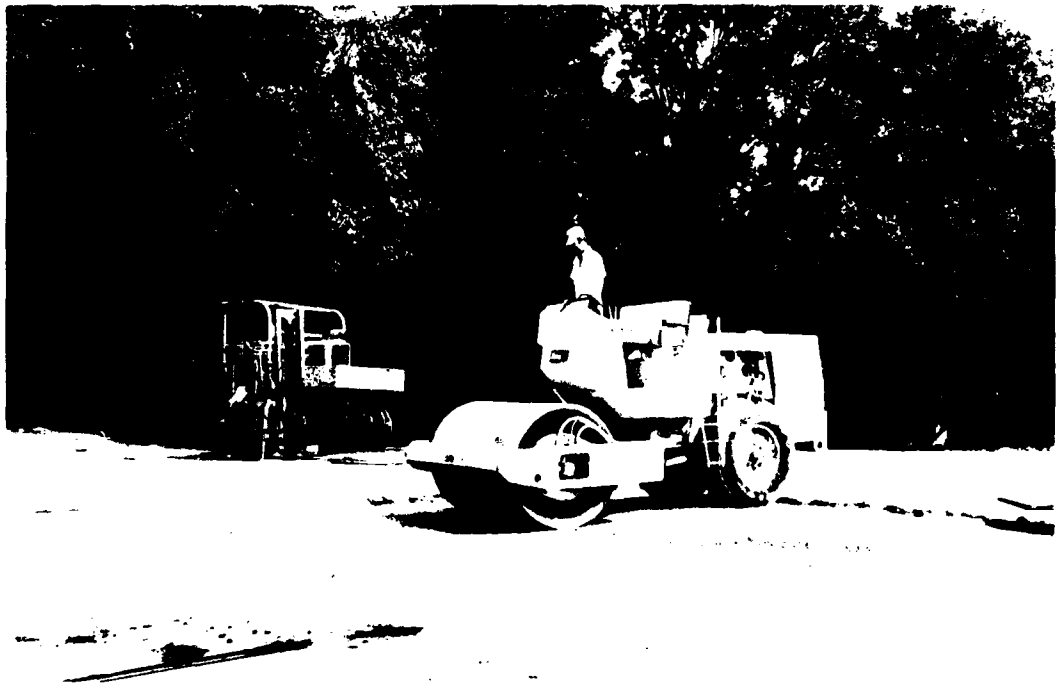

Photo 58. Rolling of the first lift with a vibratory steel-wheel roller in crater 6

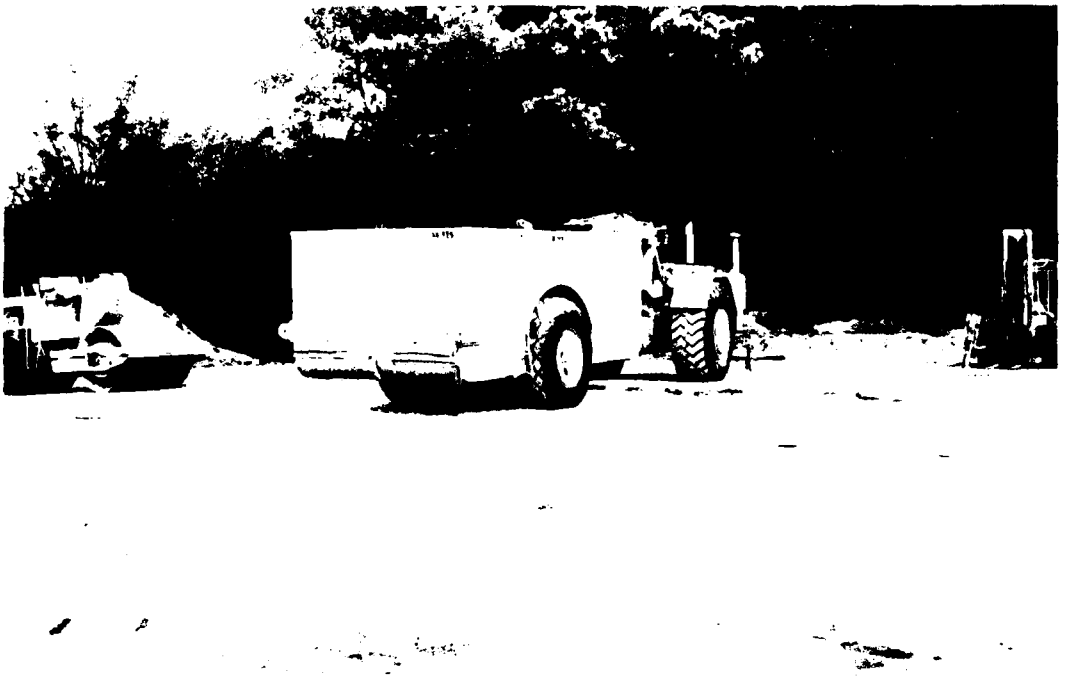

Photo 59. Rolling crushed stone with 110,000-lb, 90-psi pneumatic-tired roller

Photo 60. Applied prime coat of SS-1 before application of asphaltic concrete in crater 6

Photo 61. Asphaltic concrete being placed into the crater

Photo 62. Spreading asphaltic concrete with motor grader in crater 6

Photo 63. Rolling asphaltic concrete with vibratory steel-wheel roller in crater 6

Photo 64. Aerial view of test section showing C-141 load cart trafficking section

Photo 65. Test section looking west with F-4C load cart operating in lane 1, and larger C-141 load cart in lane 2

Photo 66. Crater 1, lane 1, prior to traffic

Photo 67. Surface of crater 1 after 380 passes of F-4C load cart

Photo 68. Close-up of limestone surface after 1020 passes of C-141 load cart

AD-A108 716 ARMY ENGINEER WATERWAYS EXPERIMENT STATION VICKSBURG--ETC F/G 13/2
BOMB CRATER REPAIR TECHNIQUES FOR PERMANENT AIRFIELDS. REPORT I--ETC(U)
OCT 81 D L COOKSEY
UNCLASSIFIED WES/MP/GL-81-12 NL

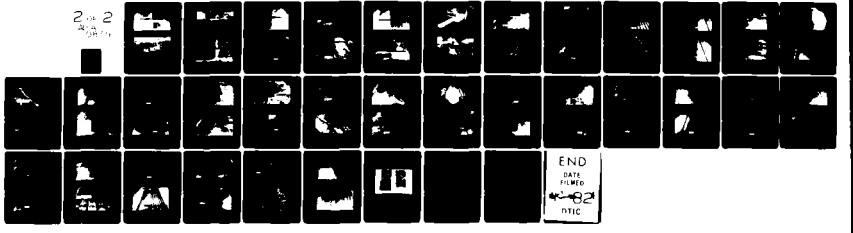

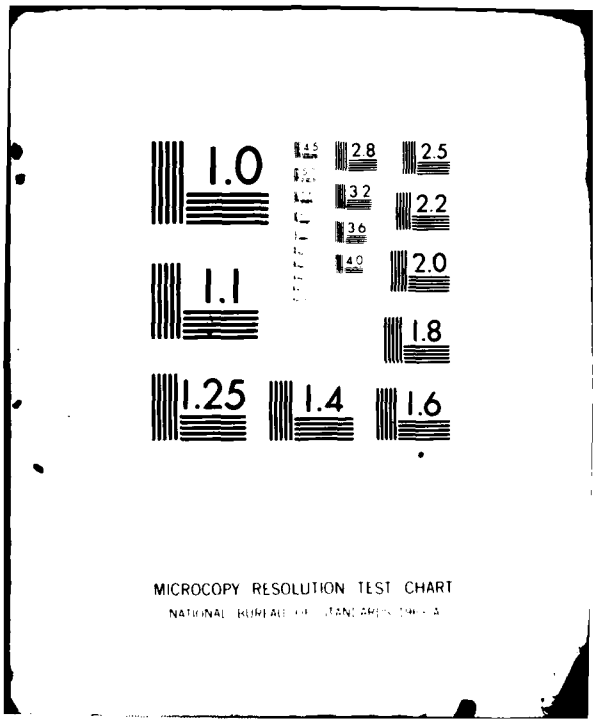
1.0
1.1
1.25
1.4
1.6
1.8
2.0
2.2
2.5
2.8
3.2
3.6
4.0
MICROCOPY RESOLUTION TEST CHART

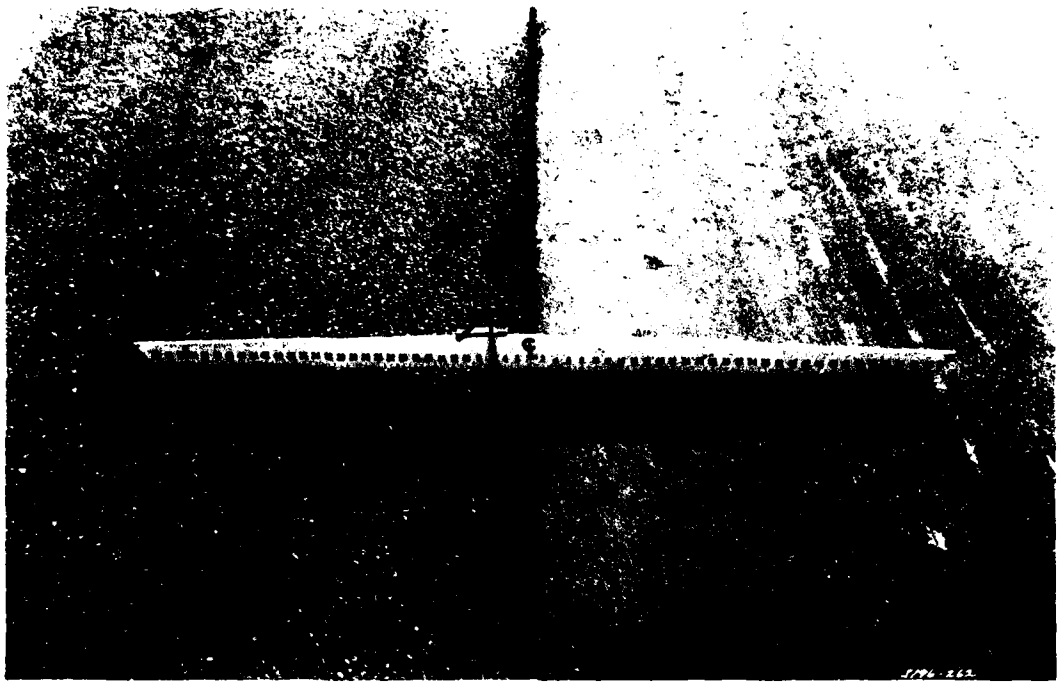

Photo 69. Rutting of limestone adjacent to asphalt after 3400 passes of C-141 loading

Photo 70. Maintenance being performed on limestone repair in crater 1

Photo 71. Pneumatic-tired roller compacting limestone which was added to crater 1 as part of normal anticipated maintenance

Photo 72. View of crater 1, lane 1, after completion of maintenance and prior to resumption of traffic

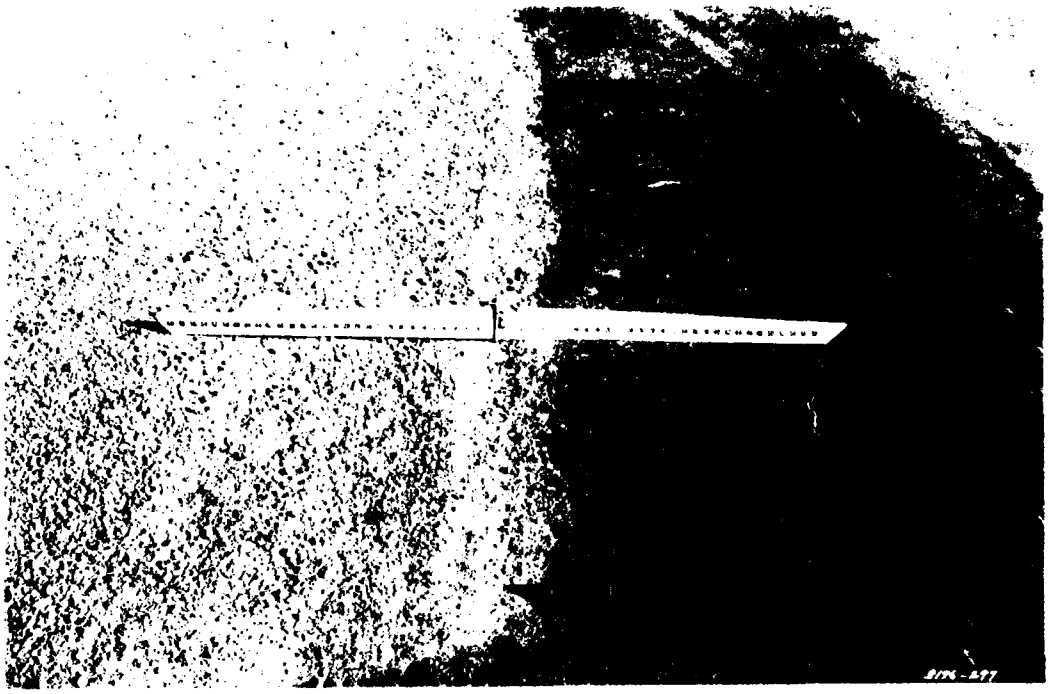

Photo 73. Repair surface of crater 1, lane 1, after 4692 passes of the C-141 load cart

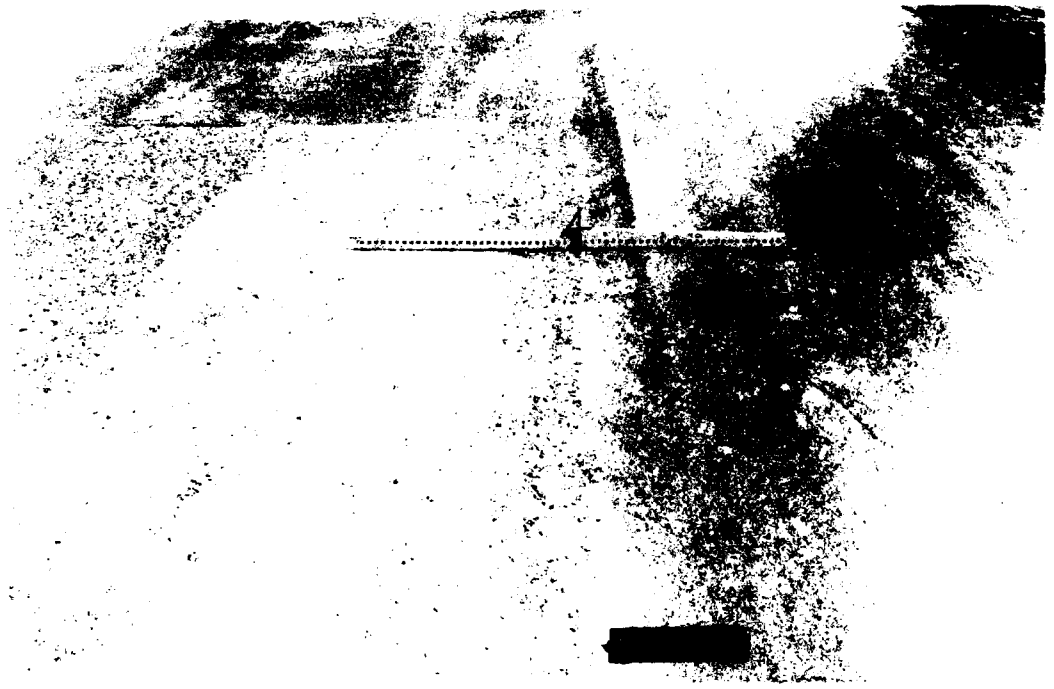

Photo 74. Overall view of crater 1, lane 1 after completion of traffic showing some minor rutting

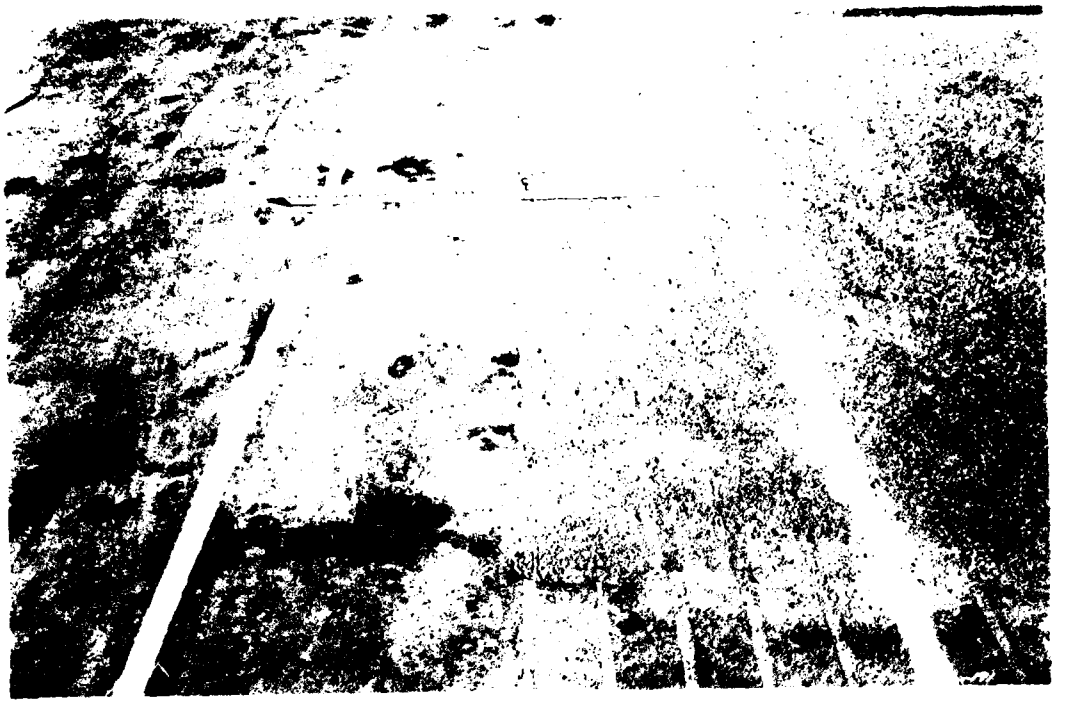

Photo 75. Surface of crater 1, lane 2, prior to traffic

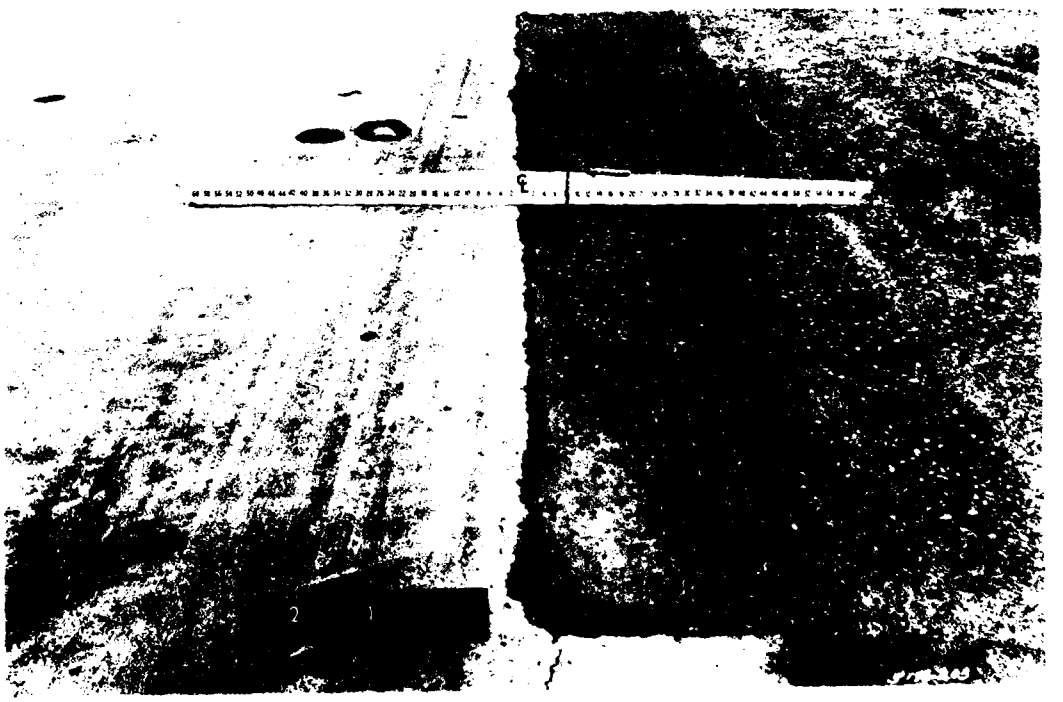

Photo 76. Surface of crater 1, lane 2, after 510 passes of the C-141 load cart

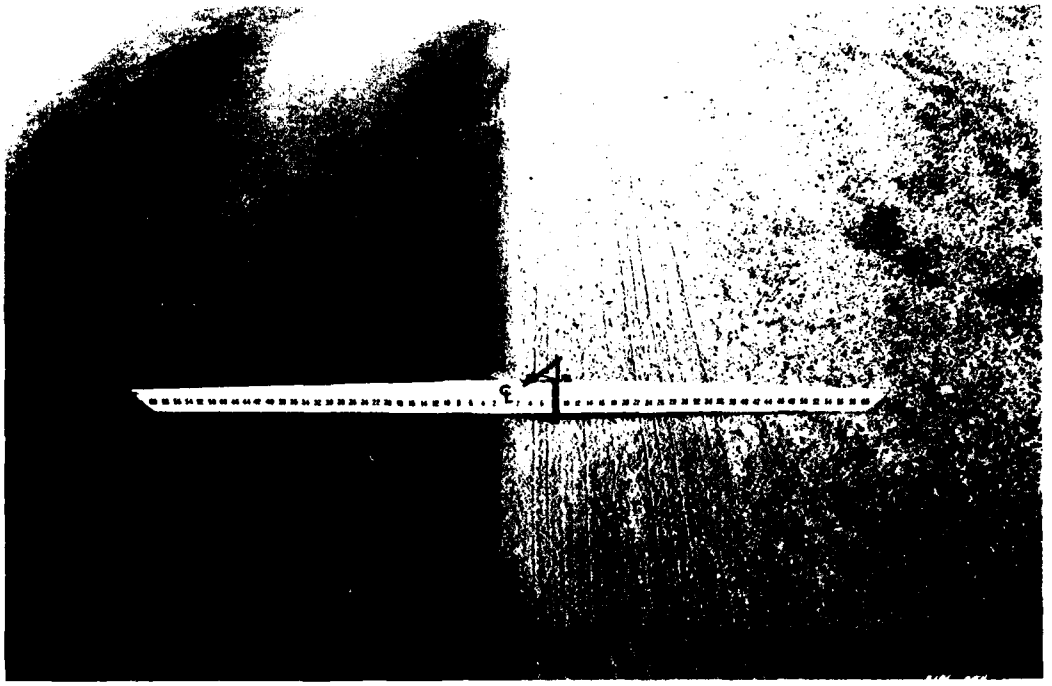

Photo 77. Crater 1, lane 2, after 1700 passes of the C-141 load cart showing a relatively smooth surface

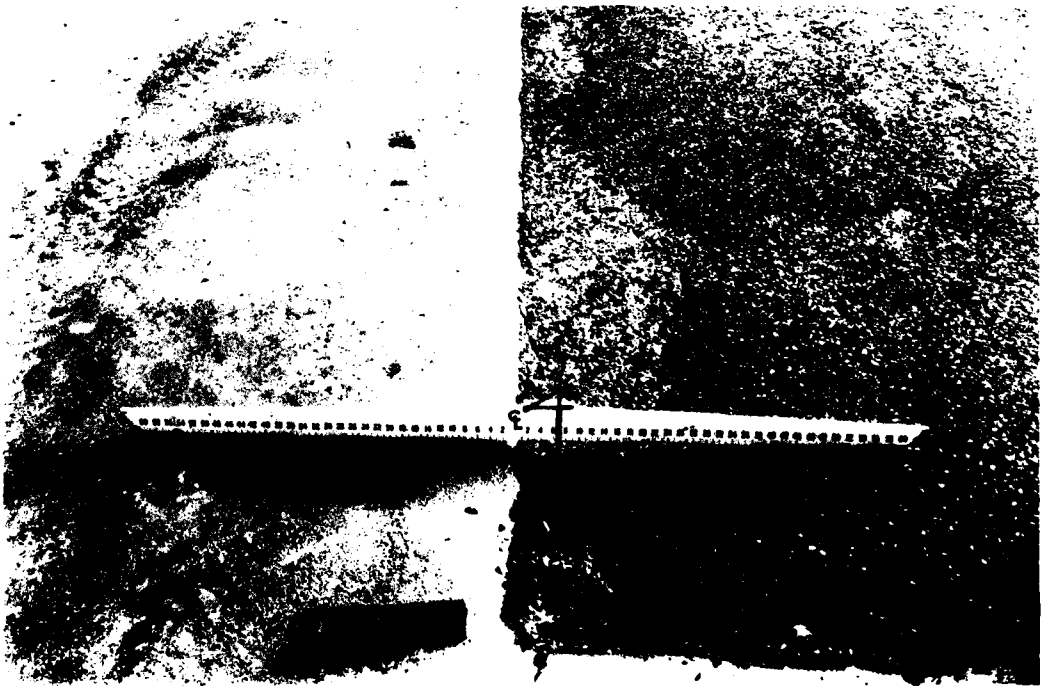

Photo 78. Rut depth of crater 1, lane 2, after 3400 passes of C-141 load cart during periods of rainfall

Photo 79. Asphaltic film being placed by hand over surface of limestone to keep individual limestone aggregates intact

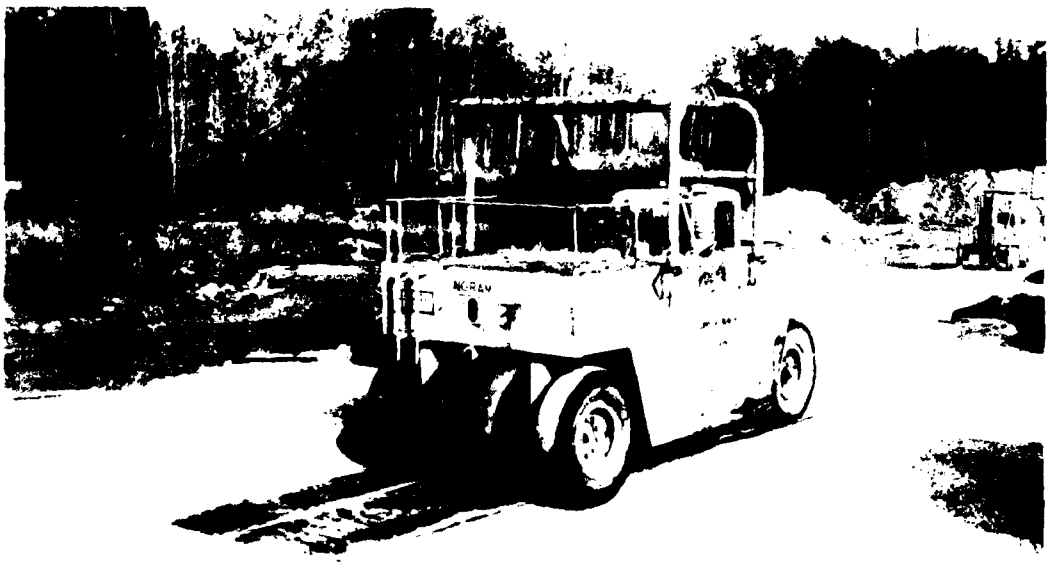

Photo 80. Rolling of asphaltic film in crater 1, lane 2, using self-propelled roller with seven tires

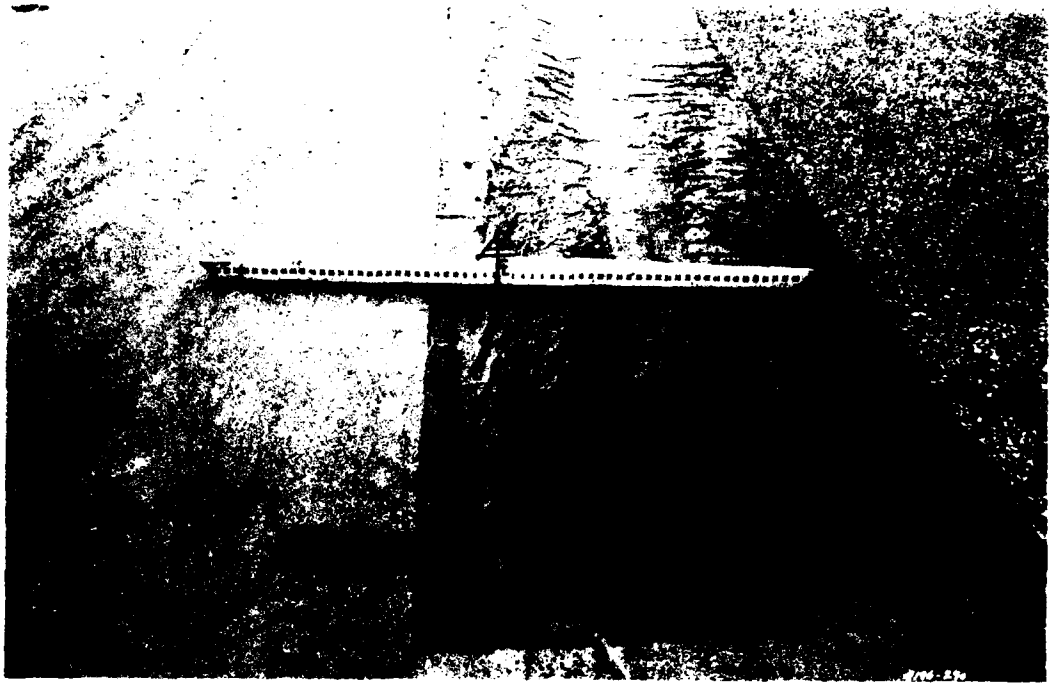

Photo 81. Surface of crater after completion of asphaltic film placement

Photo 82. Wrinkles in the asphalt-coated fabric after 10 passes of the C-141 load cart

Photo 83. End of fabric rolled back to show condition of bottom surface after loss of bond

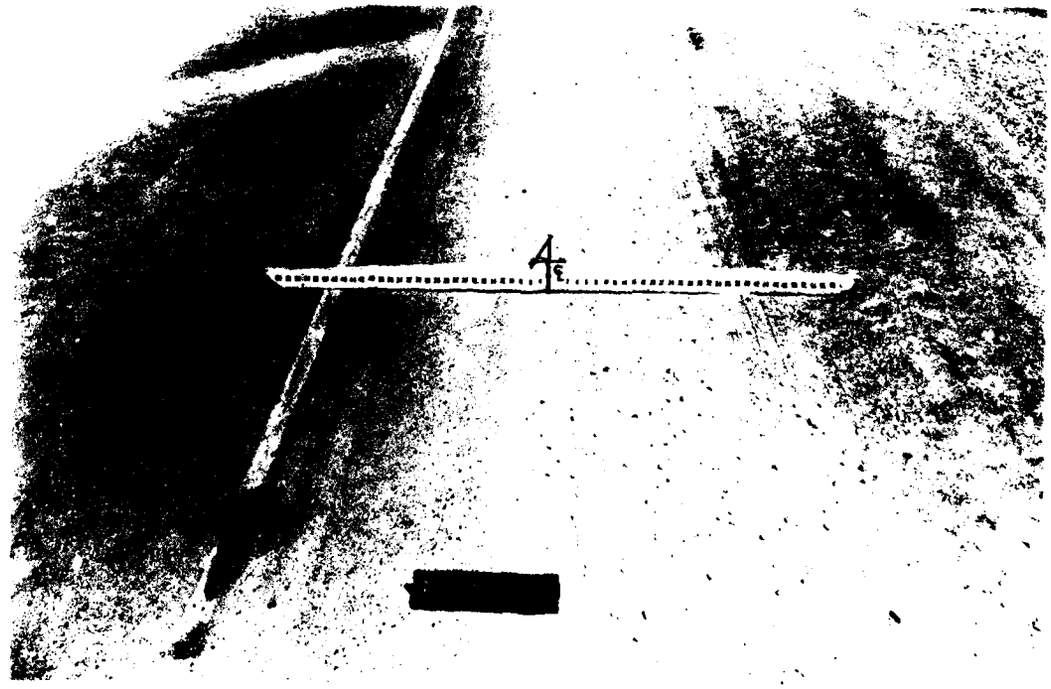

Photo 84. Crater 1 showing condition after traffic in lane 2 after 5100 passes

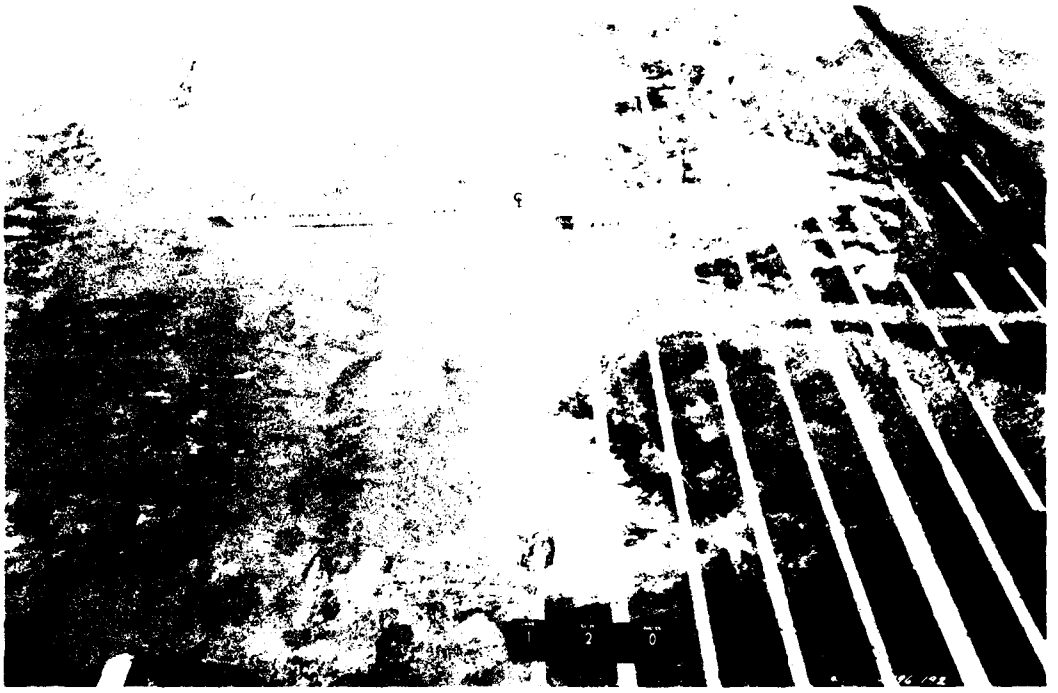

Photo 85. Crater 2, lane 2, just after grout placement and prior to traffic. Free water was quite evident on the surface of the repair

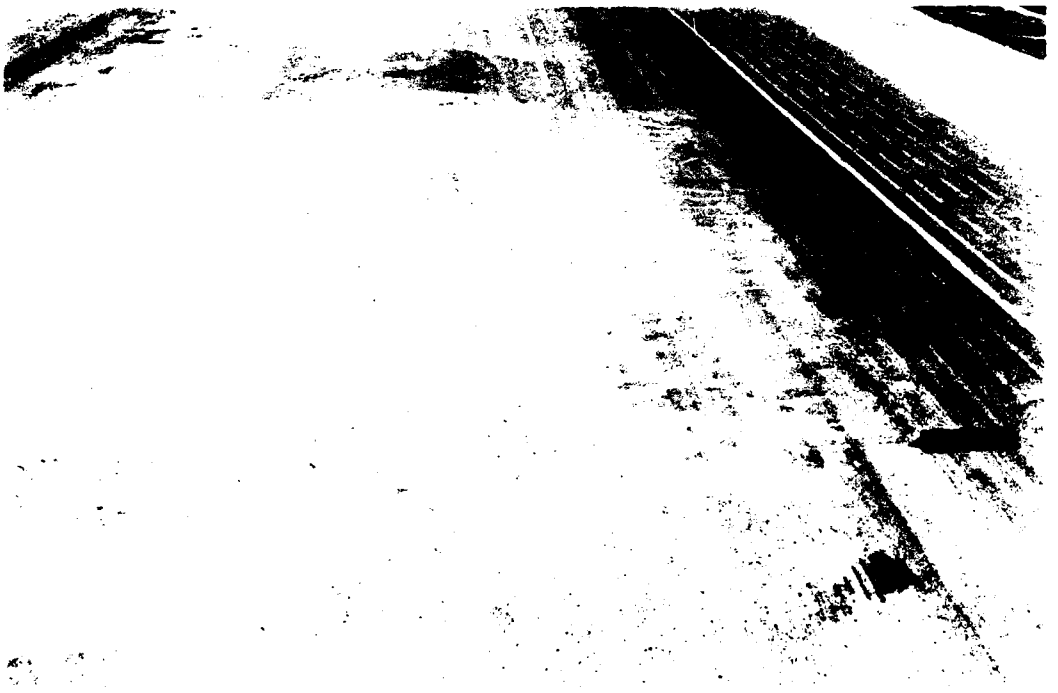

Photo 86. Corner breaks, transverse cracks, and some spalling after 340 passes of the C-141 load cart, crater 2, lane 1

Photo 87. Increased spalling and more pronounced corner breaks and transverse cracks in crater 2, lane 1, after 1020 passes of the C-141 load cart

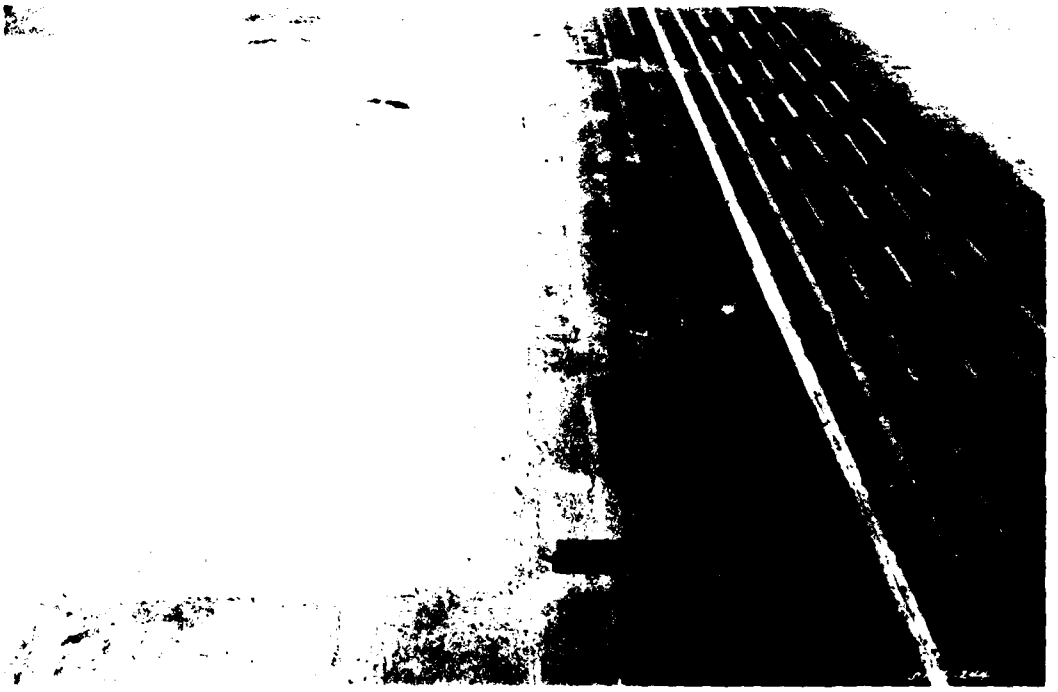

Photo 88. View of crater 2, lane 1, after 1700 passes of the C-141 load cart showing visible spalling, especially at locations of moment transfer devices

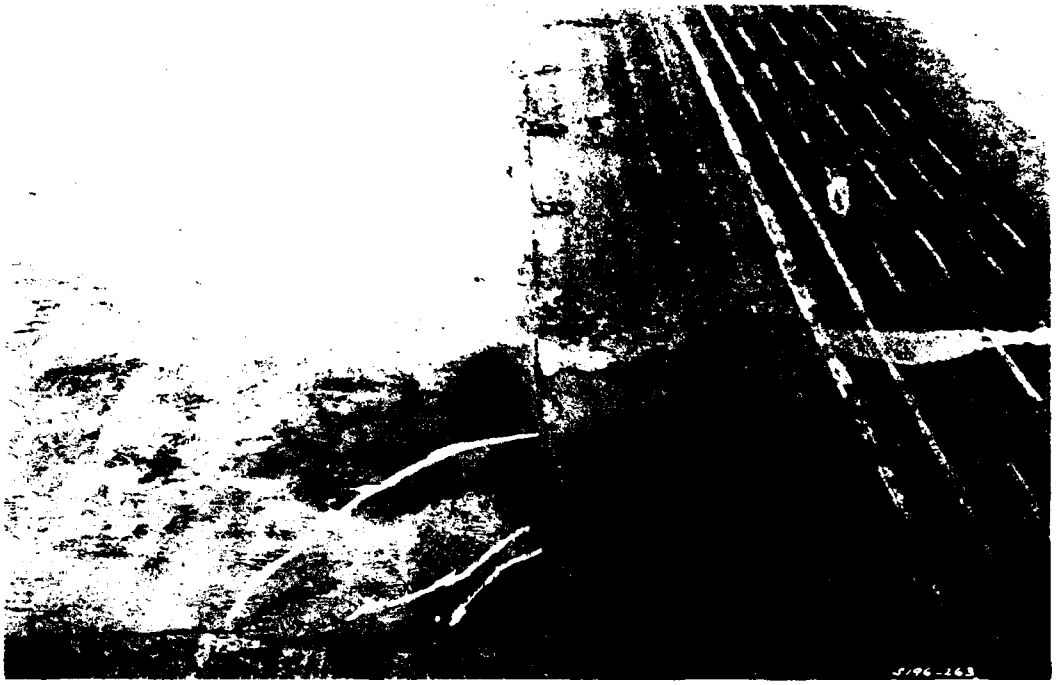

Photo 89. Crater 2, lane 1, after 3400 passes of the C-141 load cart, showing some progression of corner breaks and spalling over the moment transfer devices

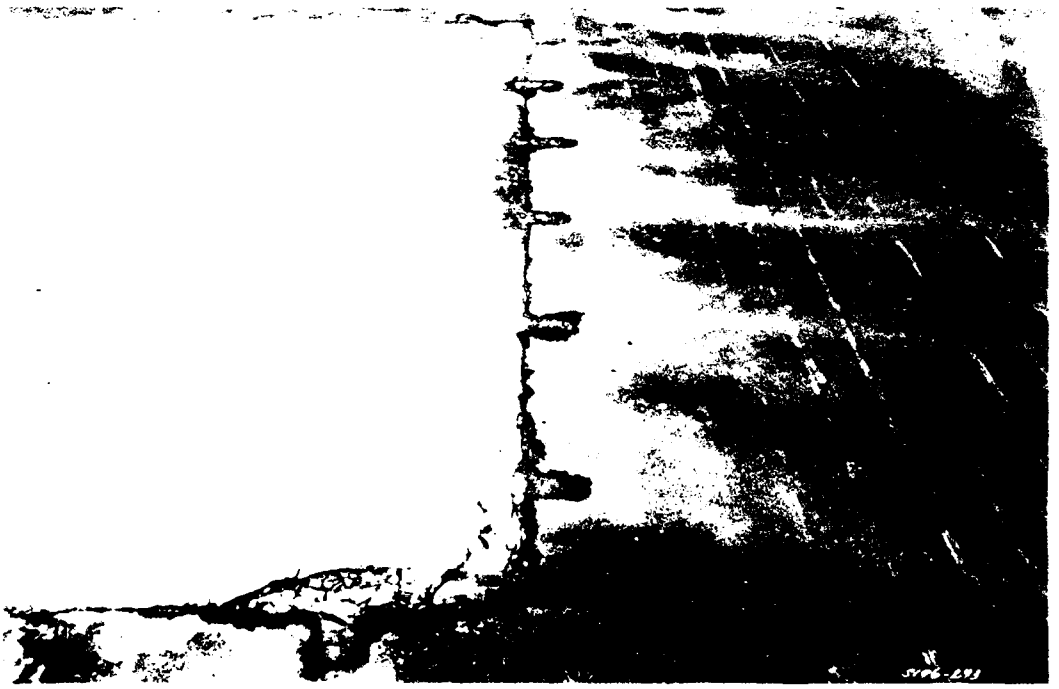

Photo 90. Increase in spalling at corners and along joints after 4692 passes of traffic

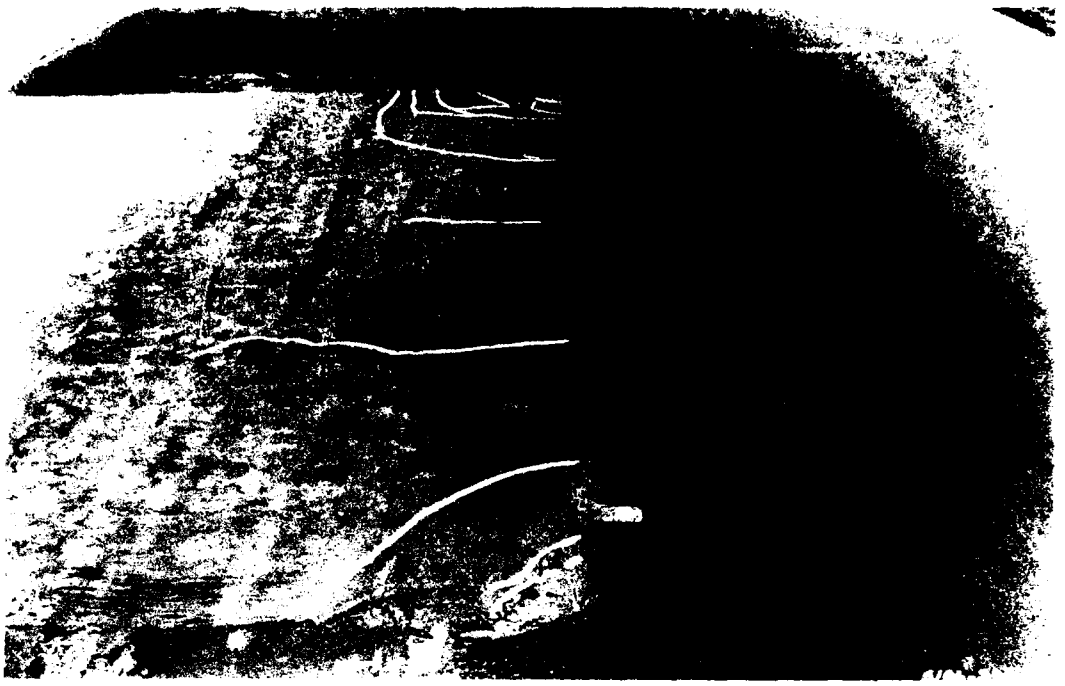

Photo 91. View of crater 2, lane 1, at completion of traffic showing some spalling of grout

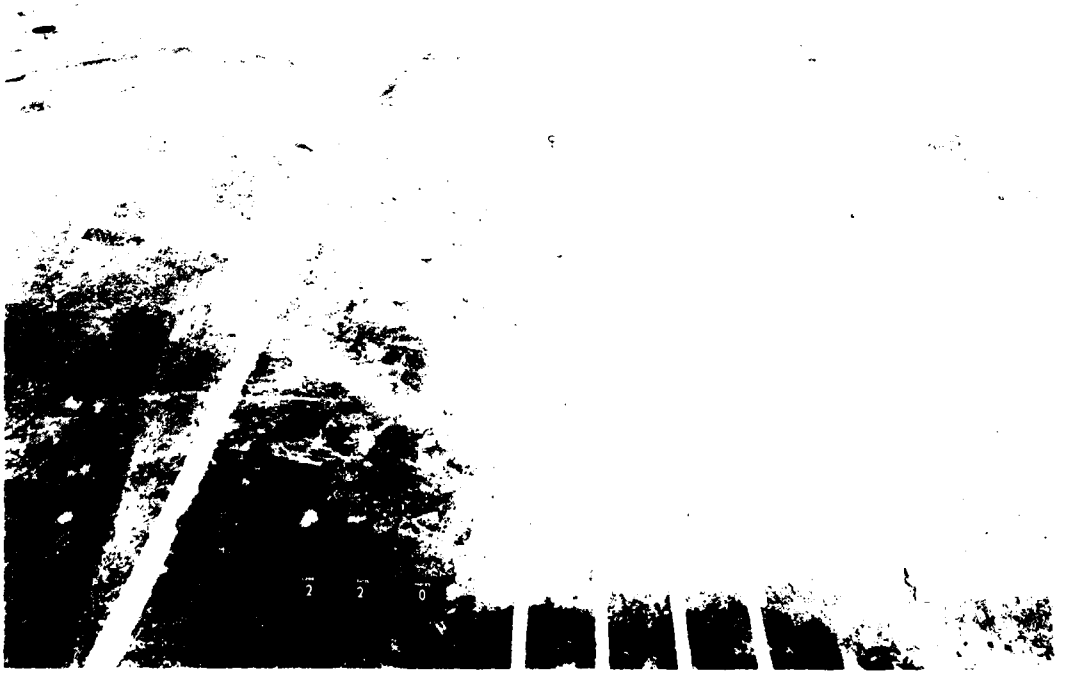

Photo 92. Crater 2, lane 2, prior to traffic, which shows the irregular surface as evidenced by water-filled depressions

Photo 93. Crater 2, lane 2, showing hairline cracks and corner breaks in crater corner after 45 hr of curing time and 510 passes of the C-141 load cart

Photo 94. Crater 2, lane 2, showing additional hairline cracks and corner breaks (painted white) after curing time increase of 43 hr with no traffic

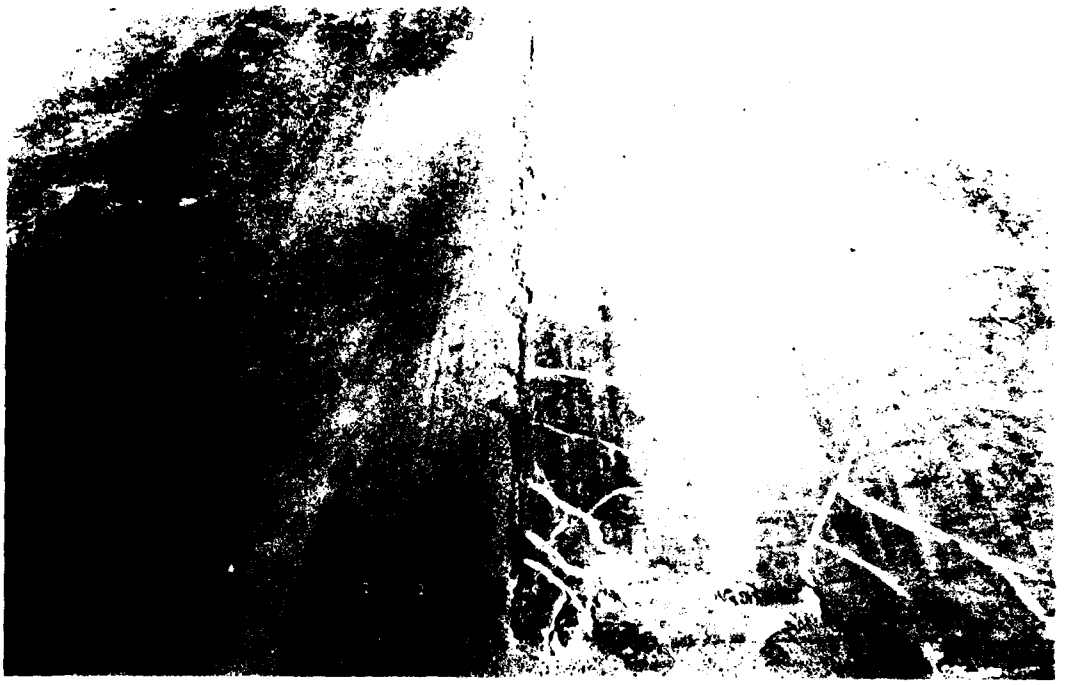

Photo 95. Increase in spalling in crater 2, lane 2, after completion of 1700 passes of the C-141 loading

Photo 96. Close-up of northeast corner of crater 2, lane 1, showing spalling after 3400 passes of the C-141 load cart

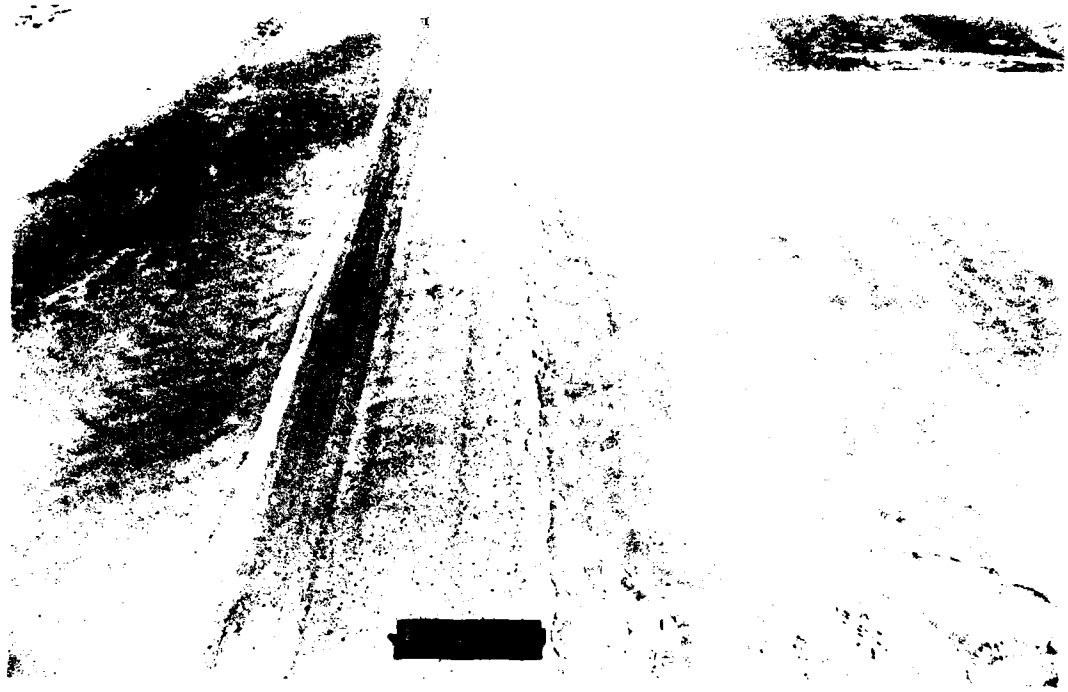

Photo 97. Crater 2, lane 2, after completion of traffic showing spalling, crack, and corner break conditions

Photo 98. Crater 3, lane 1, shortly after grout placement showing indications of water-filled depressions

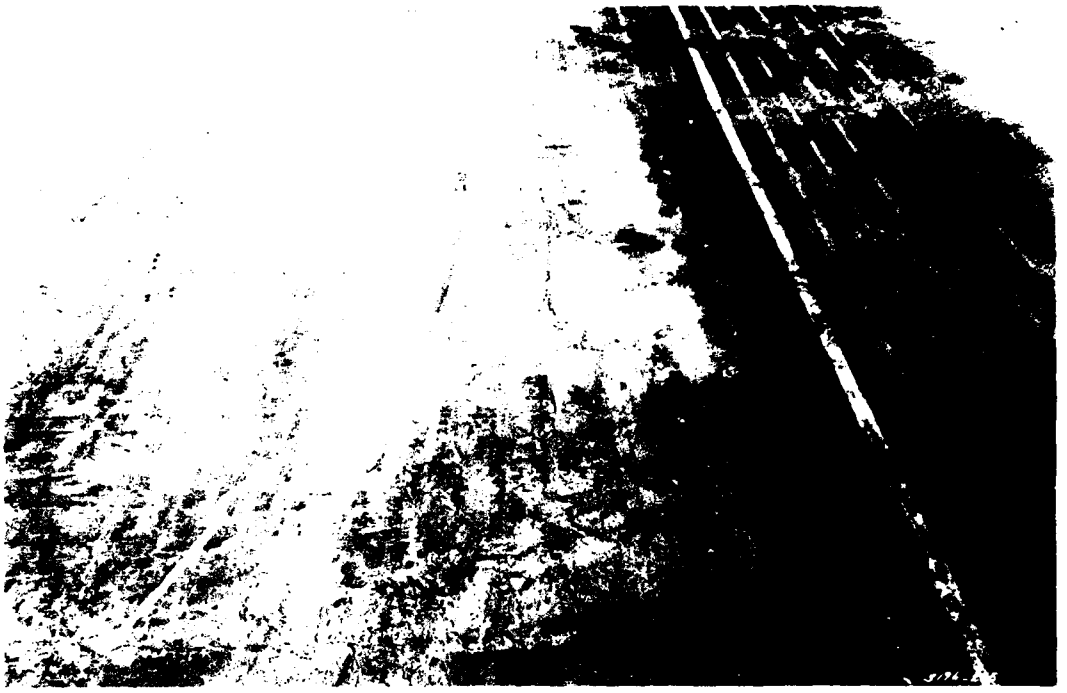

Photo 99. Crater 3, lane 1, showing initial corner breaks in repair and indications of minor spalling

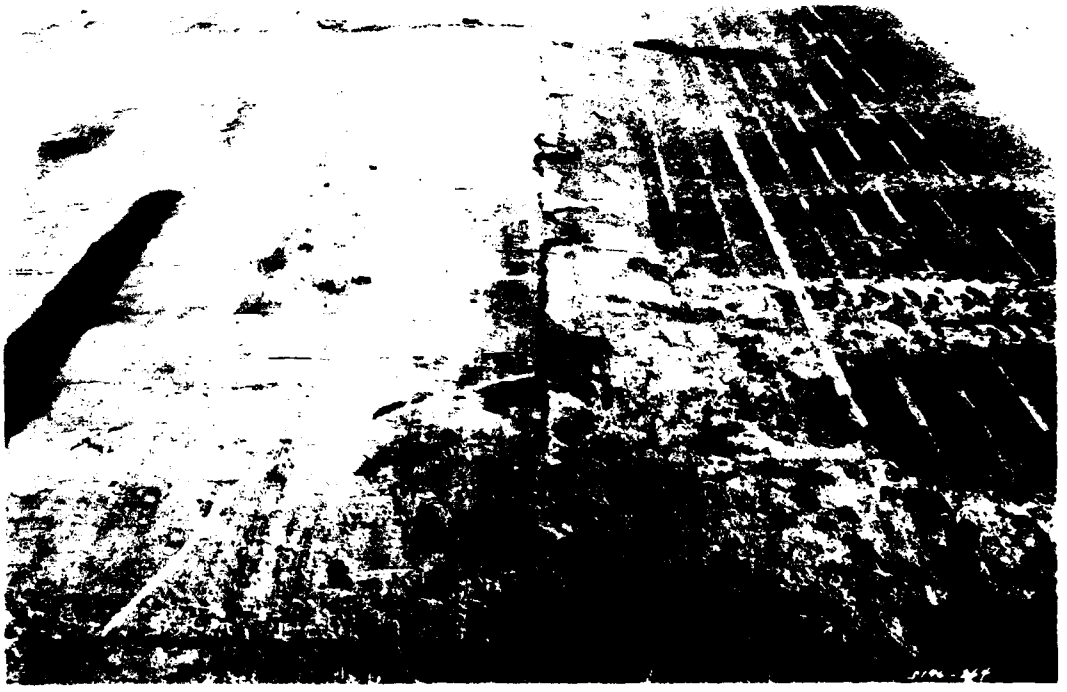

Photo 100. Additional corner breaks in crater 3, lane 1, after 3400 passes of the C-141 loading

Photo 101. Crater 3, lane 1, after 4692 passes of C-141 traffic showing spalling at joints of crater

Photo 102. Crater 3, lane 1, at completion of traffic showing test pit after repair

Photo 103. Crater 3, lane 2, after placement of grout and prior to initiation of traffic

Photo 104. Crater 3, lane 2, initial signs of stress developing after 510 passes of C-141 loading which was begun within 16 hr of grout placement

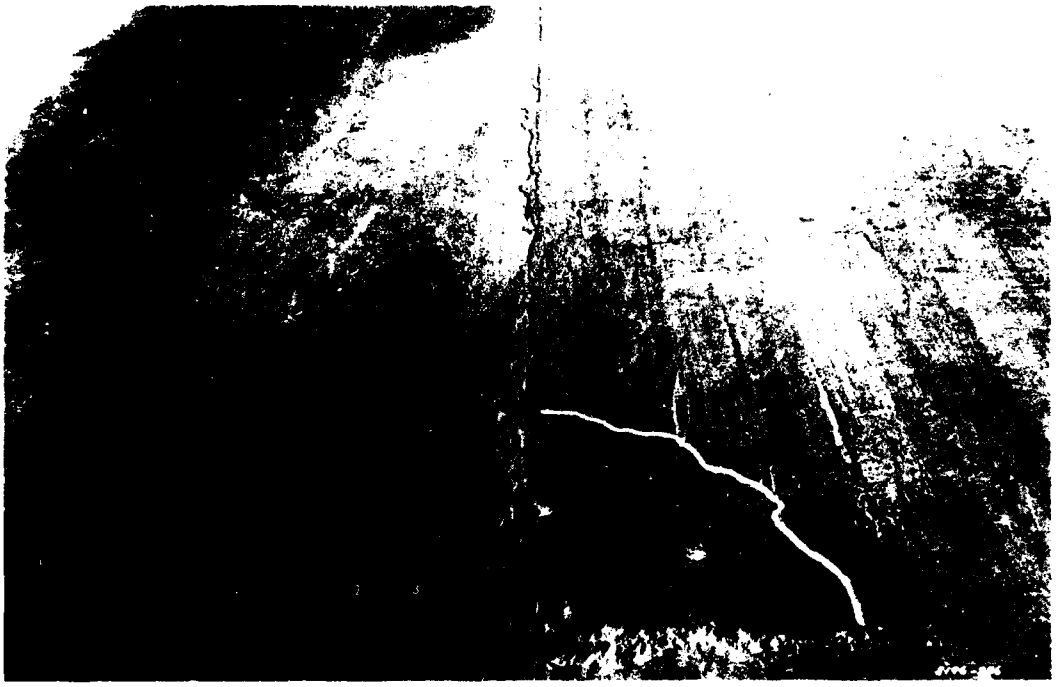

Photo 105. Crater 3, lane 3, corner breaks and spalling occurring after 1700 passes of the C-141 loading

Photo 106. Crater 3, lane 2, view of increased spalling at repair corner and along joint after 3400 passes of the C-141 load cart

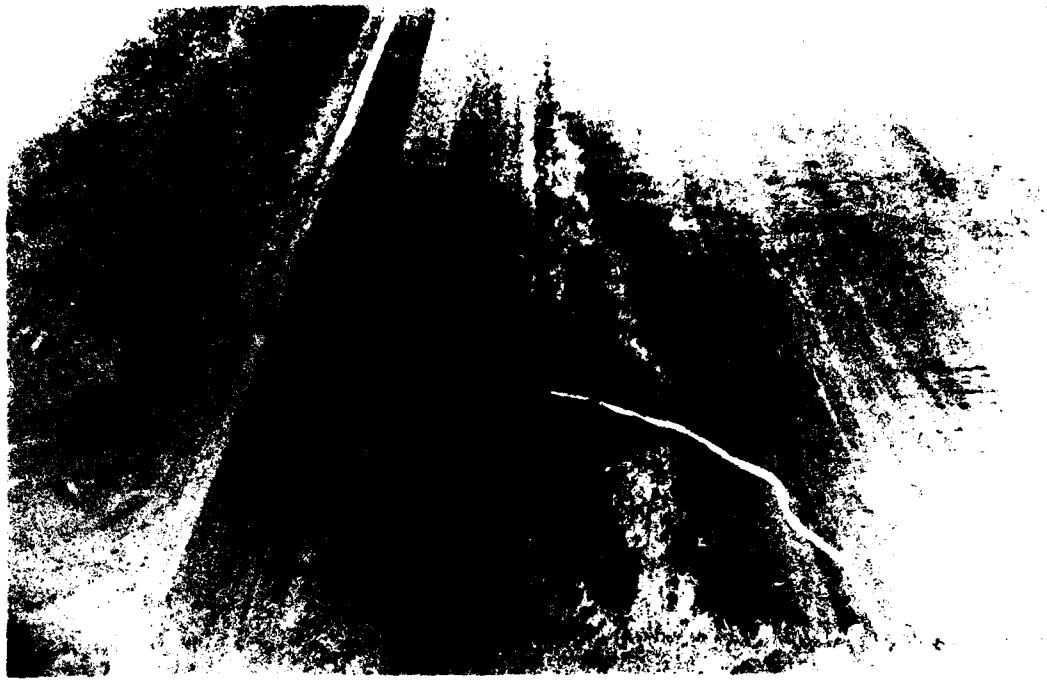

Photo 107. Crater 3, lane 2, after completion of traffic showing spalling along joints

Photo 108. View of crater 4, lane 1, after 7 days curing time of portland cement and prior to application of traffic

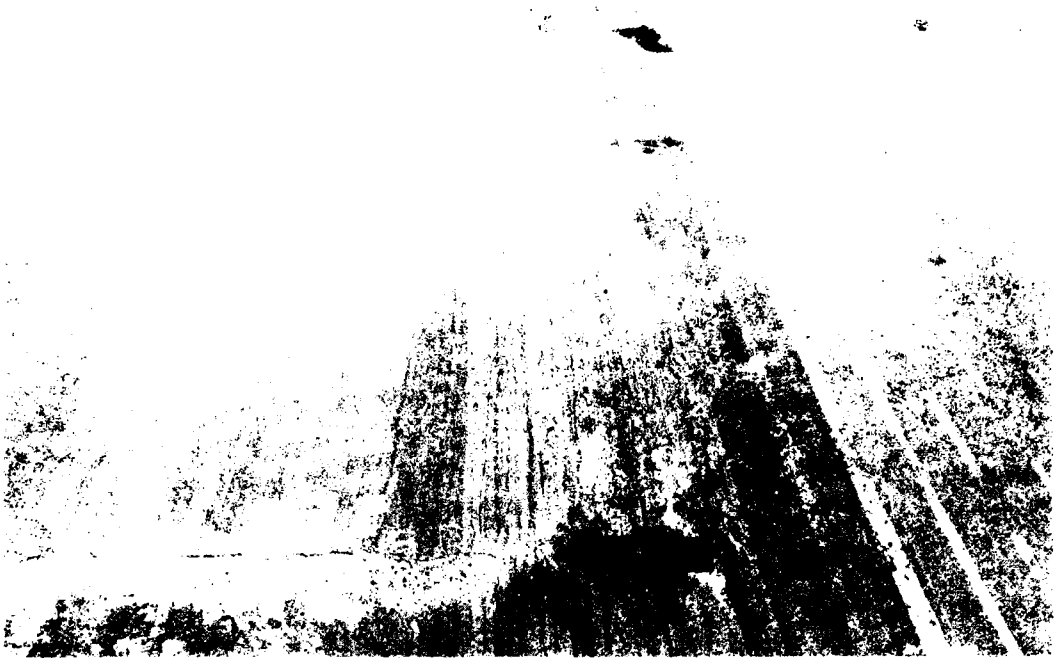

Photo 109. Crater 4, lane 1, initial corner break in crater repair after 760 passes of the F-4C load cart and 680 passes of the C-141 load cart

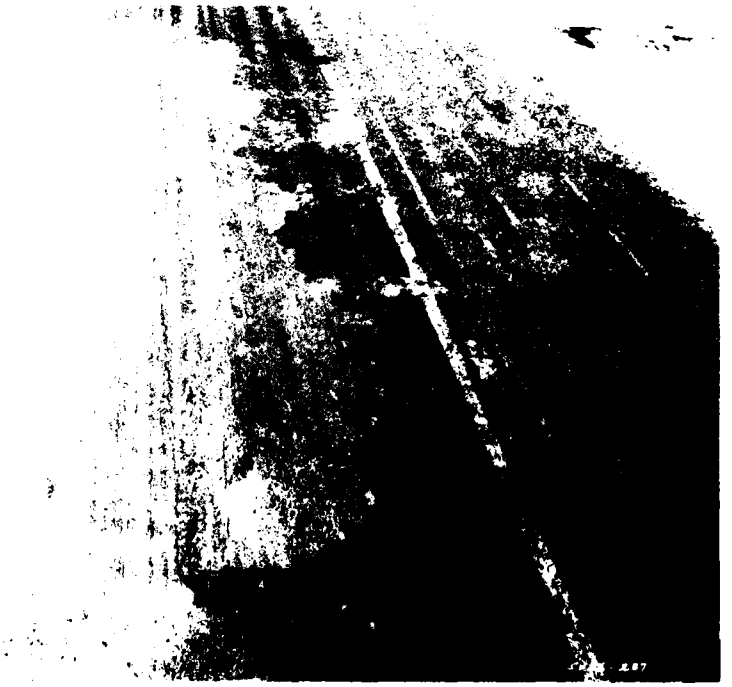

Photo 110. Crater 4, lane 1, additional crack in crater repair after 1020 passes of the C-141 load cart

Photo 111. Overall view of crater 4, lane 1, after 4692 passes of the C-141 load cart showing some minor spalling

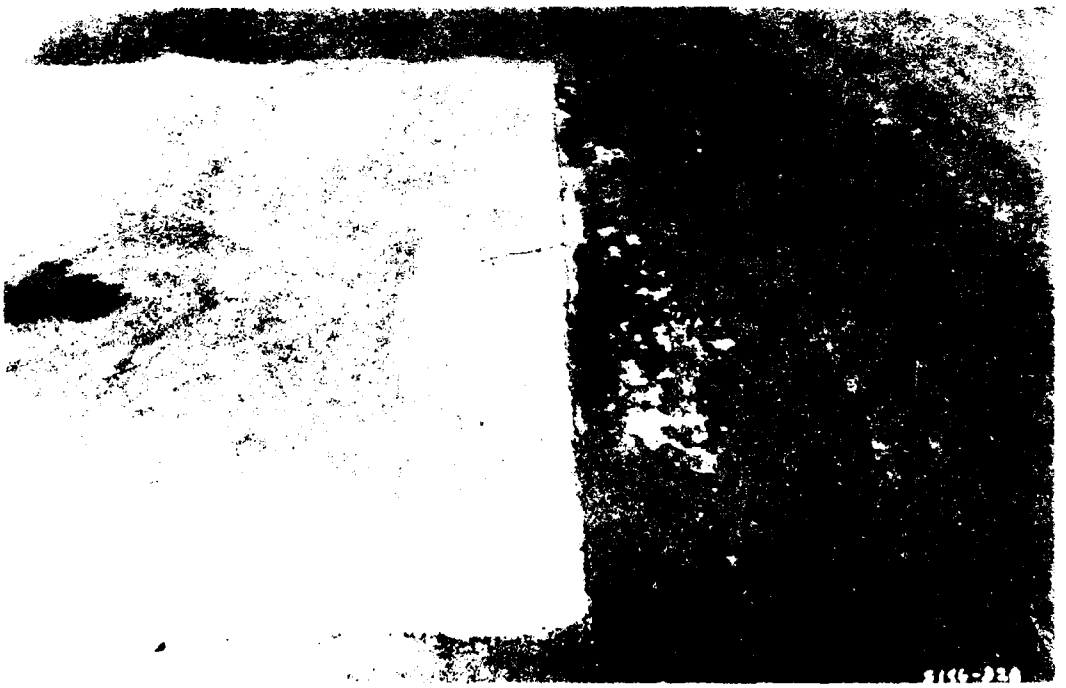

Photo 112. Crater 4, lane 1, after completion of traffic showing absence of major spalling

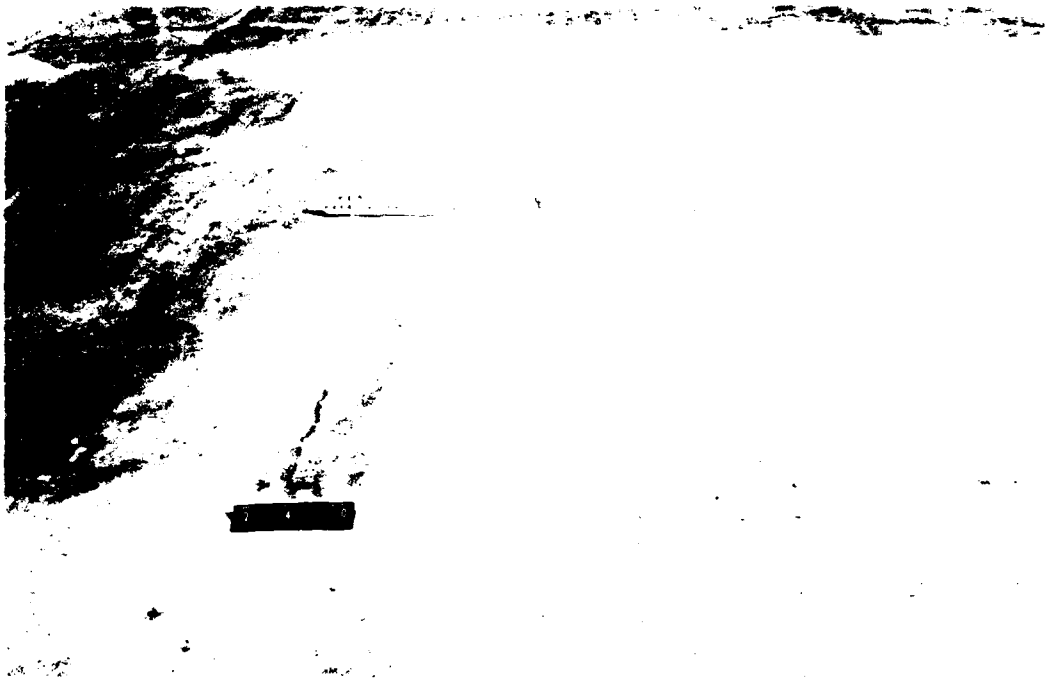

Photo 113. Crater 4, lane 2, 7 days after placement of portland cement concrete and just prior to traffic

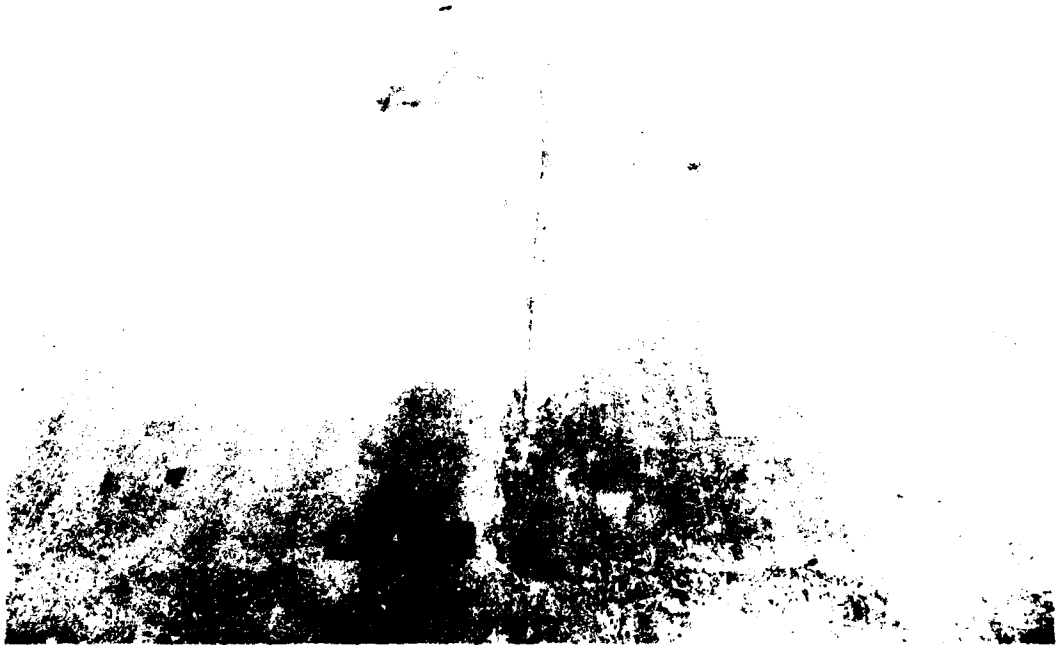

Photo 114. Crater 4, lane 2, no breaks in crater after 1020 passes of the C-141 load cart

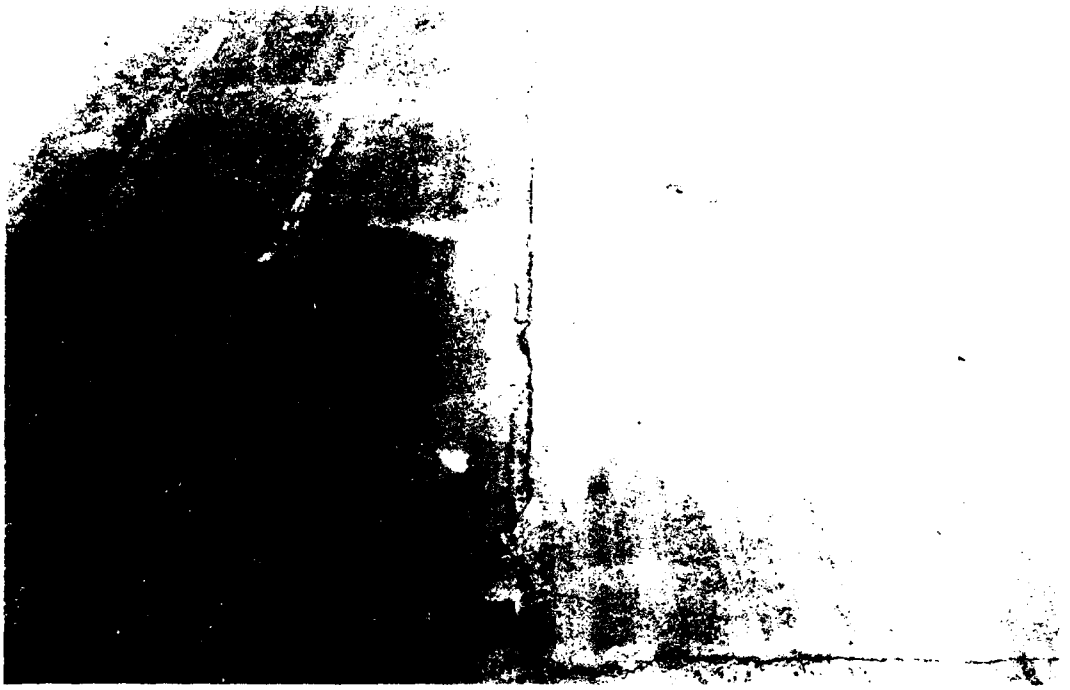

Photo 115. Crater 4, lane 2, after 3400 passes of traffic showing no corner breaks or cracks

Photo 116. Crater 4, lane 2, with a relatively smooth surface after completion of traffic

Photo 117. Unevenness of repair in crater 5, lane 1, prior to traffic

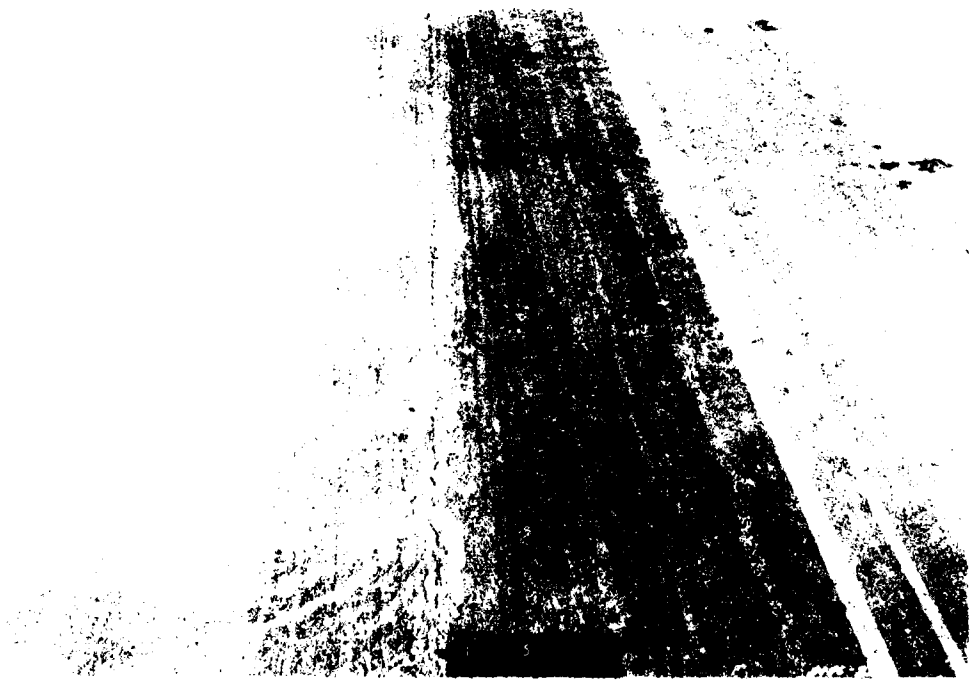

Photo 118. Crater 5, lane 1, initial corner break after 680 passes of C-141 traffic

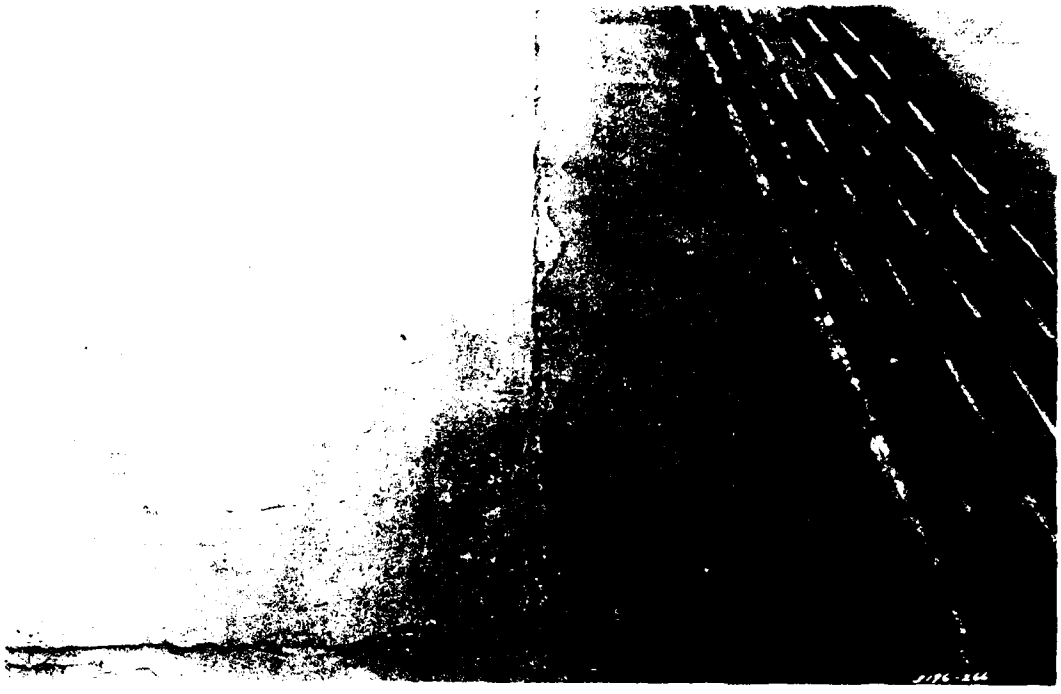

Photo 119. View of crater 5, lane 1, after 3400 passes of the C-141 load cart showing only minor spalling and a further increase in corner breaks

Photo 120. Crater 5, lane 1, no additional corner breaks after 4692 passes although there was some increase in spalling

Photo 121. Crater 5, lane 2, showing portland cement concrete repair just prior to traffic

Photo 122. Crater 5, lane 2, after 1020 passes of the C-141 load cart with no major corner breaks and minor spalling

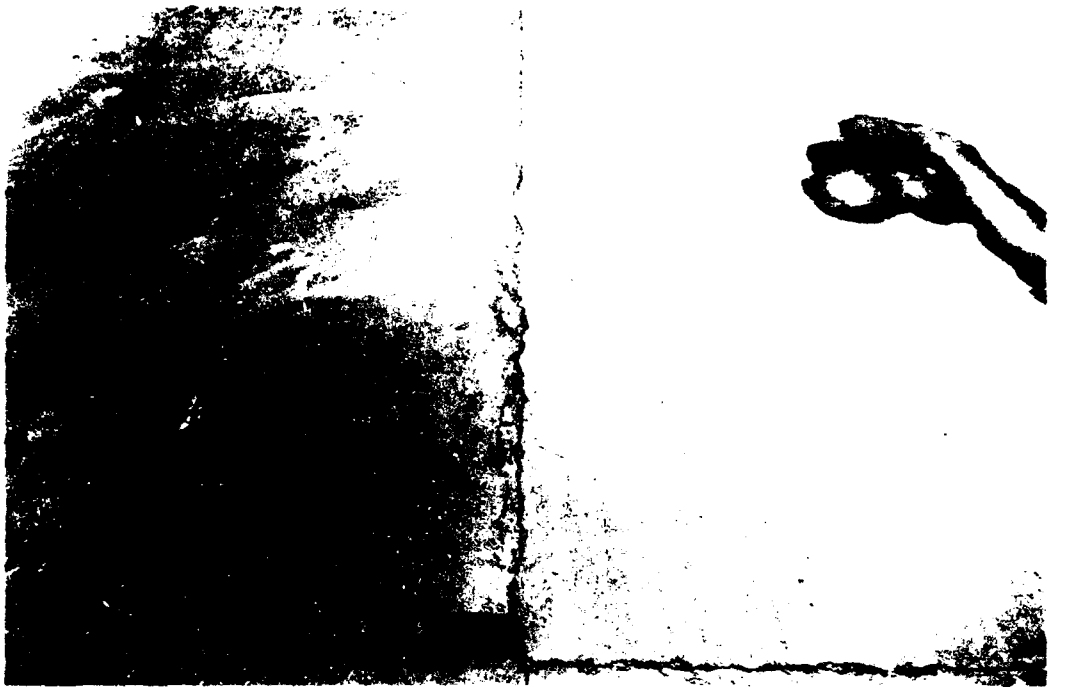

Photo 123. Crater 5, lane 2, no major corner breaks after 3400 passes of traffic and minor spalling at joints

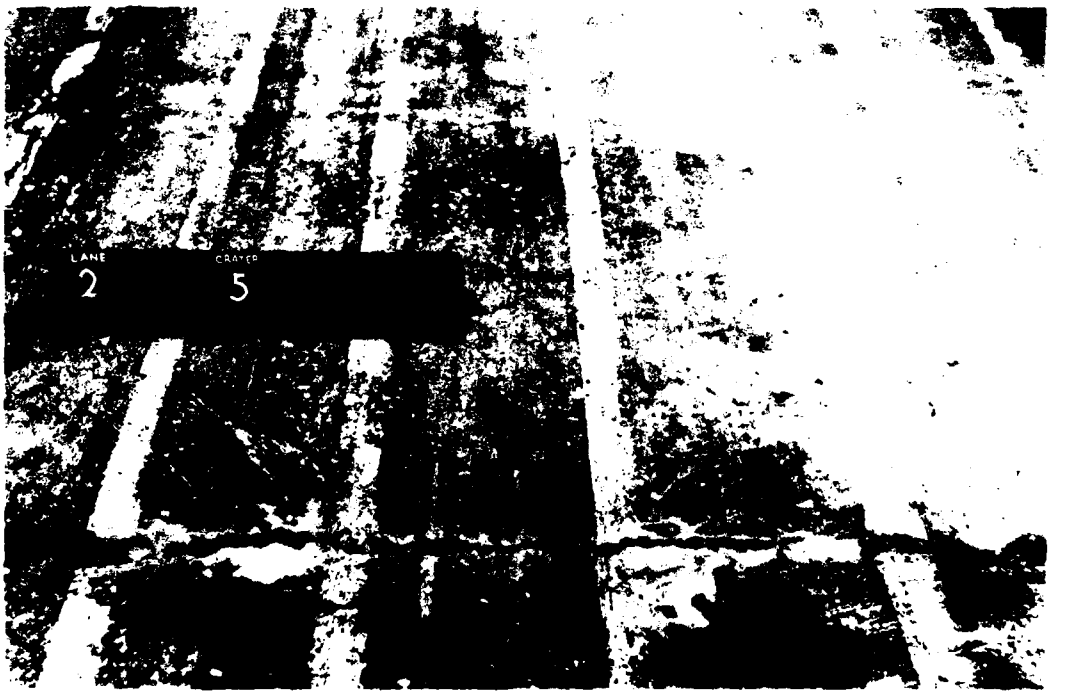

Photo 124. Subgrade material pumping at corner of crater 5, lane 2, after 3876 passes of C-141 traffic

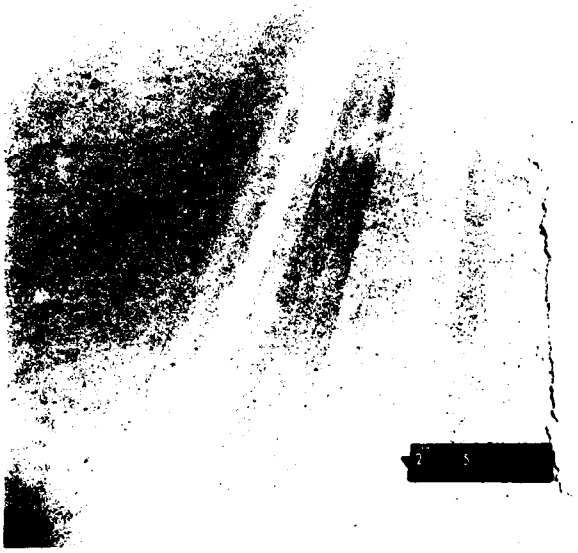

Photo 125. View of crater 5, lane 2, after completion of trafficking with C-141 load cart

Photo 126. Crater 6, lane 2, prior to traffic

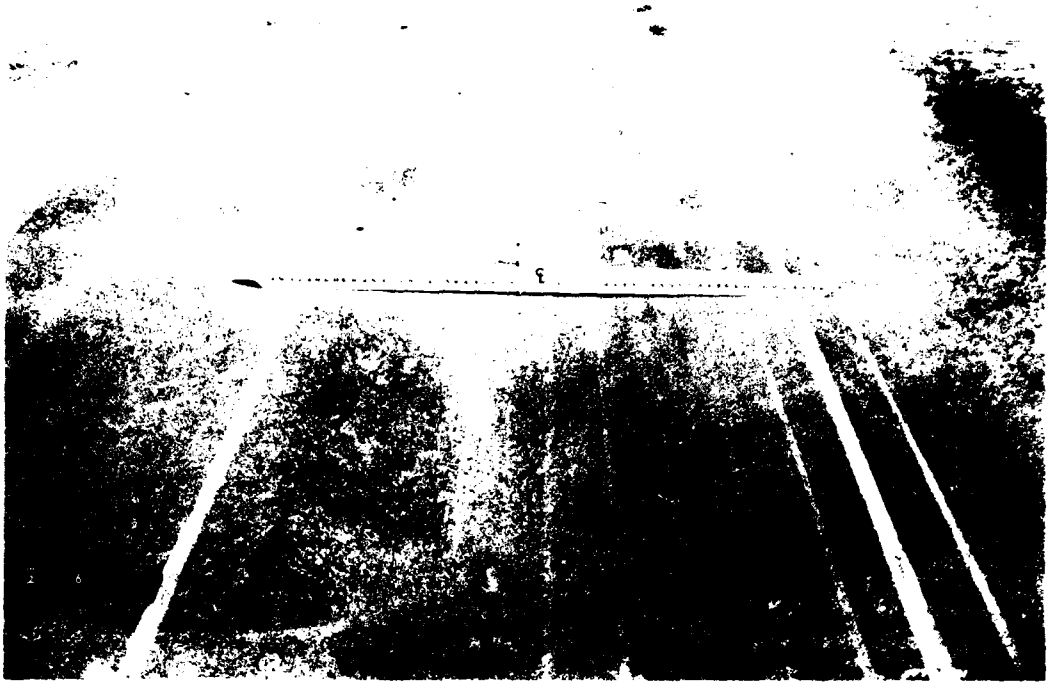

Photo 127. Crater 6, lane 2, after 1020 passes of C-141 traffic

Photo 128. Crater 6, lane 2, after 3400 passes showing longitudinal fatigue cracks

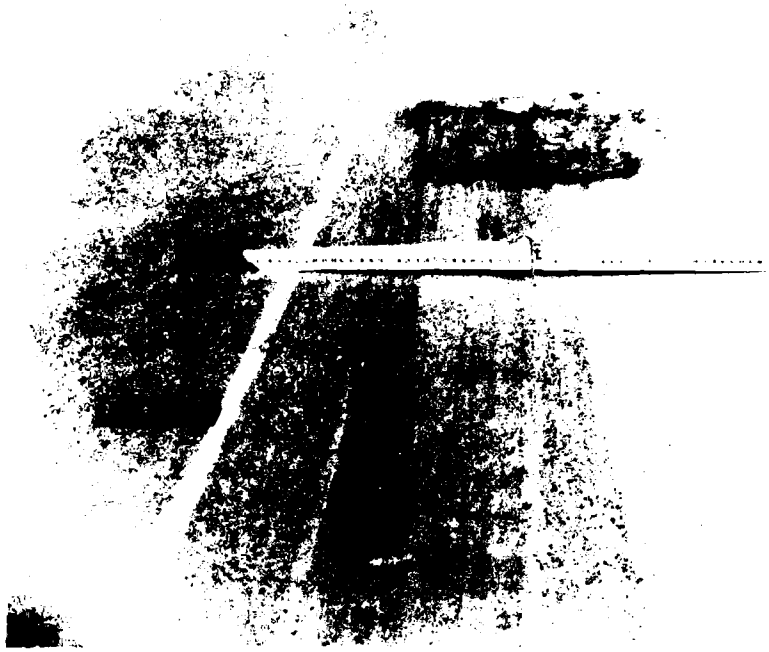

Photo 129. Crater 6, lane 2, showing condition after 5100 passes

Photo 130. Cracking in vicinity of crater 1 that occurred in slab 5 after 3774 passes of C-141 traffic

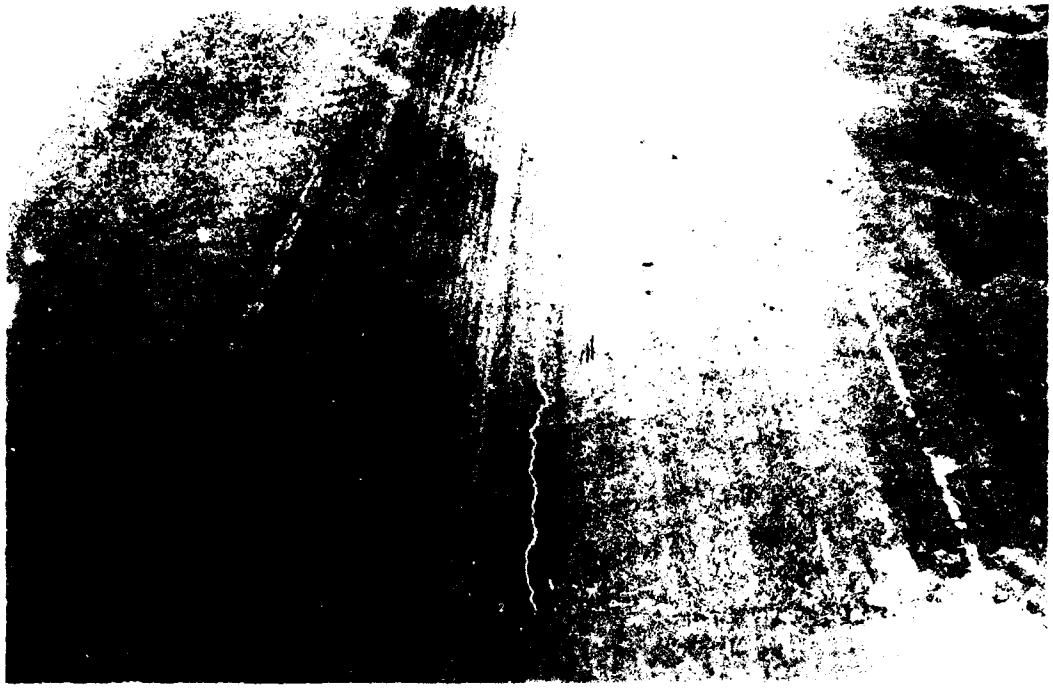

Photo 131. Reflective crack that occurred over construction joint in lane 2

Photo 132. Reflective cracking indicating corner breaks and keyed joint failure after 2856 passes of the C-141 load cart

Photo 133. Cross section of concrete core taken through keyed joint showing failure of male portion of key

In accordance with letter from DAEN-RDC, DAEN-AST dated 22 July 1977, Subject: Facsimile Catalog Cards for Laboratory Technical Publications, a facsimile catalog card in Library of Congress MARC format is reproduced below.

Cooksey, David L.
Bomb crater repair techniques for permanent airfields : Report 1 : Series 1 tests / by David L. Cooksey (Geotechnical Laboratory, U.S. Army Engineer Waterways Experiment Station). -- Vicksburg, Miss. : The Station ; Springfield, Va. : available from NTIS, 1981.
49, [74] p. : ill., ports. ; 27 cm. -- (Technical report / U.S. Army Engineer Waterways Experiment Station ; GL-81-12, Report 1)
Cover title.
"October 1981."
"Prepared for Office, Chief of Engineers, U.S. Army under Project AT40, Task CO, Work Unit 002."
Bibliography: p. 45-49.

1. Air bases--Runways. 2. Airports--Runways. 3. Blast effects. 4. Cratering. I. U.S. Army Engineer Waterways Experiment Station. Geotechnical Laboratory. II. Title.

Cooksey, David L.
Bomb crater repair techniques for permanent airfields : ... 1981.
(Card 2)

III. Series: Technical report (U.S. Army Engineer Waterways Experiment Station) ; GL-81-12, Report 1.
TA7.W34 no.GL-81-12 Report 1


FILME
8